# HIGH RESOLUTION SONAR FOR THE ARCHAEOLOGICAL INVESTIGATION OF MARINE AGGREGATE DEPOSITS

FINAL PROJECT REPORT

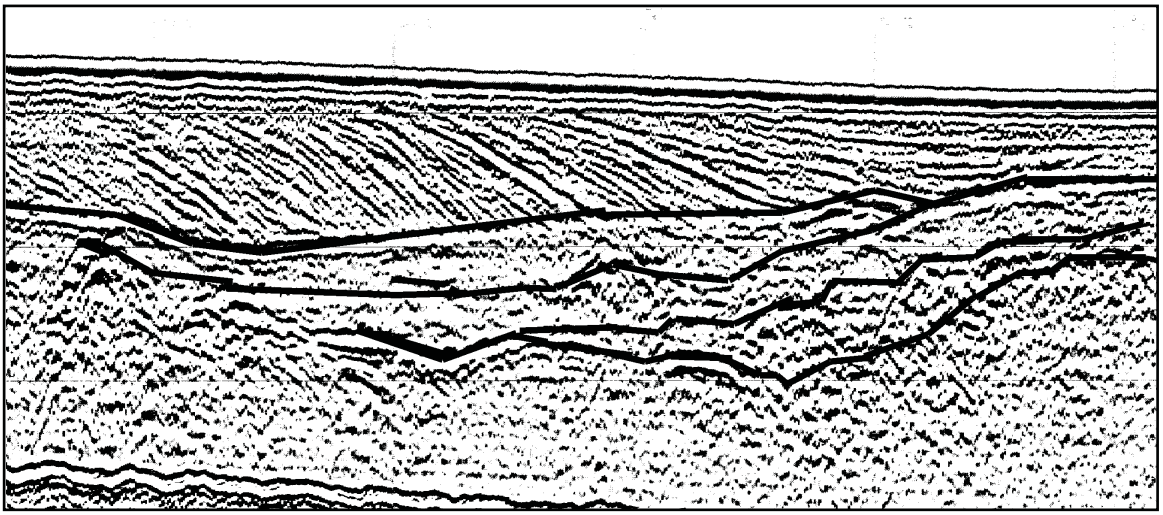

*by*

*Dr Justin Dix[1,2],Dr Alex Bastos[2], Ruth Plets[2], Dr Jonathan Bull[2] and Dr Tim Henstock[2]*

*School of Humanities (Archaeology)[1] and School of Ocean and Earth Science[2], University of Southampton*

*CONTENTS*

# 1. INTRODUCTION

Penetrative and non-penetrative sonar systems have been periodically used for the investigation of marine archaeological sites for at least the last four decades. Such sonar systems have been used to investigate both wreck sites (e.g. Rule, 1982) and latterly submerged landscapes, where the data has been used to provide a back-drop to a series of pre-historic archaeological studies (e.g. Ballard et al., 2000; Dix, 2001; Quinn et al., 2002). Unfortunately, the success of these systems for such investigations has been highly variable and as such, the archaeological community has understandably viewed such methodologies with a high degree of scepticism. However, more often than not the poor results obtained from sonar surveys have actually been the result of incorrect choice and use of equipment as well as more fundamental misconceptions of the acoustics of archaeological materials.

The last decade has seen an increase in research that specifically addresses the use of high-resolution sonar to identify marine archaeological materials (e.g. Quinn et al., 1998a; Momber & Geen, 2000; Lawrence & Bates, 2001; Arnott et al., 2002). The majority of the published work has focused on the use of Chirp sub-bottom profiling systems (e.g. Quinn et al. 1997; 1998a and b; Quinn et al., 2000). These are swept frequency sources capable of producing high-resolution imagery to a sub-seabed depth of c. 20m particularly in fine grained materials. These systems have been demonstrably shown to detect archaeological material (shipwrecks) buried beneath the seabed (e.g. Quinn et al. 1998a; Quinn 2001) and to reconstruct Holocene (Mesolithic - Neolithic) landscapes (e.g. Dix et al., 1998, 2001; Cooper et al., 2002a).

However, there are two fundamental problems with the Chirp sonar systems as the current technology stands: firstly, their ability to penetrate coarse grained stratigraphies (medium to coarse sands and gravels) is inconsistent, and secondly, as with all sonar profiling systems they only acquire two-dimensional data ("slices through the seabed") and consequently object or structure detection frequently depends on the spacing of the survey lines which may achieve a minimum separation of only 5 m and more typically 10 – 100m. The first of these issues is particularly pertinent to the aggregates industry, as their target deposits are these coarser grained materials. The aggregate industry has therefore understandably failed to embrace Chirp technology and continues to deploy lower frequency, higher energy, sources (Boomers) which more reliably penetrate coarse seabeds. These systems provide the aggregate companies with the majority of the data they require for prospection purposes. The company's principal aim being to identify the deposit and calculate aggregate volume from the identification of it's upper and lower reflectors. However, due to an inherent trade-off between penetration and resolution of sonar systems the vertical and horizontal resolution capabilities of the Boomer systems means that they are frequently incapable of detecting small buried objects (< c. 0.5 m) or identifying internal stratification, particularly of fine grained layers, within the aggregate volume.

This lack of detailed structural information is a major problem from both the archaeologist's and the aggregate industry perspective. The former are obviously interested in the identification of buried artefacts (e.g. wrecks) but are equally interested in the aggregate deposits as potential secondary (and even tertiary) contexts of Palaeolithic material. As is being shown by the work of Hosfield (1999, 2001, ALSF 3361) and others if we are to fully realise the potential of secondary contexts, such as fluvial terrace gravels, we have to be able to understand the complexity of the aggregate deposit geometry. Further, one of the major dilemmas with secondary context archaeological material is finding suitable methods of dating these coarse

grained deposits. From the extensive archaeological studies of terrestrial aggregate deposits, it is evident that, intercalated, fine grained and frequently highly organic horizons can provide essential datable material for reconstructing depositional events and thus constraining the archaeological material they contain. Consequently, the identification of such horizons can be a major criteria determining the usefulness of anyone site. From the aggregate industry perspective, in addition to the intrinsic archaeological importance of the material, the presence of large quantities of wood/metal and/or fine grained organic sediments significantly degrade the quality, and therefore profitability of the aggregate deposit itself.

This project aimed therefore to tackle these two fundamental problems to the detailed archaeological investigation of coarse grained aggregate deposits. This aim was achieved through the optimisation of new Chirp sources, developed by the School of Ocean and Earth Science, University of Southampton, in conjunction with GeoAcoustics Ltd, Great Yarmouth, specifically for the penetration of coarse grained materials. These sources have been deployed in both 2D and 3D modes. The latter has utilised a brand new design for the acquisition of high-resolution data volumes (a SOES-GeoAcoustics Ltd design) capable of imaging objects and layers beneath the seabed that are greater than 0.5 m in lateral extent, thicker than 0.2 m and down to a depth of 15 m beneath the seabed. This work has encompassed extant data collected in 2002, during the initial trial period of the SOES 3D-Chirp system, as well as extant core and seismic data made available by Hanson Marine Ltd. The sites targeted for data acquisition as well as those already surveyed have all been of intrinsic archaeological importance and in many cases will compliment other ALSF projects already funded (e.g. Imperial College, Hampshire & Wight Trust for Maritime Archaeology and Hosfield PD 3361).

# 2. RATIONALE

## 2.1. Introduction

Over the last thirty years a variety of marine seismic reflection techniques have been used to investigate a range of submerged archaeological sites (e.g. Frey 1971; Chauhan and Almeida 1988; Rao 1988; Redknap 1990). The aims of these early investigations have focused principally on prospection for wreck sites and their success has been limited by the workers accessibility to appropriate state-of-the-art technology. In addition, the majority of such early systems were incapable of; producing an acoustic pulse with sufficient resolution to be able to identify artefact material; providing data in a format facilitating post-acquisition image enhancement; and operating in the shallow water depths found over many archaeological sites.

Recent work by Quinn et al. (1998a; 1999; 2001) has shown the ability of such Chirp systems for identifying buried wreck material in a range of sedimentary environments. Intuitively, however, it is regarded that coarse grained substrates do not provide an ideal environment for the preservation of archaeological material (e.g. Muckleroy, 1978). Yet as has been seen from the recent concern over sites such as the Stirling Castle (ADU, 2002), excellent preservation can be found at least in environments characterised by very coarse grained sands. This causes a problem in that Chirp sources traditionally lack the penetrating power to interrogate coarse grained substrates, whilst higher energy, lower frequency sources (Boomer and Sparker), as used by the aggregate industry do not possess the resolution capability for detailed target identification. Further, the two-dimensional nature of both systems means that the chances of interrogating wreck sites, at least from a prospection stand-point, is more down to chance than design. Consequently, the identification of buried artefact sites is rarely achieved by current acoustic surveys undertaken for aggregate prospection or licence area Environmental Impact Assessment.

By comparison to the use of acoustics for identifying wreck sites (at least in fine grained sequences), it wasn't until the nineteen-eighties that seismic reflection surveys started to be used for the investigation of submerged landscapes specifically for archaeological reconstruction's (e.g. Stright, 1986; van Andel & Llanos, 1983; Garrison, 1992). The majority of this early work aimed purely to identify primary context sites (the Submarine Human Occupation Sites - 'SHOS' of Flemming, 1998). Considering that primary context sites represent the minority of Palaeolithic sites on land (< 1%?) it was not surprising that Patterson (1981) maintained that "… legislation required commercial companies to undertake *pointless* acoustic surveys which would *never reveal* archaeological data.".

In the late nineties the use of acoustics for investigating submerged landscapes specifically to provide a back-drop to archaeological investigations was re-visited with some degree of success (e.g. Ballard et al., 2000; Cooper et al., 2002b; Dix, 2000; Quinn et al., 2002). However, to the authors knowledge there has still not been any specific projects undertaken to directly identify secondary contexts. Further, as highlighted by Westley & Dix (2004) there has yet to be any archaeological investigation of tertiary contexts (primary and secondary deposits that have been re-worked by submarine processes during marine transgressions and regressions). This dearth in the use of acoustics for the investigation of submerged secondary and tertiary contexts is not only a problem in terms of identifying site specific material of

direct archaeological importance. The lack of such work misses a perfect opportunity to provide fundamental data on the three-dimensional geometry of secondary contexts, and in particular fluvial terrace sequences. This information could be vital for our investigation of terrestrial let alone submerged secondary context sites.

Despite the fact that the study of fluvial river terraces has a long history in both the geomorphological and archaeological communities, as a number of recent articles have identified the sedimentary architecture of individual terrace systems is still poorly understood (Maddy et al., 2001; Lewis et al., 2001; Dollar, 2002). This is because all of the work on the three-dimensional geometry of such deposits has inevitably been restricted to investigation of natural or human induced section cuts and spot core/borehole data. Although integration of such sporadic datasets can provide excellent interpretations (e.g. Maddy et al., 1998; Lewis et al., 2001) they are labour intensive and effectively only provide information on a scale of a few 10's metres and the recognition of regionally extensive unconformities is not possible (Lewis et al., 2001). Rumsby (2000) echoes this concern when he suggests that such detailed interpretations require detailed vertical and lateral dimensions of units, information that is frequently not available.

From a geomorphological perspective therefore, the critical components of such high-resolution studies of terrace systems are a well defined sedimentary architecture and strong geochronological constraints (Maddy et al., 2001). These are required as researchers attempt to asses the dominance of local hydro-geological vs regional climatic controls on fluvial development (Vandenberghe and Maddy, 2001). From an archaeological perspective such detailed knowledge of the stratigraphic location (in both time and space) of lithic artefacts would enable a reduction in the time-depth mixing problems associated with such secondary contexts. For example on a single terrace level artefacts may span a 70,000 year period and represent accumulation from a drainage basin 10's $km^2$ (Hosfield, 2001).

From work by the aggregate industry (Bellamy, 1995), government scientists (BGS: Hamblin et al., 1992) and academics (Velegrakis et al., 1999) the published literature has shown that there are significant terrace deposits on the submerged sections of the north-west European continental shelf. Similarly, the marine extraction industry has collected a large volume of unpublished material that undoubtedly has identified such features elsewhere on the continental shelf (Draper-Ali, 1996).Where the industrial data has been published, the papers have focused on the Late Quaternary evolution of such sites and has not specifically attempted to use this knowledge for archaeological purposes, albeit subsequent authors have (e.g. Bridgeland, 2000; 2001).

The typical surface-tow and sub-tow boomer systems used for the prospection of offshore aggregate deposits (Selby, 1992), and the majority of current academic research into submerged coarse grained structures, are capable of identifying submerged river terraces. In certain instances they are also capable of identifying large scale cut-and-fill sequences (see frontispiece figure). Yet these systems inherently lack the vertical and horizontal resolution to potentially image the all important small-scale (decimetre) internal stratigraphic architecture that maybe required for accurate reconstruction. Similarly, the typical survey line spacing optimum for aggregate prospection ranges between 100 and 500 m (Selby, 1992) and is therefore at a scale close to the opportunistic sections of the terrestrial deposits. If we are to investigate the aggregate licensing areas, and for that matter any coarse grained seabeds for primary (wreck or SHOS), secondary or tertiary contexts we

require systems that are capable of providing high-resolution full coverage imagery of the seabed.

## 2.2. High-frequency Chirp Sources for the penetration of coarse grained aggregate deposits

### 2.2.1. Chirp Sources

Chirp is a high-resolution, wide bandwidth (typically operating in the frequency range of 400 Hz to 24 kHz), frequency-modulated (FM) sub-bottom profiling system that is capable of obtaining cross-sectional profiles of the seabed. The system has a vertical resolution of decimetres and typical penetration depths of 20 to 30 m in fine grained (clays to fine sands) unconsolidated sediments. These systems can operate in shallow water depths (> 2.5m) and can acquire data in an industry standard format (SEG-Y) which enables its straightforward transfer to off-line processing packages. Post-acquisition processing of the data can significantly improve the final data image (see Quinn et al., 1998a) and is an essential pre-requisite to the extraction of quantitative information on the physical properties of sub-surface reflectors/targets.

Chirp systems were first developed at the University of Rhode Island (URI) under a program that started in 1981 (Schock and LeBlanc, 1990). The investigators found the existing systems (e.g. boomer, sparker, pinger) insufficient for quantitative measurements. These systems showed poor pulse repeatability (the variations in the amplitude and phase of the transmitted pulse for different transmissions), low signal to noise ratio (SNR), and poor vertical resolution caused by source ringing and inadequate system bandwidth. The chirp system was designed to overcome these deficiencies. Chirp systems comprise calibrated, linear electronics that are capable of producing a highly repeatable source signature (Schock and LeBlanc, 1990). The transmitted FM signal is corrected for the source and receiver phase and amplitude responses, this ensures that the signal sent into the transducers is the same as the signal that actually enters the water column. Due to the wide bandwidth of the signal optimum penetration as well as resolution can be achieved. The SNR is improved through matched filter processing by correlating the reflection data with the transmitted pulse.

Both horizontal and vertical theoretical resolution limits can be determined for Chirp sources. Quinn (1998) suggests that the theoretical limits of vertical resolution ($R_v$) of a source can be defined by the following equation:

$$2/\Delta f \geq R_v \geq 1/\Delta f$$

Where $\Delta f$ is the bandwidth of the source (i.e. the range of frequencies within a swept pulse). The limits of the horizontal resolution ($R_h$) of Chirp sources can be constrained by:

$$V_p\, twt/2 \tan \theta_d/2 \geq R_h \geq V_p/2 \sqrt{twt/f_d}$$

Where twt is the two-way travel time to a target, $\theta_d$ the beam angle and $f_d$ is the dominant frequency of the source. It should be noted that attenuation of the chirp pulse by the sediments it passes through would have a detrimental affect on both the vertical and horizontal resolution of the system. This is because attenuation results in a downshifting of the dominant frequency ($f_d$) and an overall decrease in the

bandwidth (Δf). The extent of this affect will depend upon the grain size of the sediment with attenuation effects being higher in gravel and sand-dominated environments than clay- and silt-rich environments. It is therefore best to calculate resolution using information from the actual data recorded rather than based on the outgoing source properties or using other quantitative measures.

As described above Chirp systems have been used to image both wreck sites and submerged landscapes (Quinn et al., 1998a and b, 1999; Dix et al., 1998, Quinn et al., 2001). The majority of these surveys have used a GeoAcoustics GeoChirp system. This emits a linearly swept pulse, 32 ms in length, which sweeps from 1.5 to 7.5 kHz and can be transmitted at an optimum rate of 4 pulses per second. The pulse is transmitted with a RMS energy of 6.4 Joules. This pulse provides a theoretical vertical resolution of 0.15 – 0.2 m and a theoretical horizontal resolution of 1.2 m in an average water depth of c. 10 m.

It is important to note that one of the key advances of Chirp technology is that the repeatability of the source signature facilitates the use of these systems for the extraction of physical properties of reflectors from Chirp data. Ironically, the majority of acoustic sources currently marketed as seabed classification systems demonstrably fail to use a repeatable source signature (or fail to demonstrate that they do!). Effectively, if you don't know what is going into the ground then you can not use the reflected signals to tell you about the properties of the seabed.

Two parameters can be extracted from Chirp data to indicate the material nature of the seabed. Bull et al. (1998) have demonstrated how the calculation of reflection coefficients can identify material type, using a wreck site (wood vs fine sand) as a successful case study. Reflection coefficients relate to the ratio of the amount of energy is reflected to the amount of energy transmitted at any acoustic boundary. In turn this ratio is controlled by the density and velocity characteristics of the seabed. Ultimately, these values can be used in an attempt to distinguish between archaeological materials (specifically wood) and sediments (Arnott et al., 2002; Dix et al., 2001). Secondly, attenuation estimates extracted from the Chirp data can also be used to provide quantitative information on seabed properties (see Robb et al., 2002) in particular grain size. However, these techniques are still the subject of significant current research and as yet there has been no attempt to look at the attenuation characteristics of archaeological materials.

### 2.2.2. Boomer Sources

Boomers are electrodynamic devices that work by a plate giving a high intensity, short duration pressure pulse. When electrical energy stored in a capacitor is discharged through a flat coil positioned immediately behind a metal piston, induced electrical current, produces electromagnetic repulsive forces to drive the piston and coil apart. The piston movement produces a pressure pulse with typical frequencies of between 100 Hz and 6 kHz, but with a dominant frequency typically in the range of 1.5-3 kHz and an output RMS energy of c. 60 J per pulse. This order of magnitude higher energy output and lower dominant frequency means Boomer systems traditionally have greater penetration depths than chirp sources (40-50 m as opposed to 20-30 m), but rather lower theoretical vertical (0.3 – 0.5 m) and horizontal (4 m in an average water depth of c. 10m) resolutions.

The poorly constrained nature of the pulse by comparison to the Chirp data prevents the possibility for match filter processing and source signature deconvolution.

Consequently boomer data tends to have a much lower SNR (the "ringing" effect typical of boomer traces) making interpretation of finer stratigraphic features difficult.

While boomer systems certainly give interpretable images of the sub-surface, boomer data has traditionally proved problematic for later processing. There are a number of reasons for this including: source signature variations (although this is becoming less of a problem with very recent systems), the relative lack of focussing of boomer systems (often hemispherical spreading), and the way in which the boomer signal becomes attenuated in sediments. Recent developments (e.g. Pinson et al, 2006) are however beginning to show good progress in the extraction of attenuation parameters from boomer data.

### 2.2.3. Chirp II

In November 2001, a team from SOES and GeoAcoustics Ltd, trialled both a new set of Chirp transducers and a series of newly designed Chirp sweeps aimed to optimise penetration and resolution. These new transducers could operate at a wider bandwidth, 1.5 kHz to 13 kHz, than those typically used over the last decade, and output a significantly higher energy pulse, 64 Joules (RMS energy per pulse). Further a variety of new sweeps functions were used including linear, quadratic and logarithmic instantaneous frequency functions as well as a number of different envelope functions. The former dictates the amount of time the pulse stays at a single frequency (i.e. it effects the dominant output frequency) whilst the latter dictates how much energy is allocated to each frequency step.

An experiment was conducted by repeatedly running a single line selecting a different sweep on each occasion (Gutowski et al., 2002). This enabled a quantitative sweep to sweep comparison both in terms of resolution and penetration. This work suggested that the optimum sweep has a box envelope function that is tapered with a sine square function at the start and end of the sweep spanning an eighth of the total time duration. Together with its linear instantaneous frequency function this results in a symmetric spectrum with a relatively high fundamental frequency. This sweep design seeks to maximise the power output over the entire time/frequency range while avoiding strong correlation noise typical for a box function sweep. This pulse showed very good resolution capabilities while at the same time having similar attenuation values to the originally used sweep. These new sources therefore provide a power output comparable to Boomer systems (64 Joules RMS energy per pulse versus 60 Joules RMS energy per pulse), whilst maintaining a significantly higher bandwidth, source signature repeatability, and consequently, improved resolution and penetration. As yet though there has been no direct assessment of this and other signatures over coarse grained seabeds, or direct line to line comparison with Boomer systems, to see if the Chirp II system can provide a creditable competitor to the established Boomer source.

## 2.3 3D-Chirp system for the investigation of coarse grained aggregate deposits

Irrespective of the advances in terms of source signature described in Section 2.2.3., there are still two major problems to be overcome for the effective detection, mapping and characterisation of archaeological objects. Firstly as the systems described so far are 2D profilers the horizontal coverage will be dictated by the line spacing employed

during a survey. Even for well-controlled (DGPS), boat based, hydrographic surveys, minimum effective line spacing can be considered of the order of 5m, hence objects smaller than this spacing are missed altogether, or at the very least are mis-located both in position and depth. Recent developments with the deployment of a variety of single and swept frequency sources on both ROV's and AUV's have gone someway to reduce the line spacing to produce pseudo-3D imagery, however both systems still have severe operational limitations. ROV's can be used to produce line spacing of less than a metre (navigational accuracy being of the order of cm's) but depending on time and cost constraints they can realistically only operate over zones approximately 100 m square (e.g. Mindell & Bingham, 2001). AUV's by contrast offer excellent potential for surveying down to 1m line spacing and have the ability to cover larger survey areas a few hundred metres square, but at present (Gregory, 2000) these systems are not cost effective and have limitations in very shallow waters with irregular bottom topography. Further, despite the potential of both of these platforms they are still producing 2D profiles and consequently objects can still be missed.

Secondly, all of the current commercially available profiling systems produce non-migrated data so reflections from targets can be incorrectly located in both a horizontal and vertical plane. Recent work at Southampton has demonstrated the potential for migration of high-frequency 2D Chirp data, however, 2D data never provides information on cross-dip variation and so in the migration of such data the migrated reflection points are constrained to lie within the plane of the section. Therefore in the presence of rapidly varying 3D topography (i.e. discrete targets as found on wreck sites) such two-dimensional migration is inevitably an imperfect process.

By contrast to the developments in high resolution sonars, lower frequency (10 – 200 Hz) acoustic acquisition systems used for oil exploration have routinely been collecting 3-dimensional datasets for the last two decades. 3D in this context means that rather than a series of 2D lines being collected and interpolation made between them to provide a 3-dimensional image of the subsurface an actual data volume is acquired and so no interpolation is necessary. This is achieved by the position of both the source and receiver being known for each source location, and hence the position of reflected waves can be accurately focussed by migration processing at their "bounce point". However, these systems are designed to image the general geometries of oil reservoirs (at a scale of 100's of metres) at several kilometres depth, and do not have the required resolution for near-surface studies. Yet many of the processing and interpretation strategies developed for the oil industry are generally applicable to high frequency devices.

The ability to collect a high frequency 3D volume would enable the acquisition of a full sub-surface volume for the survey area resulting in the minimum dimensions of the objects to be detected being dependent on the acoustic characteristics of the source and receiver array rather than the survey design. Further accurate location of both source and receiver groups will facilitate full three-dimensional migration in which reflection points can be migrated in any azimuthal direction. The ability to conduct full 3D migration has three primary effects: reflections from dipping reflectors will be correctly repositioned; energy scattered from small features will be focused at the scatterer location; the output volume will be evenly sampled in all three dimensions. The first two of these also act to improve the lateral resolution of the data from the scale of a Fresnel zone (typically 2-3m for these targets) to theoretically close to a

wavelength (10 – 20 cm). The limit on the lateral resolution of the data will be ultimately controlled by spatial aliasing criteria based on the horizontal apparent wavelength of the arrivals.

The successful design and development criteria required for a high-resolution 3D-sonar system for the detection, location and identification of archaeological materials and/or their sedimentary contexts, in decreasing order of importance are as follows:

- Accurate (centimetric) location of source and receivers for within line and between line data integration and hence full geo-rectification of 3D volume
- Ability to control area of insonification and hence coverage rate
- Optimisation of vertical and horizontal resolution parameters
- High signal-to-noise-ratio to improve image quality and acoustic characterisation of acoustic targets.
- Knowledge of the acoustic properties of target objects.

As part of a major EPSRC-MOD Joint Grant Scheme (2001-2004) a 3D Chirp system had been designed and built by a consortium led by the School of Ocean and Earth Science and including the Institute of Sound and Vibration Research, the School of Mechanical Engineering (both University of Southampton) and GeoAcoustics Ltd. This EH funded project will be able to provide much needed companion funding to extend and finalize the configuration of the 3D Chirp system as well as to enable the acquisition of a true 3D dataset from an archaeological site in a coarse grained stratigraphy.

## 2.4 Summary

Over the last twenty years the growth and development of the offshore extraction and construction industries have increasingly threatened the submerged archaeological resource. Over the same period our knowledge of the archaeological potential of submerged environments (in terms of both historic and pre-historic material) has been recognised by the Academic community, the Heritage organisations and the seabed developers at both national and international levels.

Similarly, over the last fifteen years the archaeological community has moved away from traditional excavation methods toward a strategy of *in situ* preservation of our cultural resource. This trend has been politically galvanised in Article 6 of the ICOMOS Charter for the Protection and Management of the Archaeological Heritage (ICOMOS, 1990), which states that "The overall objective of archaeological heritage management should be the preservation of monuments and sites *in situ"*. Further, this directive also emphasises that the choice of conservation strategies to be deployed should be achieved through non-destructive, non-intrusive survey rather than excavation.

It is therefore suggested that high-resolution acoustics can play a vital role in both the exploration of the seabed for archaeological materials and landscapes and the non-intrusive survey of sites once discovered. In the past archaeologists have had to make-do with systems that were intrinsically inappropriate for the task in hand. Invariably this was due to the lack of finances available to the archaeological community for *a*

*priori* research in to such developments. This new climate of recognition of the archaeological potential of submerged environments and the recent availability of research funds such as the ALSF must therefore be capitalised on by the archaeological community for the development of acoustic systems specifically designed to identify and map archaeological materials.

The coarse grained deposits typical of aggregate licensing areas represents one of the toughest challenges for archaeological acoustics. Not only do these areas contain a wide range of archaeological materials, from historic wreck fragments to Palaeolithic and Mesolithic material deposited within secondary and tertiary contexts, but they also represent a very difficult substrate to penetrate whilst maintaining an appropriate vertical and horizontal resolution.

This project design aims to test and optimise new acoustic techniques expressly designed to identify objects and structures within these acoustically complex environments. If successful, these techniques should enable the archaeologist to not only further our understanding of submerged archaeological sites but also glean invaluable insights to terrestrial contexts that have to date been difficult to interrogate.

# 3. AIMS AND OBJECTIVES

The Rationale described in Section 2 sets out our current understanding of high-resolution acoustic sources for the interrogation of sub-seabed archaeology. It highlights that although sonar systems have been deployed for many decades for archaeological investigations, current systems are incapable of resolving small objects and structures in the coarse grained stratigraphies (sands and gravels) typical of aggregate licensing areas. Sections 2.2.3 and 2.3 suggest that new Chirp sources deployed in 2D and 3D modes offer the potential to interrogate these "difficult" seabeds with sufficient resolution to identify artefactual material as well as the detailed geometry of the secondary and tertiary contexts in which it is deposited.

## 3.1. Aims

The primary aims of this project are four-fold:

1. To identify an optimum Chirp pulse for the penetration of coarse grained (sand and gravel) deposits whilst maintaining typical decimetre resolution and high SNR imagery.
2. To demonstrate the capabilities of this Chirp II source for the archaeological investigation of coarse grained aggregate deposits.
3. To demonstrate the capabilities of the SOES 3D-Chirp system for the mapping and characterisation of an archaeological site within an aggregate licensing area.
4. To disseminate the results of the research project to the academic community, the aggregates industry and the general public.

Aims one to three will be achieved through the surveying of a series of archaeologically significant localities which have been chosen specifically to satisfy a series of secondary aims pertinent to the agenda of the ALSF:

5. To identify if the "Solent River System" represented a single or multiple drainage systems, and the implications of drainage morphology for our understanding of the Upper Palaeolithic and Mesolithic archaeology of the area.
6. To establish the internal stratigraphy of a single terrace deposit, in order to further constrain the time-depth history of these secondary contexts.
7. To map out a buried wreck site in a coarse grained environment.

## 3.2. Objectives

The overall project aims will be realised through a series of objectives in three phases:

### 3.2.1. Phase 1: *Boomer vs Chirp II Comparison – Solent Area Survey*

**Objective 1 –** The processing of c. 350 km's of Boomer and Chirp II data already acquired from two 5 km x 3 km blocks one each at the head of the East and West Solent.

**Objective 2 –** Quantitative analysis of the penetration and resolution capabilities of a Boomer and Chirp II system from a selection of co-incident lines taken from each block.

**Objective 3 –** If required iterative re-assessment of chosen Chirp II pulse in order to optimise resolution and penetration in coarse stratigraphies.

**Objective 4 –** Pesudo-3D palaeogeographic interpretation of Chirp II and Boomer datasets from Solent system.

**Objective 5 –** Integration of interpretation from Objective 4 with extant archaeological and palaeogeographic work on the Solent River system and appropriate ALSF funded projects.

### 3.2.2. Phase 2: *Chirp II core calibration – the internal stratigraphy of secondary contexts*

**Objective 6** – Study of the survey archives (both seismic traces and core logs) of Hanson Marine Ltd. for the identification of a calibrated terrace deposit for 2D investigation using a Chirp II source.

**Objective 7** – Close line spacing (c. 10 - 50 m) survey of terrace deposit using Chirp II source. Lines will be run over specific core localities to ensure lithological calibration is possible.

**Objective 8 –** Processing of Chirp II dataset from core calibration survey.

**Objective 9 –** Core logging (density and velocity profiles and grain size data) using GeoTek Core Logger of Hanson Marine Ltd. core.

**Objective 10 –** Production of synthetic seismogram for direct quantitative comparison with Chirp II data over core site and the calculation of actual resolution parameters.

**Objective 11 –** Pseudo-3D interpretation of internal stratigraphy of terrace deposit and comparison with published terrestrial examples.

**Objective 12 –** Integration of results of pseudo-3D geometry with work on Secondary Contexts of Hosfield (PD 3361).

### 3.2.3. Phase 3: *3D-Chirp for the archaeological mapping in aggregate deposits*

**Objective 13 –** Choice of either a wreck site or terrace deposit mapping for 3D volume investigation – to be made in discussion with Project Officer (I. Oxley) and Wessex Archaeology (as part of PD: Wrecks on the seabed: assessment evaluation and recording).

**Objective 14** – Acquisition of 3D data volume from site identified in Objective 13 and using optimum source signature as defined in Objective 2.

**Objective 15 –** Processing of 3D data volume acquired in Objective 14.

**Objective 16** – Archaeological interpretation of 3D data volume.

**Objective 17** – Quantitative and qualitative assessment of 3D-Chirp for investigation of archaeological sites in aggregate licence areas.

### 3.2.4. *Dissemination*

**Objective 18** - Provision of the project report and submission of synthesis papers to national and international conferences and internationally refereed journals.

# 4. PHASE 1: Boomer vs Chirp II Comparison – Solent Area Survey

## 4.1. Introduction

Phase 2 has been successfully completed but with the focus on Objectives 1, 4 and 5. As will be described in Section 5 below the full characterization of the relative penetrative and resolution capabilities has been undertaken as part of an extended Phase 2. However, over the last twelve months new seismic processing approaches developed at the National Oceanography Centre has enabled the integration of an additional 135 line kilometres of Boomer and Chirp data. This data has been fully interpreted and has been integrated in to the final palaeogeographic reconstruction for this region by a Masters of Research student, Charles Howarth at no additional cost to the project. The following text represents the penultimate draft of a paper for submission to the Journal of the Geological Society of London. The final draft, which is being dealt with at present, is having this additional data added to it.

## 4.2. Late Quaternary palaeogeography and seismic stratigraphy of the central Solent river system (Bastos, Dix, Howarth, Bull & Henstock).

### 4.2.1. *Introduction*

During Pleistocene lowstand periods, the English Channel was characterised by a large alluvial plain dominated by a major river system called the Channel River (Fleuve Manche) (Gibbard, 1988; Lericolais et al., 2003). During these periods, a number of rivers, such as Seine, Somme, Solent, Arun, and others, formed a network of tributaries of the main Channel River. These incised palaeovalleys are, since the last post-glacial marine transgression, offshore extensions of the coastal rivers and can be observed as submarine topographic features or infilled valleys over the English Channel (Hamblin et al., 1992). As part of this palaeosystem, the Solent River was one of the major northern tributaries of the Channel River. Terrestrial and offshore evidences suggest that a major Solent River system was established during the Pleistocene, integrating all the rivers from the southern margin of the Hampshire Basin.

The palaeogeographic reconstruction of the Solent River has been object of numerous investigations (Fox, 1862; Reid, 1905; West, 1980, Allen and Gibbard, 1993; Bridgland, 1996; Velegrakis et al., 1999, and Tomalin, 2000). This river system developed throughout the Pleistocene and significant modifications to its valley have taken place during every interglacial highstand period. The widely accepted reconstruction of the Solent system during the Pleistocene shows a major river flowing eastward from the River Frome, in Dorset, towards the East Solent, where it would meet with a major southeast flowing river connected to the south, with the English Channel palaeovalley (Fox, 1862; Reid, 1905; and West, 1980) (Fig. 1).

Evidences of the evolution of the Solent River during the Pleistocene have been described, especially, in terms of the occurrence of onshore gravel terrace deposits. Allen and Gibbard (1994) have recognised different generations of terrace systems

from Dorchester (Dorset) across Poole and Bournemouth to the southern area of New Forest (West Solent) and in Southampton area. The reconstruction of these terraces shows that throughout the Pleistocene, the Solent River migrated towards the southeast.

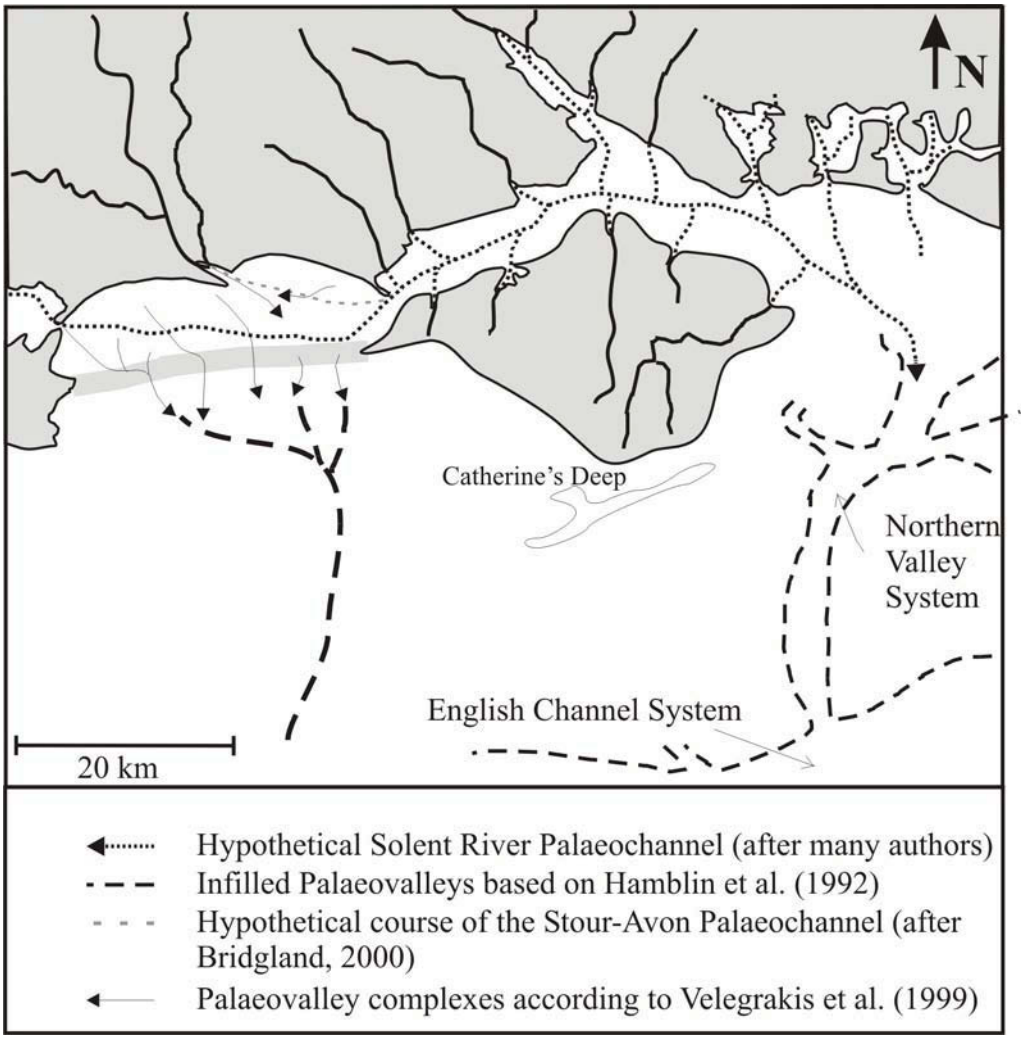


Figure 1: Hypothetical course of the Solent River system after numerous authors (including Hamblin et al., 1992; Velegrakis et al., 1999; Bridgeland, 2000).

The occurrence of buried palaeochannels offshore has been described by different investigators (Dyer, 1975; Hamblin et al., 1992, Velegrakis et al., 1999). Dyer (1975), analysing seismic sections over the Solent and Christchurch Bay, showed that the Solent River system was incised to a base level of at least -46 m OD in the East Solent. Over the West Solent, no buried palaeochannels were identified; however, the author suggested a possible continuation of the Solent River valley through the West Solent into Christchurch Bay, where a single buried channel was detected at -12 m OD.

A significant contribution for the understanding of the system evolution was provided by the seismic investigation undertaken by Velegrakis et al. (1999) in Poole and Christchurch bays. These authors have identified seven Palaeovalley complexes

over the area. These channel complexes were formed by southwardly river channels, indicating that the Solent River system was disrupted irreversibly by southerly river flows before the Flandrian Transgression. Another relevant aspect of this investigation is that no evidence of a W-E buried Solent River channel was found offshore, over Poole and Christchurch bays.

Based upon this background, it is safe to assume that during Late Devensian time there was no major W-E Solent River, at least as an extension of the river Frome, as described for Early and Middle Pleistocene times. However, the existence of a Solent River system flowing across the West Solent can not be ruled out. A possible interpretation would be that during Late Devensian, the Solent River system would be an extension of the Stour-Avon system (Hooper and Kelland, 1974; Bridgland, 2000), but this hypothesis has been rejected by Wright (1982), Dixon (1986) and Velegrakis et al. (1999). The latter authors identified a palaeovalley (Palaeovalley VII) in the notheastern part of Christchurch Bay, which is possibly the same buried channel that Dyer (1975) had identified previously. The Palaeovalley VII of Velegrakis et al. (1999) shows a gradient towards the WNW, which is in the opposite direction to that expected if the channel was a tributary of the Solent River. Thus, to consider the Solent River as an extension of the Stour-Avon system, its drainage would have flowed through the modern Hurst Narrows area. Unfortunately, after the drowning and formation of the West Solent, the Hurst Narrows has been the subject of intensive seabed erosion and, therefore, any pre-Flandrian sedimentary record has been destroyed.

As a consequence, there is still no definitive answer to the reconstruction of the Solent palaeodrainage. Hence, considering the absence of a major west-east river channel in Poole and Christchurch bays, one can consider that the West Solent represented a segmented drainage with a dominantly southerly flow. This was initially proposed by Reid (1905), who hypothesized the occurrence of a West Solent Isthmus separating two major river systems flowing southward: West Solent and Southampton Water-East Solent. Another possible explanation for the absence of a major single river channel is poly-cyclic erosion of the bedrock during lowstand and highstand phases of the Pleistocene.

The objective of this contribution is to investigate the offshore palaeogeography and the seismic stratigraphy sequences of the central part of the Solent River System. The present investigation addresses the uncertainties regarding the central Solent area by exploring the hypothesis of connectivity between West and East Solent palaeodrainage systems and by examining the difference between the associated seismic sequences.

### 4.2.2. *Methods*

#### 4.2.2.1. *Data Acquisition*

Two seismic surveys were undertaken over the study area. Initially, two 5 km x 3 km blocks in West and East Solent were surveyed using Boomer (300 Joules Geoacustics) and Chirp II sources, during July and August 2002 (Fig. 2). A total of 200 km of Boomer data and 150 km of Chirp II data were acquired. Subsequently, in order to merge the two blocks surveyed initially, a seismic survey, using a Boomer source, was conducted around the tip of the Isle of Wight, off Cowes. This survey area will be referred here as the central area. A total of 50 km of seismic lines were

acquired during this survey. During both surveys, digital seismic data were acquired using the Geoacoustics Sonar Enhance System. Navigation was obtained using a Trimble DGPS system, with an average accuracy of 1 m.


Figure 2. Location of the seismic lines collected over the Central Solent. Black lines represent Boomer sections and grey lines are Chirp sections. The location of the seismic sections presented here as examples are also shown.

#### **4.2.2.2.** *Data Processing and Interpretation*

Post-processing of Boomer and Chirp II data was undertaken using a standard industry seismic processing package, Promax. The first phase in the processing sequence consisted of integrating navigational data to (SEG-Y) trace headers and reducing the water level to the Lowest Astronomical Tide (Chart Datum). The tidal level correction was applied using data from a tidal gauge located at Calshot Spit (for location, see Fig. 2). Both data sets (boomer and chirp II) were subjected to this phase. Subsequently, the data sets were processed applying different sequences of conventional algorithms, in order to produce the best possible result in terms of the quality of the final image.

The software Geoframe (Geoquest-Schlumberger) was used to interpret the seismic sections and to produce bedrock-depth and isopach contour maps. This software allows the user to digitise an interpreted seismic reflector, creating a surface map of a

specific horizon. The depth of the bedrock was then calculated using an average seismic velocity of 1500 m/s for sea water and 1600 m/s for the sedimentary deposit. The calculated depth was reduced to the UK Ordnance Survey Datum (OD), for subsequent comparison. Interpretation of the seismic sections was based upon internal seismic reflection patterns and the external shape of seismic facies, as described by Mitchum et al. (1977). The concepts of seismic stratigraphic sequences, as described by Posamentier et al. (1988) were also used.

#### 4.2.3. *Seismic Reflectors*

Three orders of seismic reflectors were distinguished within the seismic sections: a major unconformity or bedrock surface; first-order reflectors associated with seismic facies boundaries; and second-order reflectors, which represent the seismic reflections within a seismic facies. The major unconformity reflector represents a bedrock erosive surface (BS) over Tertiary rocks. This erosive surface is usually characterised by a high amplitude reflector that defines different morphological features within the study areas, including the palaeovalleys of the Late Quaternary Solent and Beaulieu rivers. A first-order reflector is defined here as a bounding unconformity and/or a seismic facies boundary. First-order reflectors were recognised mainly over the East Solent area, usually associated with the channel infilling and terrace sequences. In the West Solent area, first-order reflectors were only recognized within the channel infilling sequences associated with the Beaulieu palaeovalley. The reflectors within a seismic facies are defined here as second-order reflectors. The configuration of these reflectors characterizes the seismic facies. Clinoforms, horizontal/sub-horizontal and chaotic reflector configurations were recognised.

#### 4.2.4. *Seismostratigraphy and Palaeogeography*

The Late Quaternary evolution of the central Solent River System is presented here based upon: (a) seismostratigraphic interpretation; and (b) palaeogeographic reconstruction of the Solent River system. Due to the distinct geological and stratigraphic characteristics of the surveyed areas, the results are presented separately for each area.

##### 4.2.4.1. *East Solent*

The East Solent area is characterised by a complex morphology of the bedrock erosive surface. The incised valleys are defined by significant erosional relief (up to 12 m) of the bedrock. Two morphologically distinct palaeovalley systems could be recognised: Palaeovalley I and Palaeovalley II (Fig. 3).

Palaeovalley system I is located to the north of the Ryde Middle Bank. It is characterised by a complex system of two main palaeochannels with an orientation of approximately WSW-ENE. These channels have an average width of 400 m and a vertical relief of up to 12 m (Fig. 4). Within the area under investigation, the mean gradient of the thalweg was calculated as 100 cm $km^{-1}$, with the altitude reaching up to -22 m OD in the western margin and –25 m OD along the eastern margin of the area. This suggests that the river used to flow eastwards. Palaeovalley system II is located just southward from the Ryde Middle Bank and comprises a single palaeochannel oriented WNW-ESE (Fig. 4). The palaeovalley is characterised by a very irregular channel floor with a vertical relief of up to 8 m and a width of 500-1000

m. The lowest altitude of the thalweg is – 32 m OD, which sets this palaeochannel in a lower altitude, if compared to the Palaeovalley system I. The thalweg gradient (approximately 120 cm $km^{-1}$) is eastward. Considering the entire extension of the East Solent and including the seismic data described by Dyer (1975), the overall thalweg gradient for the East Solent is 75 cm $km^{-1}$.

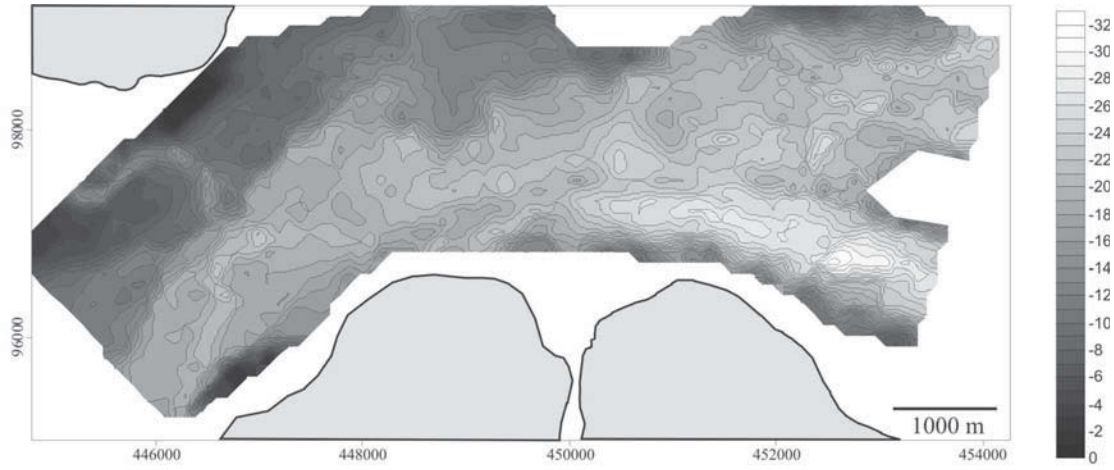


Figure 3. Bedrock contour map based on the interpretation of the Boomer sections. Contours are metres and related to OD.

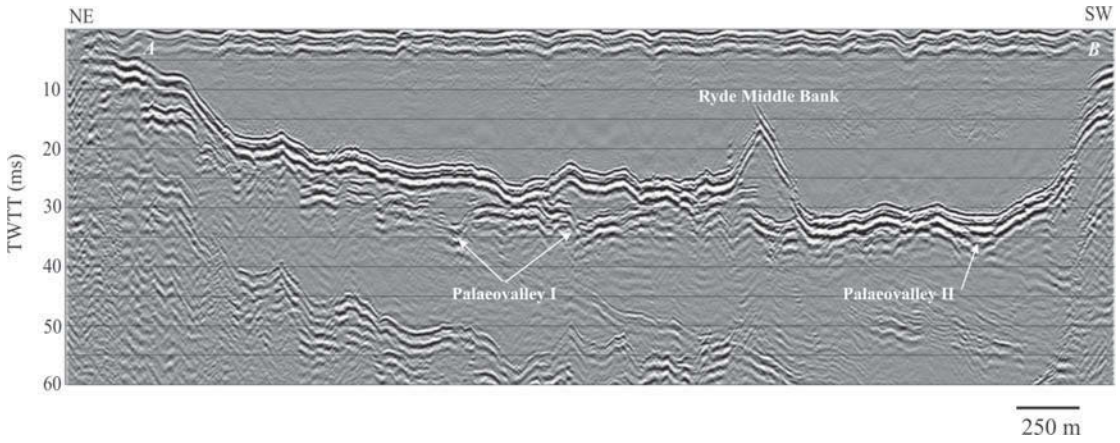


Figure 4. Boomer cross section over the East Solent, showing the two palaeovalley systems and the Ryde Middle Bank (For location, see Figure 2).

Overall, the thickness of the unconsolidated sediments varies significantly over the area due to the irregular characteristic of the BS. The thickest sedimentary sequence was observed at the northeastern extreme of the area (see Fig. 5). The sequence is approximately 13 m thick (assuming an average sound speed of 1600 m/s in unconsolidated sediments) and is associated with a palaeochannel of the Palaeovalley system I. The western end of the Ryde Middle Bank also presents an approximate 12 m thick deposit over the BS.

In terms of the seismostratigraphic evolution of the East Solent area, the sedimentary sequences may be described as a modern inner shelf/estuarine sequence overlying palaeochannel infill deposits. Locally, fluvial terrace sequences are also observed, but their geographical distribution is limited within the survey area.

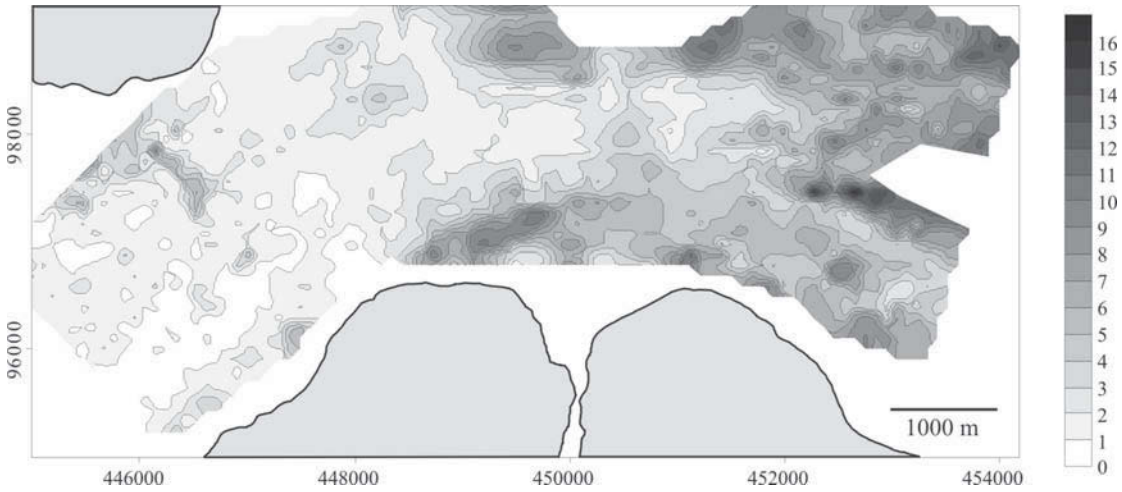


Figure 5. Isopach map based upon the interpretation of the Boomer sections and using an average seismic velocity of 1600 m/s. Contours are in metres.

Based upon the seismic characteristic of the first-order reflector (or bounding surface) and the configuration of second-order reflectors, different seismic units were recognized within the sedimentary deposits (Fig. 6).

Unit Va lies directly upon the palaeochannel bedrock surface, defining the base of the valley infill sequence. This unit has been mainly observed in the Palaeovalley system I, where its thickness does not exceed 2m. Its internal reflection pattern is characterised by medium to high amplitude reflectors, showing a rather discontinuous and sometimes chaotic pattern. This seismic facies unit has been interpreted as a possible basal coarse-grained (probably gravel) deposit associated with a fluvial regime (Fig. 6).

Another unit ($Va_2$) representing the lowstand fluvial regime has also been recognised in both palaeovalley systems. Unit $Va_2$ lies directly on the bedrock surface and its thickness can reach up to 7 m in the Palaeovalley system II (Fig. 7). Although this unit is also observed in system I, its occurrence is limited, and its thickness does not exceed 2 m. This seismic facies is characterised by steeply dipping point-source reflectors, which is an indicative of gravelly-rich sediments. $Va_2$ can be interpreted as a coarse-grained lateral channel migration deposit associated with a fluvial regime.

The main seismic facies within the valley infill sequence is represented by unit Vb (Fig. 6). Unit Vb is observed in both Palaeovalley systems, where it usually onlap the bedrock surface or unit Va, where it is present. Locally, it may also downlap the bedrock surface. Its thickness can reach up to 7 m in the northeast end of Palaeovalley I. This seismic facies is characterised by low to medium amplitude, parallel to sub-parallel reflectors. The top of unit Vb is defined by an erosive surface which may represent the upper boundary of the valley infill sequence. In the seismic

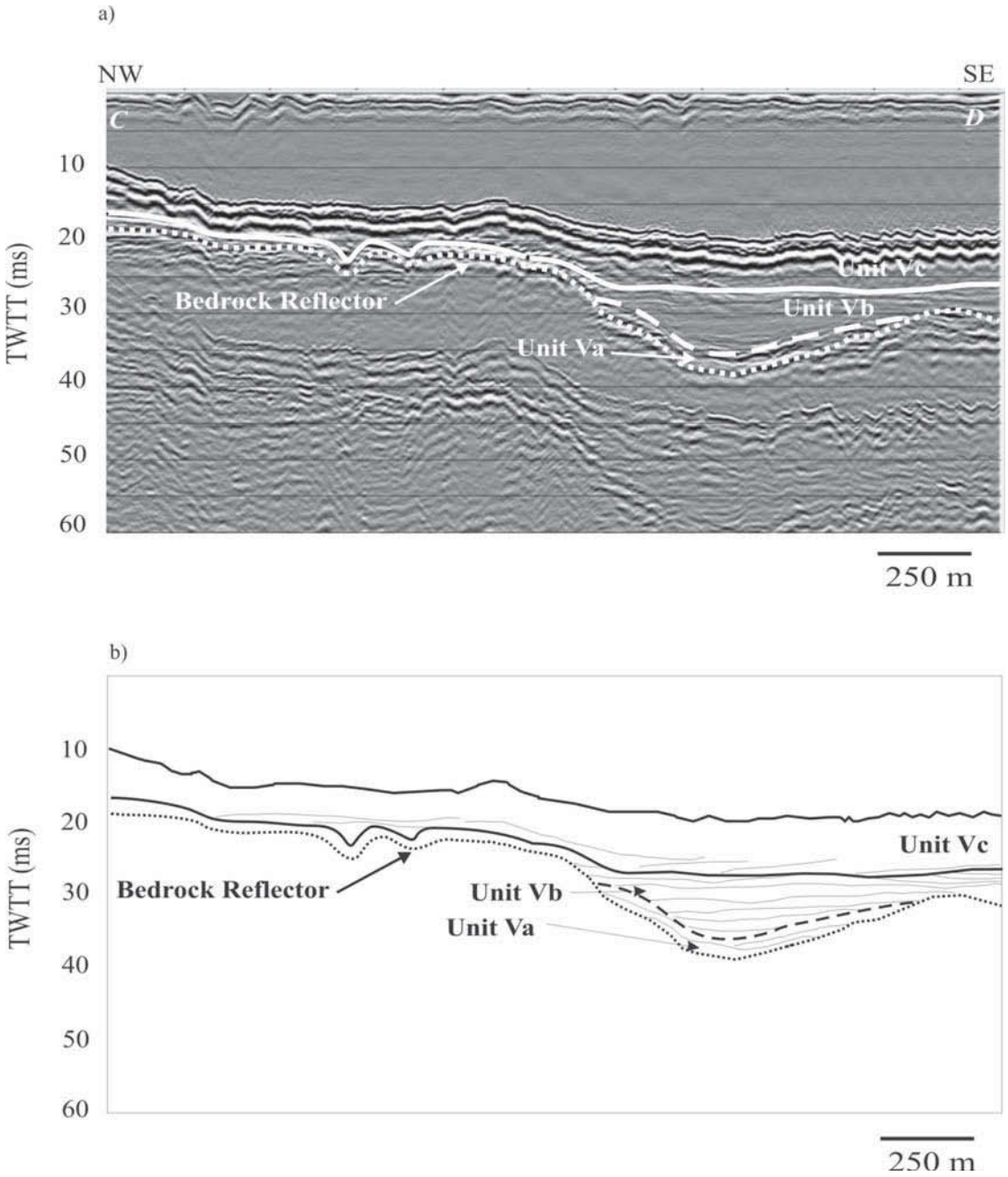


Figure 6. Boomer section showing the (a) different seismic units (Va, Vb, and Vc) observed over the East Solent, and (b) the interpretation of the seismic line (For location, see Figure 2).

sections, this erosive surface can be defined by different reflection terminations, such as: onlap, toplap and erosional truncations. This discontinuity may be indicative of a (shallow) marine erosive surface. On top of this surface, lies the seismic unit Vc. This unit can be characterised by low to high amplitude, discontinuous dipping reflectors (Fig. 6). This seismic facies is being interpreted as a modern inner shelf (or estuarine) deposit that have been formed under prevailing (or very similar) hydrodynamic conditions. As mentioned before, towards the western margin of the area, where no palaeochannel is observed, unit Vc can possibly rest directly on top of the bedrock erosive surface. A sub-unit, $Vc_2$, has been recognised in relation to the internal structure of the Ryde Middle Bank (Fig. 8). The Bank appears to be on top of a

bedrock erosive surface and along its western end, a possible infilled palaeochannel was observed. The bank seismic facies is characterised by gently dipping parallel reflectors, clearly observed in the Chirp II sections. In shallower areas over the Bank, it was not possible to observe neither the internal structure nor the bedrock surface, because of very shallow multiple reflectors.

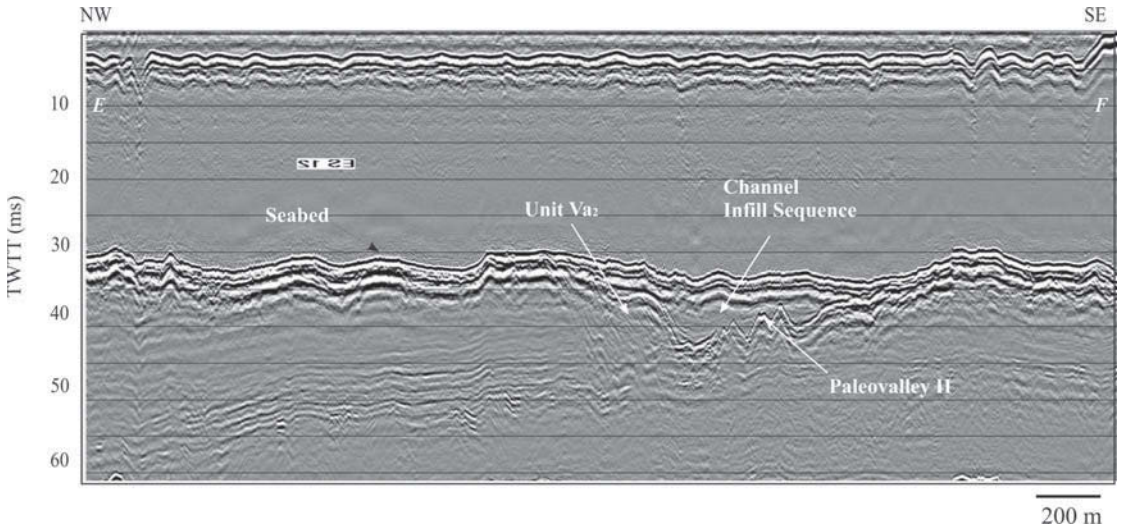


Figure 7. Boomer section showing the seismic unit $Va_2$.

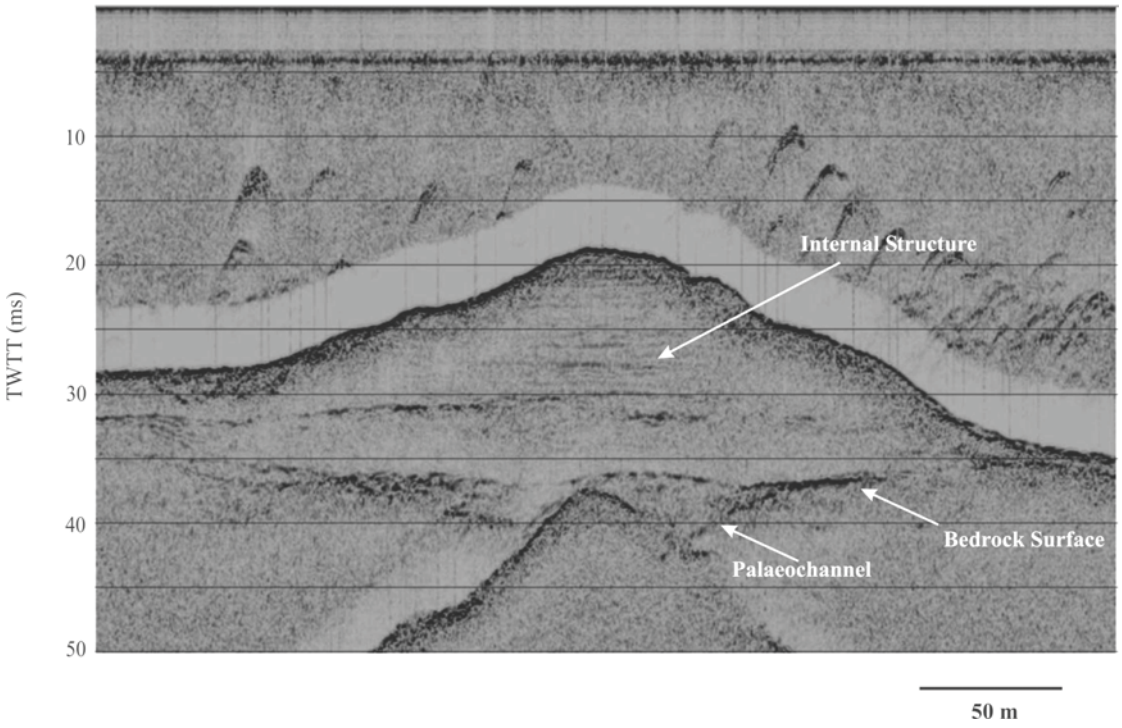


Figure 8. Chirp section across the western end of the Ryde Middle Bank. The section shows the internal structure of the bank and the presence of a possible palaeochannel running beneath the modern bank (For location, see Figure 2).

Seismic unit Ta was interpreted as terrace deposit. This unit is observed associated with both Palaeovalley systems (Fig. 9). However, because it usually occurs in associated very shallow water areas, its extension could not be totally traced. It is characterised by low to medium amplitude, parallel to sub-parallel, flat and dipping reflectors. In Palaeovalley I, the altitude of the terrace unit Ta varies, east to west, from approximately -15 to -13 m OD, showing an eastward gradient of 110 cm $km^{-1}$. In Palaeovalley II, its altitude ranges from -15 to -18 m OD, showing an eastward gradient of 125 cm $km^{-1}$. This unit can be interpreted as a possible low-energy deposit associated with a river floodplain.

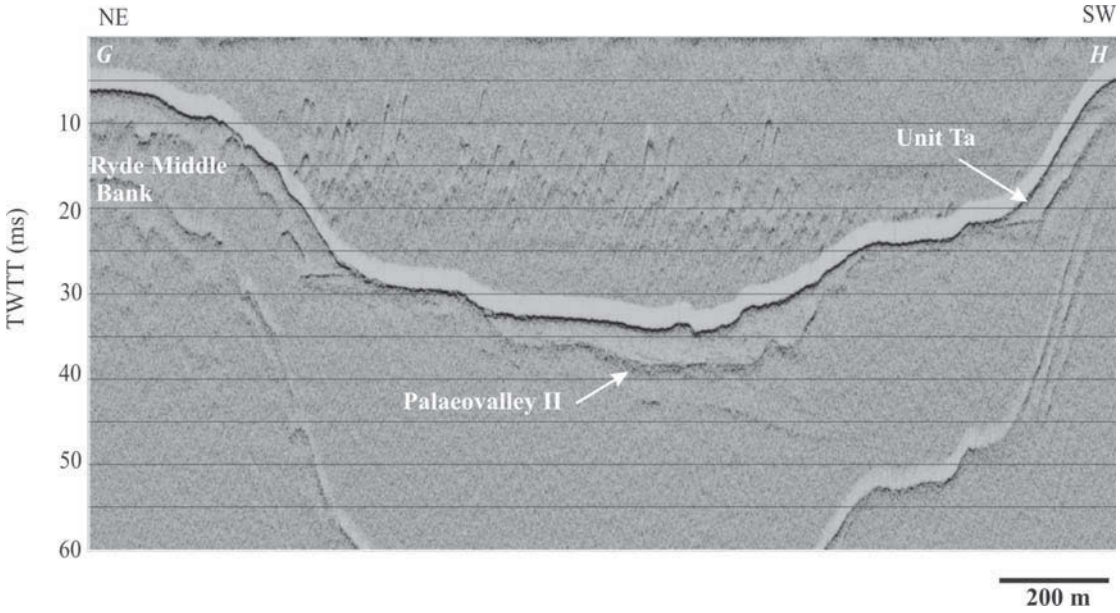


Figure 9. Chirp section across the Palaeovalley II showing the infill sequences of the palaeochannel and the terrace unit Ta (For location, see Figure 2).

The sedimentary sequences observed over the area can be identified as a Type-1 incised-valley depositional sequence as described by Posamentier and Vail (1988). This depositional sequence is characterised by a lowstand, transgressive and highstand system tracts. These are represented, respectively, by units Va, Vb and $Vc/Vc_2$. Unit Ta represents a geomorphological river terrace associated to the lowstand period when Va was deposited.

#### **4.2.4.2.** *West Solent*

The West Solent area is characterised by a thin sediment veneer overlying the bedrock erosive surface (Figs. 3 and 5). Locally, the sediment veneer can be absent and the seafloor consists of exposed bedrock. Overall, the sediment thickness rarely reaches 2 m and the only exception for this pattern is the presence of a palaeovalley associated to the Beaulieu river (Fig. 5).

The bedrock surface is being interpreted as a transgressive surface. It defines different morphological features over this area, including (Fig. 3): (a) a main channel with a SW-NE direction; (b) a possible palaeochannel thalweg within the wide channel; (c) a "morphological" terrace defining the northwest margin of the main channel; and (d) the Beaulieu river associated palaeochannel.

The main feature dominating the West Solent area is a wide channel (or a palaeoalluvial plain) running with a SW-NE direction with a possible meandering palaeochannel thalweg associated (Fig. 10). This alluvial plain is approximately 1000 m wide and it has a vertical relief of about 7 m along its northern margin. In terms of sediment thickness, only a thin sediment veneer occurs over the bedrock surface, but locally, bedrock is exposed on the seabed. The thickest deposits are associated with the thalweg region, but they do not exceed 2.5 m. The average altitude of the palaeoalluvial plain is – 18m OD and the lowest altitude of the possible thalweg is – 20 m OD, with a very gentle northeast gradient (30 cm $km^{-1}$).

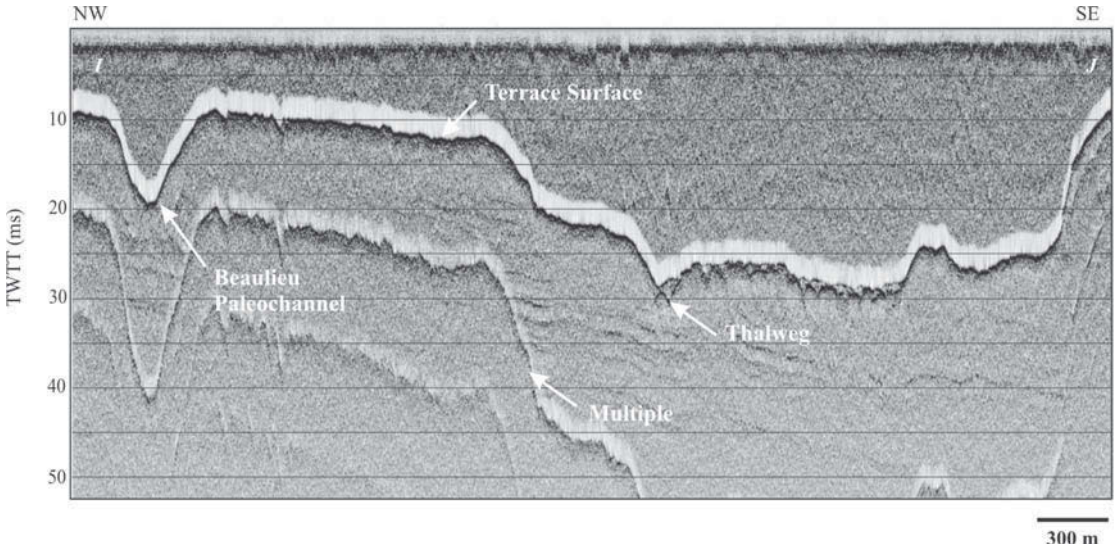


Figure 10. Chirp section across the West Solent showing a remnant thalweg and the interpreted terrace surface associated with Pennington Gravel (For location, see Figure 2).

The palaeoalluvial plain is defined by the bedrock erosive surface, hence it is being interpreted as a remnant transgressive surface. The thalweg is observed on the seismic sections and its extension has been defined using the bedrock surface map. Unfortunately, it was not possible to determine the nature of the thin sedimentary deposit associated with the thalweg. Consequently, it is not possible to verify if this deposit is a (preserved) remnant basal or infill channel deposit or if it is a modern deposit in equilibrium with the prevailing hydrodynamic conditions.

The northern margin of the alluvial plain is well defined by a "step" on the bedrock surface. This "step" or cliff line has a SW-NE direction and a vertical relief of about 7 m. The top of this feature lies at -12 m OD. Cutting through this morphological terrace, the Beaulieu river palaeochannel is up to 200 m wide and its thalweg lies at -17 m OD (Fig. 3). It has the thickest sedimentary deposit over the area, reaching up to 5 m in thickness (Fig. 5).

From a seismostratigraphic perspective, the West Solent area apparently does not show any significant record of lowstand sequences. In terms of remnant morphological features, the area is characterised by the morphology of the bedrock erosive surface that, in this case, probably represents the last transgressive surface (Fig. 11).

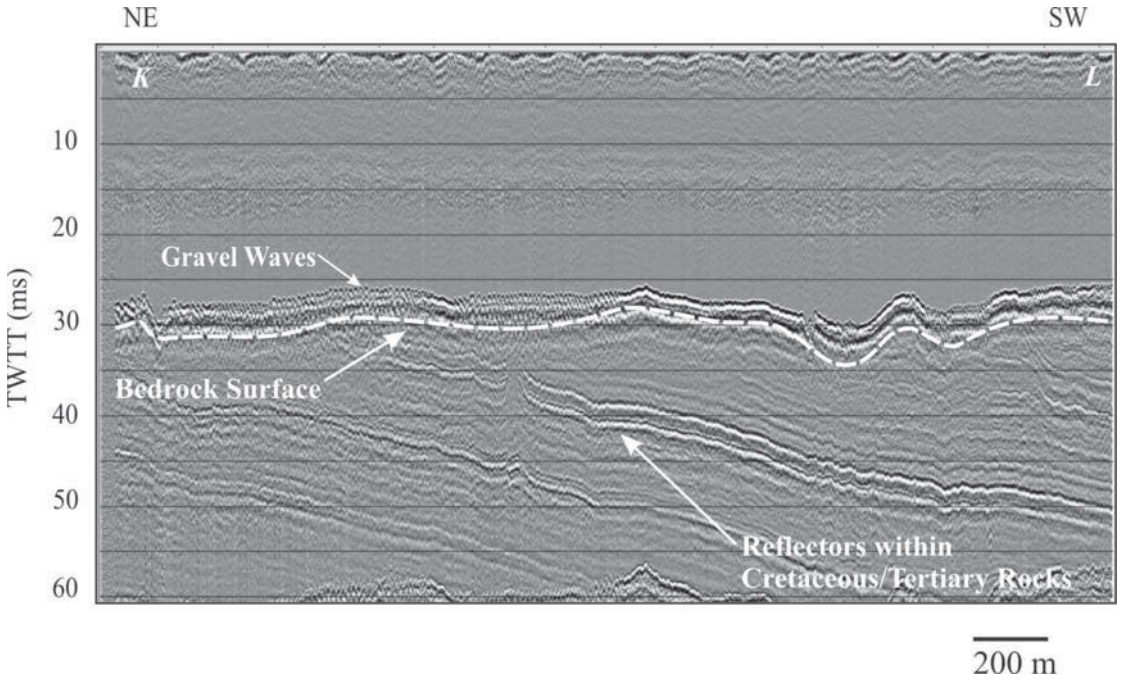


Figure 11. Boomer section over the West Solent showing the character of the bedrock surface and the thin deposit covering it (For location, see Figure 2).

#### **4.2.4.3.** *Central Area*

The central area can be described as a transitional area between the West and East Solent. It is characterised by both the occurrence of infilled palaeovalleys and thin sediment veneer areas overlying the bedrock erosive surface (Figs. 3 and 5). A main palaeovalley system is observed along the southern edge of the area. This palaeovalley is the extension of the Palaeovalley II described for the East Solent area and can be observed farther to the West, passing the Medina River mouth. The altitude of its thalweg ranges from – 22 m, off Medina River mouth, to -27 m in the eastern edge. This palaeovalley is characterised by infill deposits, however, it was not possible to define a transition between lowstand and highstand sequences (Fig. 12). Evidence of another palaeovalley can be observed on the northeast part of the area. The occurrence of this palaeovalley is limited within the survey area, still, it may represent a southerly flow channel associated with Southampton Water. It has a NW-SE direction, with a gradient towards SE. Its thalweg altitude is about – 20 m OD.

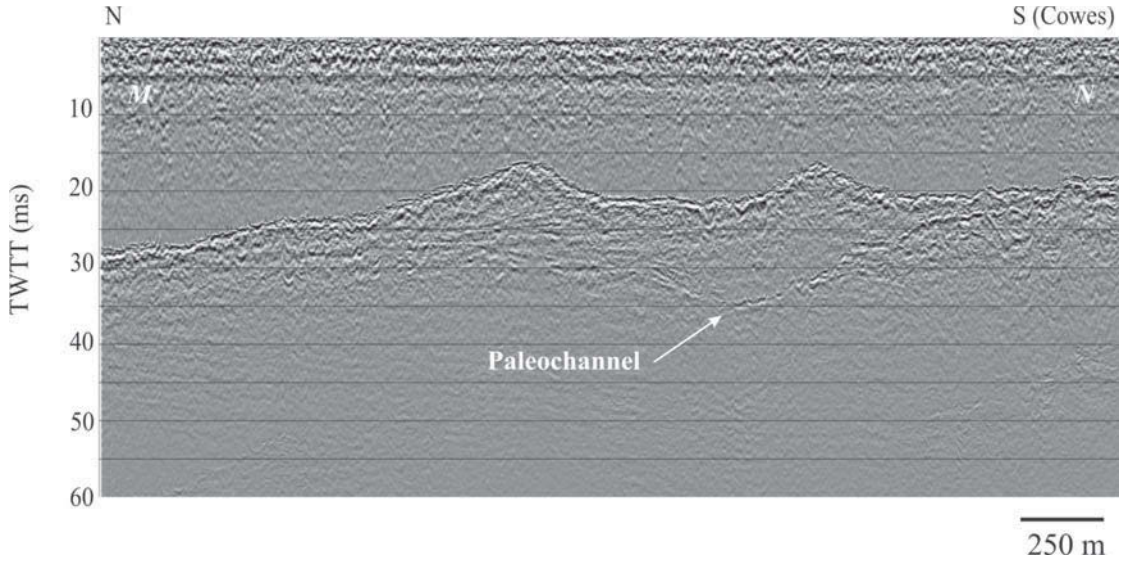


Figure 12. Boomer section across the central area showing a palaeochannel just off Cowes (Isle of Wight) (For location, see Figure 2).

#### 4.2.5. *Discussion*

The results of the present investigation have allowed the palaeogeographic reconstruction of the central Solent River system, during the Late Quaternary. Palaeovalley systems were recognised in the seismic sections along the West and East Solent areas; these are usually defined by a bedrock erosive surface which defines the distinct incised valley systems. Terrace deposits were also observed in both areas.

##### 4.2.5.1. *Incised Valleys*

The fall of sea-level during the last glacial phase left a sub aerial exposed continental shelf, causing excavation of alluvial and bedrock incision. As a result, the drainage network is rejuvenated and extended farther to the new shoreline position. This is a general trend observed worldwide and it is not different for the Solent system.

The incised channels recognised in the seismic sections are characterised by the erosion of the bedrock, indicating a change in base level, which is related to the drop in sea-level during the last glacial stage. Bedrock incision left a significant erosional relief that reaches up to 12 m along the East Solent area. The area is then characterised by poly-cyclic bedrock incised channels, with no evidence of older Pleistocene channels related to previous glacial periods. Throughout the area, terrace surfaces were recognised in association with the incised channels, which indicates the fluvial landscape evolution of the Solent River system. In the case of the West Solent, the typical terrace "staircase" (Allen and Gibbard, 1993) associated with the bedrock-defined valley running along the modern West Solent, indicates that the fluvial valley has migrated southeast, during the Quaternary. The same can not be established to the East Solent, yet, as research is still being carried out on the terrace deposits along the northern margin of Southampton Water and East Solent. Another characteristics of the incised channels observed in this study is the low potential for channel fluvial sequence preservation. Although two fluvial sequences were recognised (Va and $Va_2$), their distribution is spatially restricted.

The characteristics of the Quaternary valley settings investigated herein indicate that they can be described as a mixed bedrock/alluvial valley system, according to Blum and Tornqvist (2000). Mixed bedrock/alluvial valleys are characterised by downward-dipping terrace surfaces and may represent long-term rates of valley incision associated with multiple lateral migration of the main channel. In a sense, the youngest terrace deposit and the complex valley fill represent the last glacial cycle. In general, this type of valley system is associated with low potential preservation of fluvial sequences within the channel, but, the fluvial landscape evolution is usually preserved.

**4.2.5.2.** *Palaeogeography*

The seismic results presented here have confirmed that West and East Solent palaeodrainage systems were connected in Pre-Flandrian times. This corroborates the concept that the palaeo Solent River used to flow north-eastward over the West Solent area, joining a major south-easterly river system flowing across Southampton Water and the East Solent. However, to support this hypothesis, some assumptions had to be considered because no evident buried channel was observed in the West Solent.

An alluvial plain, defined by the bedrock erosive surface, has been interpreted over the West Solent, together with a possible associated thalweg. This channel/thalweg system is being interpreted as the base-level of a possible Late Devensian river system. Though, because no buried channel was observed, it is difficult to verify whether this bedrock surface represents the real base of the channel, or quantify the erosion produced during the Flandrian Transgression and by modern tidal scouring (see, for example, the seabed at Hurst Narrows). Consequently, the altitude of the river system over this area is an approximation. It is then suggested that the bedrock surface partly resembles the channel and the associated thalweg, as shown in the bedrock contour map (Fig. 3).

The West Solent channel shows a low gradient (30 cm $km^{-1}$), which probably can be extrapolated for the entire West Solent area. Comparable low gradients in this area have been observed by Allen and Gibbard (1994) in the Lepe Gravel terrace deposit (35 cm $km^{-1}$) (Fig. 13). The terrace identified in this investigation at -12 m OD can possibly be related to the Pennington Gravel deposits described by Allen and Gibbard (1994). If so, the Pennington Gravel would also show a low gradient of about 40 cm $km^{-1}$. Allen et al. (1996) recognised an organic bed interstratified with fluvial gravels that form the Pennington Gravel. These authors have then identified two units within the Pennington Gravel. A Pennington Lower Gravel would have been deposited under a cold climate, probably in Wolstonian time. The organic bed occurs between -3.9 to -5.3m OD and the authors suggest an early Ipswichian age. Pollen analysis indicates a temperate flora of interglacial character, while fauna assemblages suggest a change from an aquatic to terrestrial environment. The Pennington Upper Gravel sequence indicates a reversal to fluvial regime and is probably of Devensian age.

The West Solent channel would be connected to a south-easterly channel system flowing across the Southampton Water and the East Solent (Fig. 14). This connection occurs around the northern tip of the Isle of Wight and is very clear over the central area. The limits of the palaeoalluvial plain can still be followed and the channel thalweg can be extrapolated and somewhat linked to the East Solent channels. A significant alteration in the morphology and gradients of the channel systems is then observed along the central area (Figs. 3 and 13). The buried valleys in the East Solent

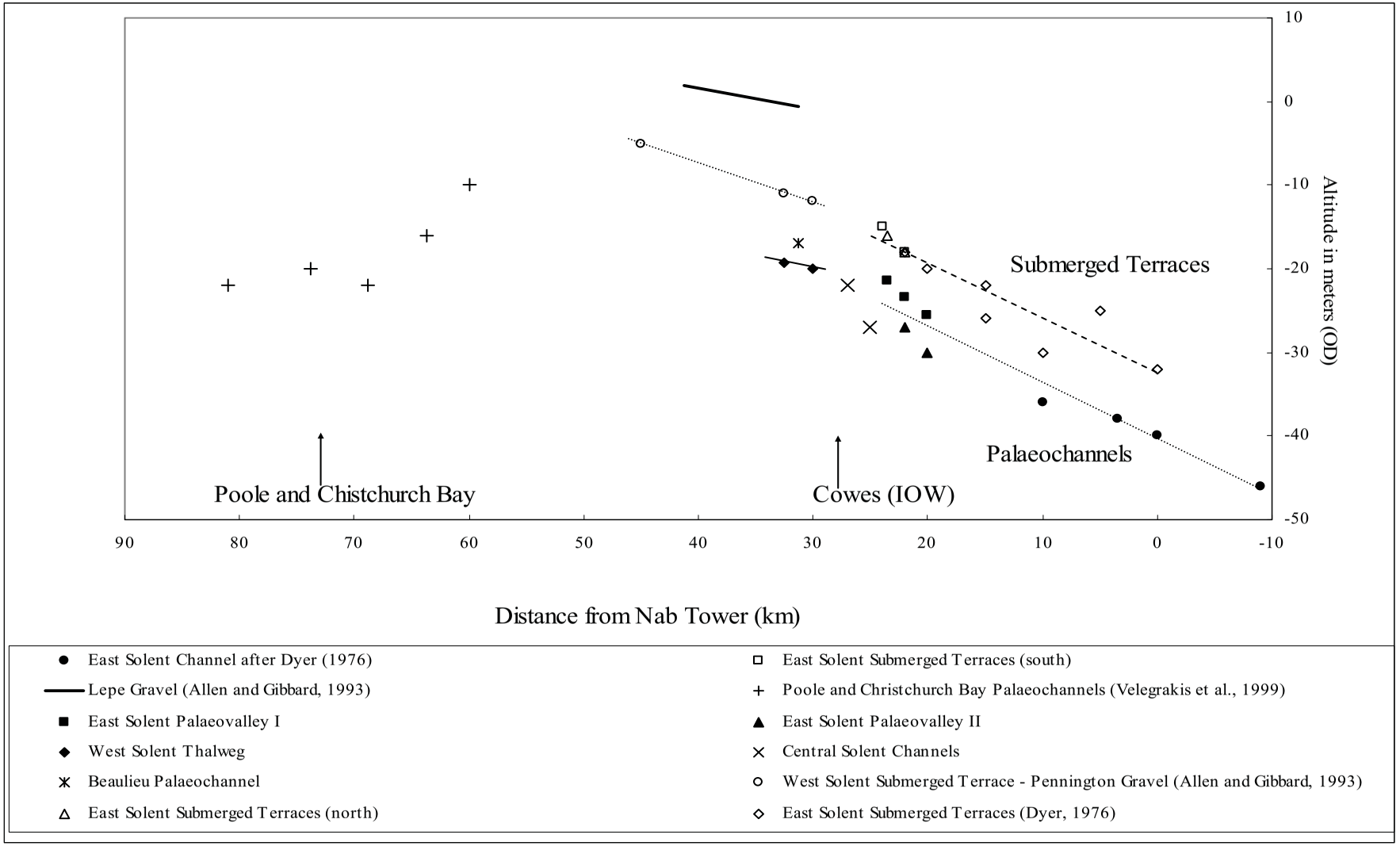


Figure 13. Profile of palaeochannel and terrace heights along the Solent. The plot shows data obtained in this investigation and also includes data from Dyer (1976), Allen and Gibbard (1993) and Velegrakis et al. (1999).

form a far more complex system of channels than in the West Solent. A change in the fluvial regime is expected to have taken place between the West and East Solent, as it is demonstrated by the morphology and higher gradients of the palaeovalley systems identified over the East Solent.

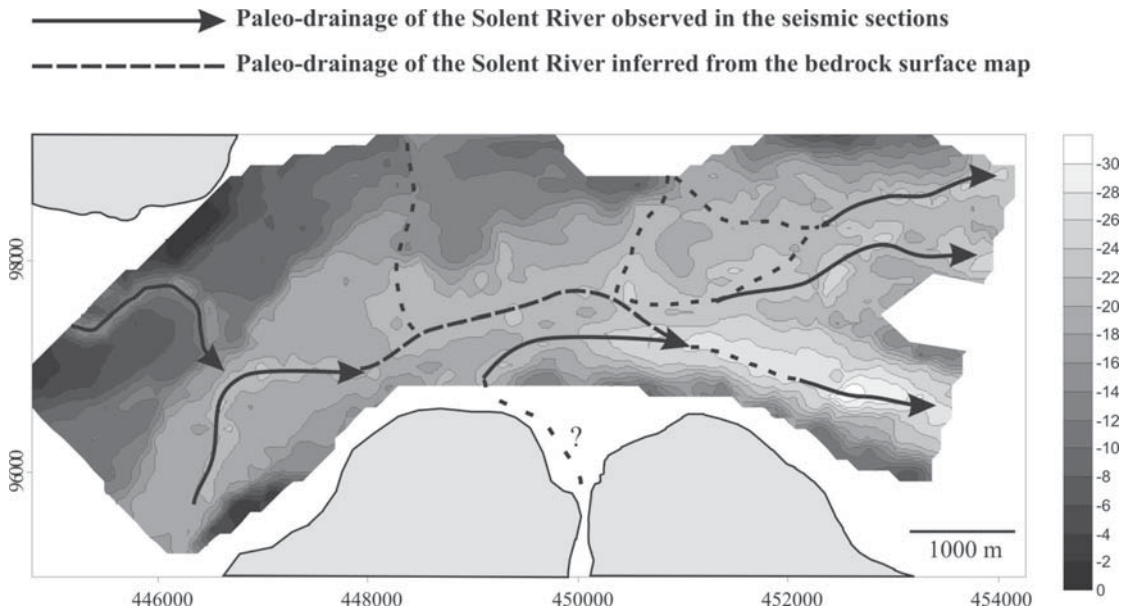


Figure 14. Palaeogeographic reconstruction of the Central Solent System.

According to Schumm (1993), the impact of base level change on the fluvial system is controlled by at least 10 variables that can be grouped as follows: 1) direction, magnitude, rate and duration of base level changes; 2) geological controls, such as lithology, structure and nature of alluvial valley; and 3) geomorphic controls, including characteristic of the exposed surface and river and valley morphology. Based on this, a possible explanation for this abrupt change in thalweg gradients from the West to the East Solent could be associated to a different fluvial response to changes in base level due to a combination of factors, including the elevation of the bedrock surface, structural patterns and change in bedrock lithology. The solid geology of the Solent system (West, 1981) shows distinct bedrock lithologies between East and West Solent. The East Solent is characterised by the occurrence of sandstones and claystones, representing the Barton Sand and Barton Clay Formations, respectively. Conversely, the northern part of the West Solent is marked by the occurrence of a marls, representing, mainly the Headon and Osborne Formations. The contact between these two characteristically distinct lithologies crosses the northern end of the West Solent (NE of the Beaulieu River) towards the mouth of the Medina River (northern tip of the Isle of Wight). It is then possible that the difference in channel gradients could be related to differential erosion of the bedrock.

There are still questions about the palaeoreconstruction of the Solent River during the Late Quaternary, but there are evidences supporting that during this period, the palaeo Solent did not flow through both Poole and Christchurch bays. With the present knowledge of the offshore palaeovalleys and bedrock topography (Velegrakis et al., 1999), it is safe to assume that, during the Late Quaternary, the Solent River as neither an extension of the Frome or Stour-Avon river systems. Considering that the

Lymington, Beaulieu, Yar and Newtown rivers extended farther into an alluvial plain in Pre-Flandrian times (Note that the present investigation has identified a buried channel associated with the Beaulieu river mouth), one can assume that a smaller Solent River used to flow north-eastward over the West Solent area and joining the major south-easterly river system flowing across Southampton Water and the East Solent.

**4.2.5.3.** *Flandian Evolution of the Solent System*

In terms of seismic stratigraphy, the interpretation of the seismic data has shown a significant discrepancy between the West and East Solent areas (Fig. 15); this is in relation to the sedimentary evolution during and after the Flandrian Transgression. The East Solent palaeovalley system is associated with a Type I incised-valley depositional sequence (Posamentier and Vail, 1988), which is characterised by the occurrence of a coarse-grained basal deposit, a channel infill transgressive deposit and a highstand or modern estuarine/inner shelf deposits, including sandbanks. Conversely, the West Solent area is characterised by the absence of a depositional sequence.

The seismostratigraphic analysis over the East Solent palaeovalley has revealed that the transgressive sequence is the dominant channel infill depositional sequence, onlapping lowstand fluvial deposits or the bedrock surface. This can be an indicative of low sedimentation rates during a relatively rapid sea-level rise (Posamentier and Vail, 1988; Allen and Posamentier, 1993). The bounding surface that separates transgressive and highstand sequences may represent a shallow marine erosive surface. Its altitude is about – 16 m OD and comparing with local sea-level curves (Waller and Long, 2004), this event would have happened around 8.0 ka BP. The preservation of the transgressive sequence seems to be limited to palaeovalley areas and where the altitude of the bedrock surface is below – 20 m OD.

In contrast, over the West Solent, the possible remnant features of a pre-transgressive age are defined based upon the morphology of the bedrock surface. The non deposition of a transgressive sequence can be attributed to the dynamic conditions over the West Solent during the Flandrian Transgression. It has been suggested that the late breaching of the eastern part of the Purbeck-Isle of Wight Chalk Ridge (7000 – 7500 BP), and consequent formation of Christchurch Bay and West Solent, has induced an abrupt change in the hydrodynamic conditions (Dyer, 1975; West, 1980; Nichols, 1987; Velegrakis et al., 1999). Probably an intensive erosion of the seafloor by strong currents has swept away most evidence of any pre-Flandrian deposit. Moreover, the present hydrodynamic conditions over Christchurch Bay and West Solent can potentially erode and rework the seabed sediments (Dyer, 1980; Velegrakis, 1994).

A comparison between the results presented by Velegrakis et al. (1999) with the ones obtained in this investigation suggests a strong connectivity between flooding and sedimentary evolution of Poole and Christchurch bays and West and East Solent. In terms of seismic sequences, it has been observed that Poole Bay and East Solent palaeochannels are characterised by preserved infilled transgressive facies sequences. In both areas a Type-1 incised-valley depositional sequence is observed. On the contrary, Christchurch Bay and West Solent show no evidence of any infilled transgressive sequence associated with the observed palaeochannels.

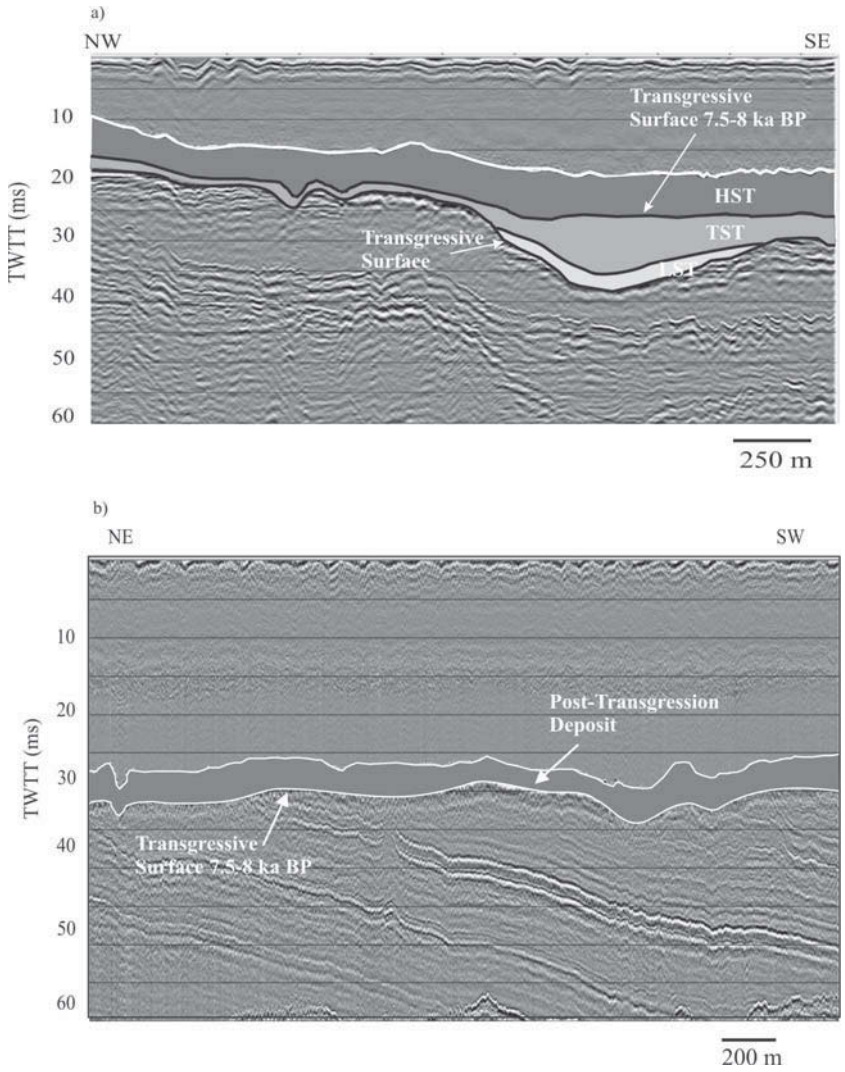


Figure 15. Summary of the different units infilling the palaeochannels over the (a) East Solent (including the transgressive surface that represents an event at 7.5 – 8 ka BP) and (b) the West Solent.

Following the conclusion of Velegrakis et al. (1999), there is evidence to suggest that the formation and evolution of Poole Bay / East Solent was different from Christchurch Bay / West Solent. Moreover, seismic stratigraphic interpretation of the East Solent sequences shows a bounding surface that could represent a change from transgressive to highstand sequences. This event would have happened around 8.0 ka BP, according to local sea-level curves. A somewhat similar age (7.5 ka BP) for the rupture of the Chalk ridge and submergence of Christchurch Bay was inferred by Velegrakis et al. (1999). Thus, it is possible that before 7.5 ka BP, the landscape in Christchurch Bay and parts of the West Solent were still dominated by alluvial plains and possible intertidal areas in the West Solent.

## 4.3. Conclusion

The offshore palaeogeography and stratigraphic evolution of the Central Solent River system has been investigated by means of high-resolution seismic surveys. The results have revealed that, during the Late Quaternary, West and East Solent

palaeodrainage systems were connected, confirming the hypothesis that the palaeo Solent River used to flow north-eastward over the West Solent area, joining a major south-easterly river system flowing across Southampton Water and the East Solent. Over this area, a significant alteration in the morphology and gradients of the channel systems is observed. The low gradient alluvial plain recognised in the West Solent develops into a higher gradient and far more complex system of channels in the East Solent.

Seismic stratigraphic analysis shows a significant difference between the West and East Solent areas in terms of the sedimentary evolution during and after the Flandrian Transgression. The seismic stratigraphy of the East Solent palaeovalley system is characterised by the occurrence of lowstand, transgressive and highstand sequences, whilst the West Solent palaeovalley is characterised by the absence of a depositional sequence. Such discrepancy indicates that the evolution of the two areas were very different. Comparing with the results of Velegrakis et al. (1999), it can be suggested that Poole Bay and East Solent evolved very similarly, with the preservation of the transgressive sequences. Christchurch Bay and West Solent, on the contrary, were drowned later and the conditions did not permit the deposition of a transgressive sequence.

Finally, the preservation of the Holocene depositional sequences within the stratigraphic record in the Solent palaeovalley systems is controlled, mainly, by local rate and chronology of sea-level rise combined with the configuration of the antecedent topography, specially the altitude of the bedrock surface and changes in hydrodynamic conditions.

# 5. PHASE 2: Chirp II core calibration – the internal geometry of secondary contexts

## 5.1. Introduction

As described in Section 3.2.2. the first objective of Phase 2 (Objective 6) was a full review of the survey archives of Hanson Marine Ltd. in order to identify potential calibrated terrace deposit for a 2D survey. A total of three whole dredging licence sites were investigated (with a total of c. 20 sets of core logs per site and full field reports). Data for an ideal coarse grained fluvial gravel "terrace" deposit was not available, but a site was chosen (Prospect Area 372-1: entrance to the East Solent) as a suitable test site. Two cores were identified, Core sites 7 and 11 (Figure 16 and 17 respectively), which included intercalated sands and gravels ideal for the sweep test procedure.

A successful Chirp II survey was undertaken over the two core sites and the adjacent area, with two preferred sweeps being utilised: a 2-5 kHz sinesq8 linear sweep and a 2.5 – 6 kHz sinesq8 linear sweep. These data were processed using established flows developed at SOC, thus satisfying Objectives 7 and 8 of the project (Sections 3.2.2.2. and 3.2.2.3. respectively). On receipt of the actual cores from Hanson for cores sites 7 and 11 (after completion of the Chirp survey) it became apparent that they were in very poor condition and consequently they were not possible to log for compressional wave velocity and density and hence construct an accurate synthetic seismogram (Objective 10 – Section 3.2.2.5.). Synthetic seismograms were produced for the East Solent Prospect area based on compressional wave velocities and densities taken from the literature and based purely on the lithological descriptions of the cores (Figure 16 and 17). These still showed broad correlation with the two seismic sections and as such demonstrated the potential of the Chirp II sources to penetrate these traditionally impenetrable sequences. However, as shall be seen these rather speculative results have been superseded by the successful completion of Phase 2 using a new dataset.

At this stage it was decided in consultation with our Project Officer to take a change in tack with the integration in to the project of a new seismic and core dataset provided by Wessex Archaeology. As part of their MIRO/ALSF funded project "Seabed Prehistory: Gauging the Effects of Marine Dredging" (Ref. 53146.02) they had consulted with representatives from the marine aggregate industry and decided to acquire data from an aggregate prospecting area within the Owers Bank Licensing block. Their project aimed to address methodologies for assessing and evaluating the potential prehistoric archaeological resource of a given area of seabed.

They allowed us access to 245 line kilometres of high resolution boomer data, along with access to 4, 6 m length vibrocores, from the outer sections of the Arun river, 10 km south of Littlehampton, off the coast of West Sussex in the English Channel. Within this broader data set Phase 2 focused on two of the cores, which through successful co-ordination with Wessex Archaeology we were able to geophysically log prior to any subsequent sampling they needed to undertake for their project. Further, we were then able to acquire Chirp II calibration data (3 sweeps) over the core locations in addition to a boomer calibration line acquired by Wessex Archaeology. These data in combination with data acquired as part of Phase 1 enabled us to successfully complete (Objective 7 to 10: Sections 3.2.2.2. to 3.2.2.5). The full results of this work are described in Section 5.1.

Unfortunately, due to these issues we were not able to acquire a high-resolution 2D Chirp II data set to fulfil Objectives 11 and 12. Although a preliminary pseudo-3D interpretation was undertaken by Dix and Bastos (Dix et al., 2004) and presented at an industry conference at the Geological Society of London, this was all based on boomer data and so has not been included here. However, these new data we did acquire enabled us to look at an additional key issue of relevance to the archaeological and dredging communities that we had not anticipated in the Project Design. This new development was the ability to identify, using remotely deployed acoustic sources, peat horizons buried at depth beneath the seabed. This capability is of real significance to the archaeological community, as they represent horizons that can provide crucial palaeo-environmental data, essential to enhancing our understanding of historic and pre-historic sites. Frequently, such data is restricted to identifying samples from cores, which although provides the necessary high-resolution data at individual sites they frequently fail to provide the more regional context of these deposits. Naturally, there is also a vital prospective element to this discovery. By contrast the aggregate industry are interested in these results as peat horizons can represent a significant contaminant to the grade quality of their deposits and so need to be avoided where possible. The full results from this work are described in Section 5.2.. This section is based on a paper that has been submitted to a Special Edition of the journal Geoarchaeology which has been dedicated to the outcomes from Round 1 ALSF projects.

As with Phase 1 we have continued to work on these data beyond the original deadline and this phase of the work includes a significant contribution from a PhD student Ruth Plets, at no additional cost to the original grant.

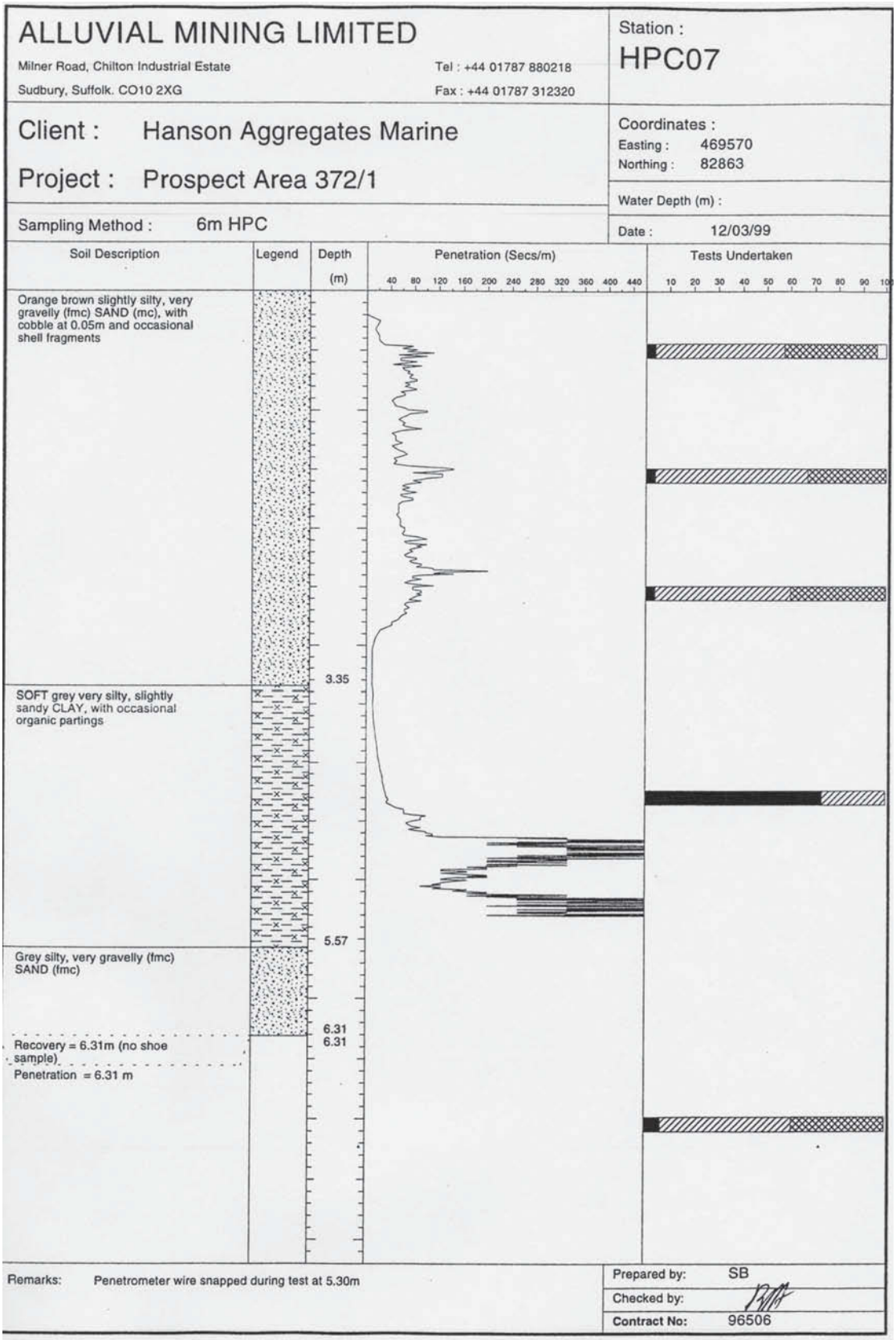


Figure 16. Copy of core log data for core site 7 from Prospect Area 372-1 (entrance to the East Solent). Courtesy of Hanson Marine Ltd.

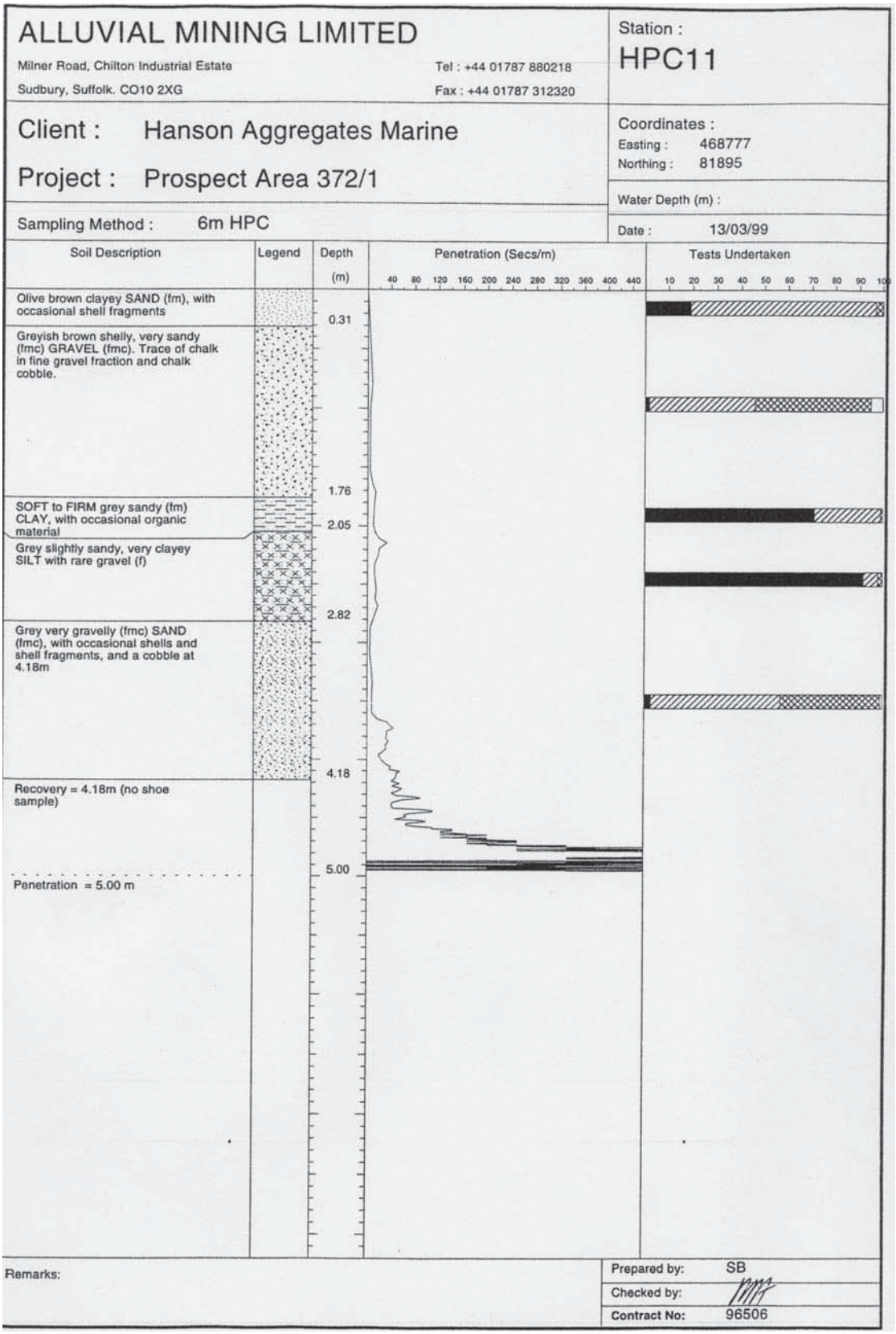


Figure 17. Copy of core log data for core site 11 from Prospect Area 372-1 (entrance to the East Solent). Courtesy of Hanson Marine Ltd.

## 5.2. Chirp II and Boomer Resolution and Penetration

In order to assess the resolution and penetration and resolution capabilities data from two locations are presented. As described in Section 5.1. the bulk of the data was collected in the palaeo-Arun area of the English Channel, approximately 10km south of Littlehampton, off the West Sussex coast. Boomer data was collected by Wessex Archaeology (Wessex Archaeology, 2004) and after an initial interpretation of the Boomer data, the area was revisited with a Chirp II source by the School of Ocean and Earth Science, University of Southampton. The locations of these surveys were targeted to specifically co-incide with two vibrocores that provided both sedimentological and geophysical calibration data. In addition data from the 2D survey taken from Ryde Middle Bank, in the East Solent (See Section 4 for survey description) will also be discussed for comparative purposes. The text from this section is ultimately is based on a preliminary draft of a paper being put together by Plets et al..

### 5.2.1. *Seismic sources and data processing*

#### 5.2.1.1. *Boomer*

As described in Section 2.2.2. Boomer systems are classified as an 'acceleration water mass source' (Mosher and Simpkin, 1999) mounted on a lightweight catamaran. The resultant acoustic pressure pulse produced by these systems is broad spectrum in nature. The properties of the Boomer source, as provided by the manufacturer (Applied Acoustic Engineering), are summarised in Table 1. Figure 18a shows the typical Boomer wavelet shape, with its accompanying power spectrum (Figure 18b). Although the power spectrum has a large frequency content (up to 15kHz), the –3dB bandwidth value is limited to 0–1.5kHz for the lower frequencies and 3-6kHz for the higher frequencies, with a drop in power between these values. The fundamental frequency is 5kHz. An 8-element hydrophone streamer, towed behind the catamaran, receives the reflected acoustic signal, which is then converted to an electric signal and recorded digitally at a sample rate of 0.028ms.

| | |
|---|---|
| Size | 38cm x 38cm depth 9cm |
| Recommended use | 100 – 200J / shot |
| Maximum energy input | 300J / shot |
| Source Level | 215dB re 1μPa @ 1m at 200J |
| Typical pulse length | 150μs |
| Reverberation time | <1/10 x initial pulse |
| Frequency content | 500Hz – 10kHz |
| Typical resolution | 10cm @ 200J |

Table 1. Characteristics of a typical Boomer source (Applied Acoustic Engineering)

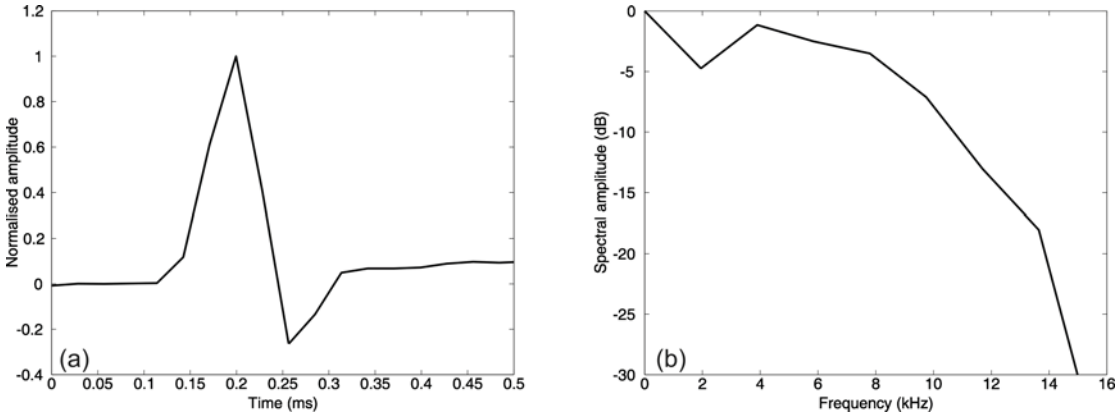


Figure 18. (a) Typical Boomer wavelet in the time domain and (b) its accompanying power spectrum.

The resolving power of an impulsive source such as the Boomer, improves as its power spectrum becomes broader and smoother, its duration becomes shorter and its shape becomes more repeatable (Verbeek and McGee, 1995). The major advantage of the Boomer system is that simply increasing the input energy can increase power in the water. As the input energy increases, lower frequencies are preferentially enhanced, resulting in longer, less repeatable wavelets, leading to a better penetration but poorer resolution (Verbeek and McGee, 1995).

The raw Boomer data was stored as SEGY files and processing was undertaken using a seismic processing package, PROMAX. The processing was kept to a minimum and the following processing flow was applied to the Boomer data:

1. *'Trace DC Removal'* to remove the bias dc or offset from the input traces
2. *'Ormsby Bandpass Filter'* to apply a frequency filter with corner frequencies 200-600-6000-10000Hz
3. *'Nomal Moveout Correction'* to correct traveltimes for offset influence
4. *'CDP/Ensemble Stack'* to stack input ensembles of stacks vertically

**5.2.1.2.** *Chirp II*

As described in Section 2.2.3. Chirp sources can be categorised as a 'controlled waveform source' (Mosher and Simpkin, 1999). The transmitted signal may be varied in pulse-length, bandwidth, pulse spectrum / Envelope Function, and in Instantaneous Frequency Function (IFF). The FM pulses are computer generated and hundreds of waveforms can easily be stored in the electronics bottle connected to the transducer from which the user can remotely choose. During this project, three source sweeps, designed by Gutowski et al. (2002), have been used (Table 2; Figure 19). Sweep 1 is an 'old' sweep which has been used for decades, but modified to have a higher energy output; Sweep 2 is a theoretically very high resolution broad-bandwidth sweep; and Sweep 3 represents a direct competitor for the Boomer source due to its similar frequency content.

As can be seen from Figure 19, the sweep (Figure 19a, d and g) gives the source function a wide bandwidth (Figure 19b, e, h), but also a long pulse length (Mosher and Simpkin, 1999). In order to maximise the output signal-to-noise ratio, this long Chirp pulse is compressed by cross-correlating the signal with a replica of the transmitted acoustic pulse, resulting in a much shorter Klauder wavelet (Figure 19g, h,

i). It is the length of this Klauder wavelet that controls the vertical resolution Gutowski et al. (2002). The main control on the length of the Klauder wavelet is the bandwidth of the signal (Table 2). The wider the initial bandwidth, the sharper the peak of the central lobe (Sheriff and Geldart, 1995). In addition, an increase in spectral bandwidth results in a decrease of the side lobes (Koefod, 1981). These two factors lead to an improved signal and, thus, to an improved vertical resolution.

| Sweep | Pulse Length | Frequency | Envelope Function | IFF | Bandwidth at –3dB | Fundamental frequency |
|---|---|---|---|---|---|---|
| 1 | 32ms | 2-7kHz | Blackmann-Harris | Linear | 1.76kHz | 4.61kHz |
| 2 | 32ms | 1.5-13kHz | Sine-Squared $8^{th}$ | Linear | 9.89kHz | 7.42kHz |
| 3 | 32ms | 2.5-6kHz | Sine-Squared $8^{th}$ | Linear | 2.95kHz | 4.35kHz |

Table 2. Properties of the selected Chirp sweeps

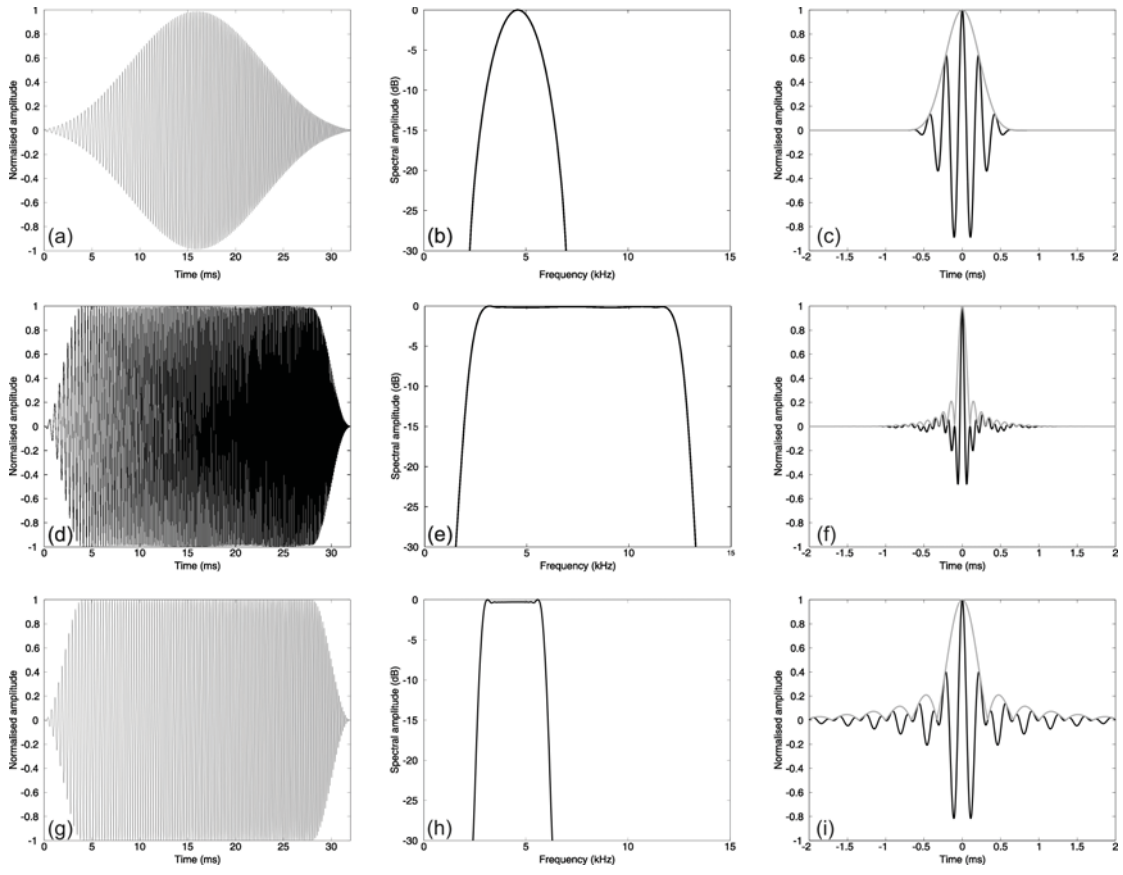


Figure 19. Time domain representation, power spectrum and Klauder wavelet with accompanying envelope (grey) of respectively Chirp Sweep 1 (a)-(b)-(c), Chirp Sweep 2 (d)-(e)-(f) and Chirp Sweep 3 (g)-(h)-(i). For detailed description of the Chirp sweeps, see Table 2.

For the survey, a quadratic array of four Chirp transducers was mounted on a catamaran. The properties of these transducers, as provided by the manufacturer (GeoAcoustics) are summarised in Table 3. The receiver array consists of a group of 8 hydrophone elements, towed behind the catamaran. The Chirp data were collected in an uncorrelated format recorded at a 0.040ms sample interval.

| | |
|---|---|
| Size | 4 transducers with a 5.5cm radius arranged in a square |
| Typical energy input | 64J / shot |
| Source Level | 205dB ± 3dB re 1μPa @ 1m at 64J |
| Typical pulse length | 32ms |
| Frequency content | 0.5kHz to >13kHz programmable |
| Typical resolution | 6cm using a 0.5 to 13.5kHz chirp |

Table 3. Characteristics of the Chirp source (GeoAcoustics)

Again the raw Chirp II data was acquired in SEGY files format and loaded into PROMAX, the data processing was also kept to a minimum:

1. *'Vibroseis Correlation'* correlates the raw uncorrelated data with the initial Chirp sweep
2. *'Automatic Gain Control'* varies the gain down the seismic section
3. *'Trace Math Transform'* applies an envelope function to the data (Reflection Strength)

### 5.2.2. *Reflection theory, cores and synthetic seismograms*

Whenever an acoustic wave, with amplitude $A_i$, encounters an interface between two layers resulting from an abrupt change in the elastic properties of the layers, the incident wave is partitioned into a transmitted wave and a reflected wave. The amplitude of the transmitted wave is $A_t$ and the amplitude of the reflected wave is $A_R$. The sum of the reflected and transmitted energy equals the energy of the incident wave. It is the acoustic impedance ($I$) which determines the relative portions of energy transmitted and reflected (Kearey and Brooks, 1991). The acoustic impedance of a material is the product of its density ($\rho$) and its P-wave velocity ($v$):

$$I = \rho v \,. \qquad (1)$$

Thus, it is the change in impedance between two materials that results in the reflection of sound. A numerical way to express the effect of such an interface is given by the reflection coefficient. The reflection coefficient ($R$) is the ratio of the amplitude of the reflected wave and the amplitude of the incident wave:

$$R_{12} = \frac{A_r}{A_i} \,. \qquad (2)$$

This measure can be related to the physical properties of the materials by using the Zoeppritz equations (Kearey and Brooks, 1991); for explanation of derivation see (Sheriff and Geldart, 1995)):

$$R_{12} = \frac{I_2 - I_1}{I_2 + I_1}, \qquad (3)$$

or

$$R_{12} = \frac{\rho_2 v_2 - \rho_1 v_1}{\rho_2 v_2 + \rho_1 v_1}, \qquad (4)$$

where $R_{12}$ is the reflection coefficient, $I_1$ is the acoustic impedance of the upper medium of the sediment and $I_2$ is the acoustic impedance of the lower medium of the sediment. It is the impedance structure of the sediment column that determines its characteristic acoustic structure and it is the contrast in impedance that should give rise to an acoustic reflection (Mayer, 1980).

The difference in impedance between all the layers/materials in the sedimentary column results in a reflectivity series. From this equation it follows that values for $R$ vary between –1 and 1, but in reality values for the reflection coefficient only rarely exceed ± 0.5 and are typically much less than ± 0.2 (Kearey and Brooks, 1991). The seismic trace that is recorded ($x(t)$) is the result of the convolution of the earth's reflection coefficient series ($r(t)$) with the sound source wavelet ($w(t)$):

$$x(t) = w(t) * r(t). \qquad (5)$$

It is clear that the wavelet produced by the source is as important in determining the character of the final seismic profile as is the earth's reflection coefficient series (Mosher and Simpkin, 1999); it is the source wavelet that will allow or disallow the resolving of individual layers.

Values for $r(t)$ can be acquired by core logging. In this study, the cores were taken within 15m of the targeted position using a 6m hydraulic vibrocorer (Wessex Archaeology, 2004). In the first instance, each core was split and logged with the Southampton Oceanography Centre's Marine Sediment Core Logger (Best and Gunn, 1999). This logging system measures the sediment bulk density (gamma ray attenuation method) and P-wave (500 kHz; transmission method) velocity down the length of the core at 2cm intervals. There are still disagreements amongst scientists on the dependence of sound speed on the used sound frequency (i.e. the dispersion), especially for the lower frequency range (McCann, 1967; Turgut and Yamamoto, 1990; Best et al, 2001; Stoll, 2001; Buckingham and Richardson, 2002; Gorgas et al., 2002; Williams et al., 2002; Robb, 2004). However, for the purposes of this study velocity is assumed to be frequency independent. After this quantitative logging, the structures, colour, texture and lithology of each core were recorded in a detailed log. For the final part of the analysis, specific units of the cores were sampled for grain size analysis. Sediment grain-size distribution was determined by dry sieving for gravel- and sand-sized particles and with a Micromeritics sedigraph for silt- and clay-sized particles.

The measurement of the bulk density and p-wave velocity with the Marine Sediment Core Logger enables a synthetic seismogram to be constructed. A synthetic seismogram is defined as an artificial seismic reflection record, manufactured from

velocity- and density-log data by convolving the reflectivity function with a waveform. It is used for comparison with an actual seismogram to aid in identifying events or in predicting how stratigraphic variation might affect a seismic record (Sheriff, 1973).

The first phase in constructing a synthetic seismogram is computing the reflectivity function. The product of velocity ($v$) and density ($\rho$), acoustic impedance ($I$) (Equation (1)) is calculated as the fundamental acoustic property of the sedimentary column. Reflection coefficients were then calculated down the length of the core at a sampling interval of 2 cm using Equations (3)/(4). The depth scale was converted to a two-way travel time scale using the measured p-wave velocity and resampled at equally spaced points of 0.027 ms.

In a second phase, the convolution of the seismic wavelet ($w(t)$) with computed reflectivity series ($r(t)$) yields the seismogram ($x(t)$) (Equation (5)).

The convolutional model assumes that the source waveform does not change as it propagates down into the earth and, hence, the intrinsic attenuation is excluded (Yilmaz, 1987).

For the Boomer, this process is relatively straightforward: the Boomer wavelet was resampled at 0.027 ms, the reflectivity series was convolved with the resampled Boomer wavelet and, in order to compare the synthetic with the real traces, the convolved trace was resampled at 0.028 ms.

The convolution of the reflectivity series with the Chirp sweeps is a longer process. Each of the 32ms Chirp sweeps was resampled at 0.027 ms before being convolved with the reflectivity series. This convolved trace was then resampled at 0.04 ms, in accordance with the sampling rate of the real acquired seismic data. In the same way as for the processing flow, the final step was to correlate this trace with the same 32 ms Chirp source wavelet (i.e. autocorrelation), but now sampled at 0.04 ms. An envelope function (Reflection Strength) is nearly always applied to Chirp data to aid visualisation, even though it means that amplitude and phase information of the original data is lost. Similarly this envelope function has been calculated for each of the synthetic traces. To do this, the instantaneous amplitude ($RS(t)$) or reflection strength needed to be computed:

$$RS(t) = [x^2(t) + y^2(t)]^{1/2}, \qquad (6)$$

where $x(t)$ is the signal itself and $y(t)$ is its quadrature. The quadrature is the 90-degree phase shifted version of the recorded signal and can be obtained by taking the Hilbert transform of $x(t)$ (Yilmaz, 1987). This envelope can now be draped over the synthetic seismogram. Note that applying this envelope function is an irreversible process; i.e. it is impossible to derive the original signal ($x(t)$), when only the reflection strength envelope has been recorded ($RS(t)$).

### 5.2.3. *Boomer and Chirp II source comparison*

Rather than looking at theoretically calculated values for penetration and vertical resolution the actual data will be used to make quantitative and qualitative comparison between the Boomer and Chirp sweeps, and between the three different Chirp sweeps. In order to achieve this three data sources were investigated: 1) a palaeo-channel infill off the coast of Littlehampton; 2) a sandbank in the East-Solent, Ryde Middle

Sandbank; and 3) a gravel deposit linked to the palaeo-channel off the coast of Littlehampton.

#### **5.2.3.1.** *Palaeo-channel fill core*

Sediments in the channel-core are dominantly silty very fine sands and with occasional intervals of millimetre-thick layers of interleaved silty very fine sand and silty clay (Figure 20). The top of the core consists of medium to coarse sand, broken shells and large pebbles. With the exception of the unit containing the pebbles, the p-wave velocity varies little throughout the core (1700 – 1750m/s; see Figure 20). Most peaks in the reflectivity profile are linked to changes in density. The density varies roughly between 1770kg/$m^3$ and 2010 kg/$m^3$, with low values corresponding to the thin clay layers and higher values to more compact sand. Values for the reflectivity coefficient are generally very low ($<\pm$ 0.01). Where they do exceed this value, negative peaks mostly correspond to clay layers and positive peaks to silty sand layers underlying the clay.

A synthetic seismogram was constructed for the core, using the method described in Section 5.2.2.. The reflectivity series (grey line in Figure 21) was convolved with the Boomer wavelet and the three Chirp sweeps, resulting in a synthetic seismogram (black line Figure 21).

For the Boomer synthetic seismogram (Figure 21a), nearly every event in the reflectivity series is resolved in the synthetic model. The very fine interlayering of silty sand and silty clay in the channel is not always resolved (e.g. C-S-C) but most of the larger peaks appear at the right depths. For the Chirp sweeps, both the reflectors without reflection strength (black line Figure 21b) and with reflection strength (dark grey envelope Figure 21b) have been modelled. Sweep 1 does not resolve the smaller reflectivity spikes very well without the reflection strength, nor are the closely spaced peaks separated (C-S-C). Once the reflection strength is applied, the major reflectors are accentuated and a layered stratigraphic pattern is easier to recognise. The synthetic seismogram constructed with Sweep 2, without reflection strength, strongly resembles the Boomer synthetic seismogram. Nearly every event in the reflectivity series results in a reflector in the synthetic model (Figure 21c). However, the fine clay-sand-clay (C-S-C) layers are still not completely resolved. Applying the reflection strength often means that reflectors, which were resolved originally, are now depicted under the same envelope, decreasing the vertical resolving power. The synthetic seismogram with Sweep 3 is comparable to that of Sweep 1. None of the closely spaced spikes are resolved (C-S-C) and reflection strength enhances the major spikes (Figure 21d).

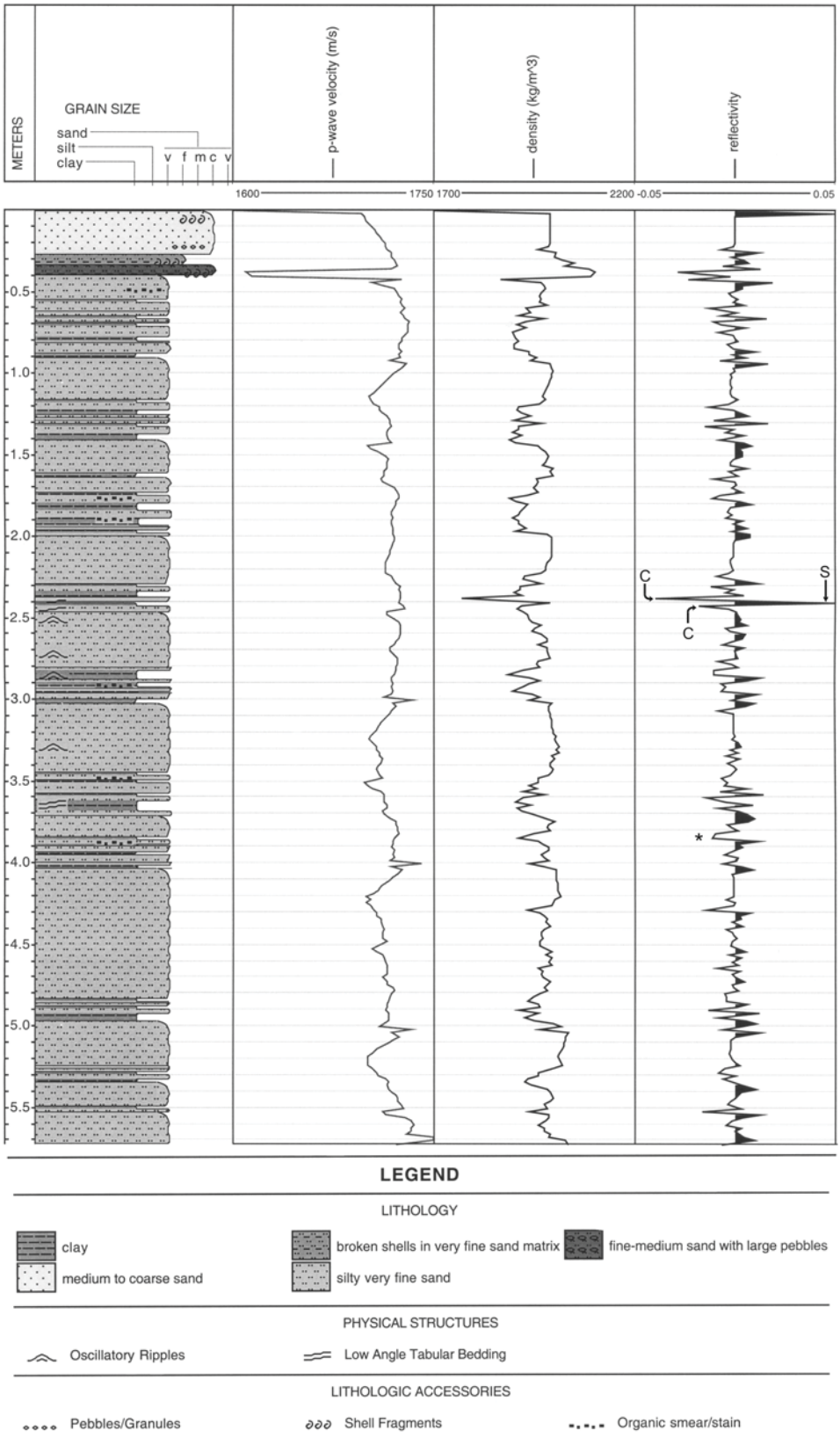


Figure 20. Log of the core recovered from the middle of the palaeo-channel. Sedimentary features, p-wave velocity ($ms^{-1}$), density ($kgm^{-3}$) and the reflectivity series are shown. C = silty clay, S = silty sand and * = silty clay layer (see Figure 21 and Figure 22 for further analysis).

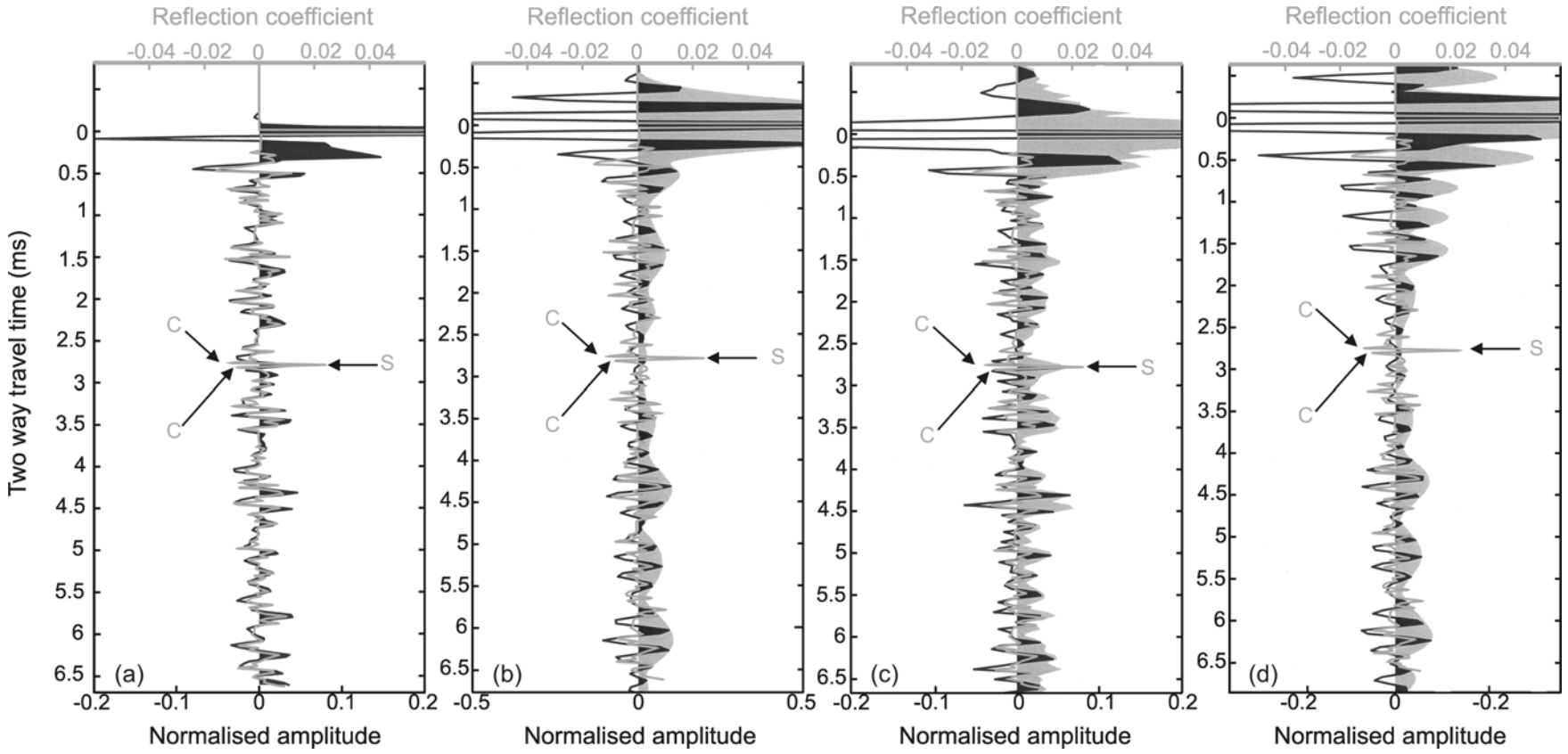


Figure 21. Synthetic seismograms constructed for the palaeo-channel core (a) convolved with the Boomer wavelet and convolved and correlated with (b) Chirp Sweep 1, (c) Chirp Sweep 2 and (d) Chirp Sweep 3. The grey line represents the reflectivity series as seen in Figure 3; the black line is the synthetic seismogram; and the dark grey envelope in (b)-(c)-(d) shows the application of reflection strength on Chirp data. C = silty clay and S = silty sand.

In addition to comparing the synthetic seismograms with the core stratigraphy it is also important to compare them against the reflection seismic data actually acquired in the field. The location of the vibrocores (with an error of 15m on either side of a central coordinate) is indicated by a white box on the seismic data. Within this box, 10 traces have been extracted and compared to the modelled synthetic seismogram.

The Boomer seismic data (Figure 22a) shows both the channel base and inclined channel infill sediments, covered by gravel. The individual traces indicate a distinct difference to the synthetic seismogram: peaks and troughs are much wider and smoother for the real traces. This is most certainly related to the shape of the Boomer wavelet: the real wavelet is inherently "ringy" and is possibly longer and wider than the manufacturer claims. One negative reflector (indicated with * in Figure 22b) can be followed throughout the ten traces and can be linked to the theoretical trace. This reflector is visible in the original data as a white reflector dipping between 49ms and 51ms in the selected white box and seems to correspond to a silty clay layer in the core (Figure 20). Other reflectors could be linked to the theoretical trace but without absolute certainty, and therefore, are not indicated on the plot.

The quality of the Chirp data acquired with Sweep 1 does not approach the quality of the Boomer data. The channel can just be picked out in the reflection strength data (Figure 23a) together with two clear dipping reflectors in the channel. The data without the reflection strength (Figure 23b) is again ringy. Although the base of the channel is still just distinguishable, only one major dipping event is vaguely recognisable (dipping between 49ms and 52ms in the selected white box). This dipping event seems to correspond to the bright reflector discussed above for the Boomer data. A negative reflector can be followed through the ten real traces and the synthetic trace (*in Figure 23c). Hardly any other reflectors, with or without reflection strength applied, can be associated with reflectors of the synthetic seismogram.

The seismic data acquired with Chirp Sweep 2 and with reflection strength applied, is of even poorer quality (Figure 24a). The base of the channel is barely visible and no dipping reflectors can be discriminated. When looking at the correlated data (Figure 24b) without reflection strength, the image improves considerably: the base of the channel is clearly obvious and the dipping reflectors of the channel infill become unmistakable. The separate traces and the synthetic trace both show many peaks and troughs (Figure 24c). As for the Boomer and Sweep 1 traces, one negative peak stands out and can be followed through all the traces, corresponding to the bright white reflector dipping between 49ms and 52ms in the selected box.

Of all the Chirp data acquired, the reflection strength data of Sweep 3 provides the best image (Figure 25a): a very hard reflector for the channel base and a number of distinctive dipping reflectors. Even the non-reflection strength data (Figure 25b), shows the basic structure of the channel and its infill sediments, despite the ringiness of the signal and data. The ringiness becomes obvious when looking at the separate traces. Again, a negative spike can be followed through all traces (* in Figure 25c).

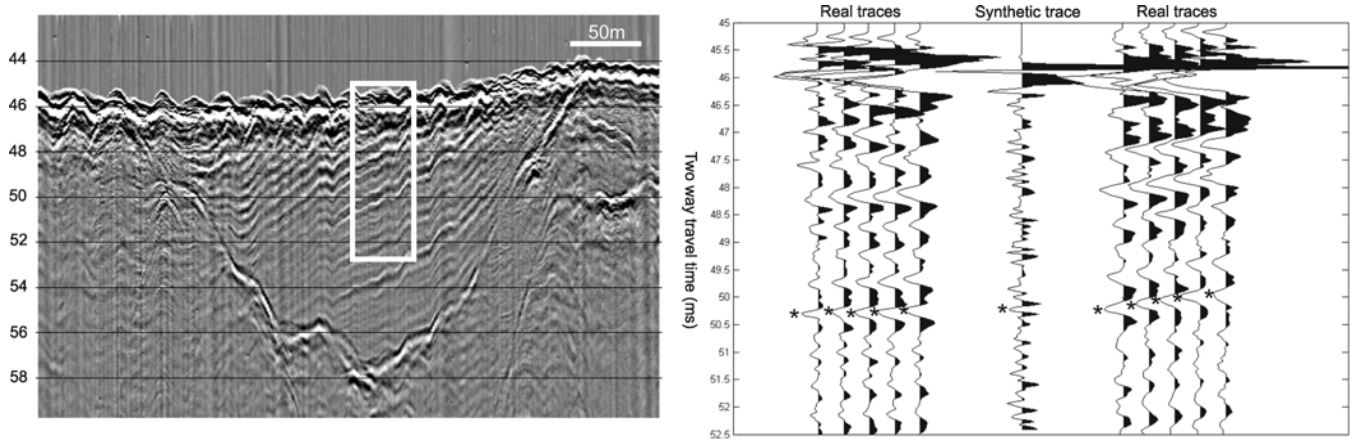


Figure 22: (a) Boomer seismic section of the palaeo-channel with (b) a comparison of real traces with the theoretical synthetic trace. * indicates a distinctive negative reflector which corresponds to a silty clay layer in the core.

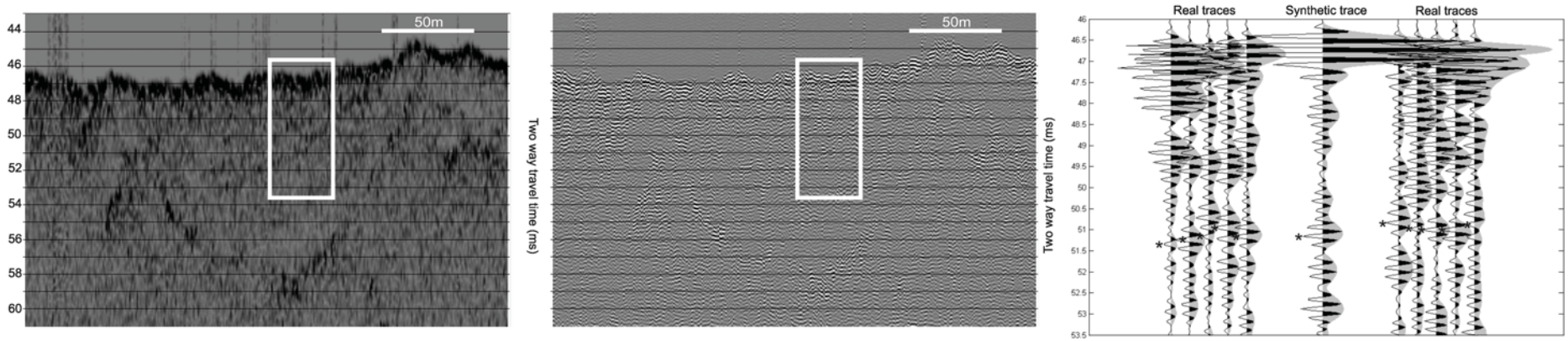


Figure 23: (a) The palaeo-channel depicted by Chirp Sweep 1, with reflection strength applied and (b) without reflection strength. (c) Shows a comparison between real Chirp Sweep 1 traces and the synthetic trace. * indicates a distinctive negative reflector which corresponds to a silty clay layer in the core.

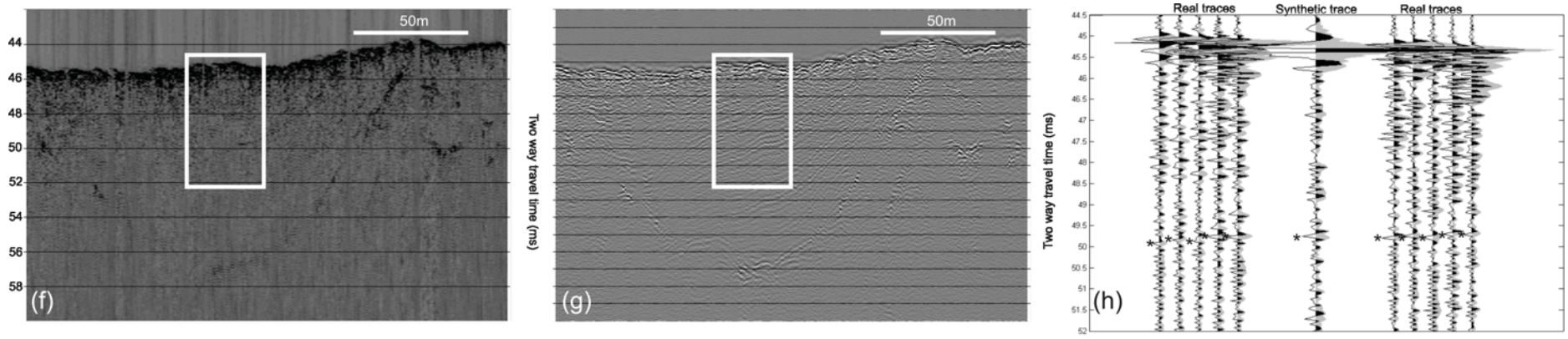


Figure 24: (a) Chirp Sweep 2 seismic data of the palaeo-channel with reflection strength applied and (b) without reflection strength. (c) Shows a comparison between real Chirp Sweep 2 traces and the synthetic trace. * indicates a distinctive negative reflector which corresponds to a silty clay layer in the core.

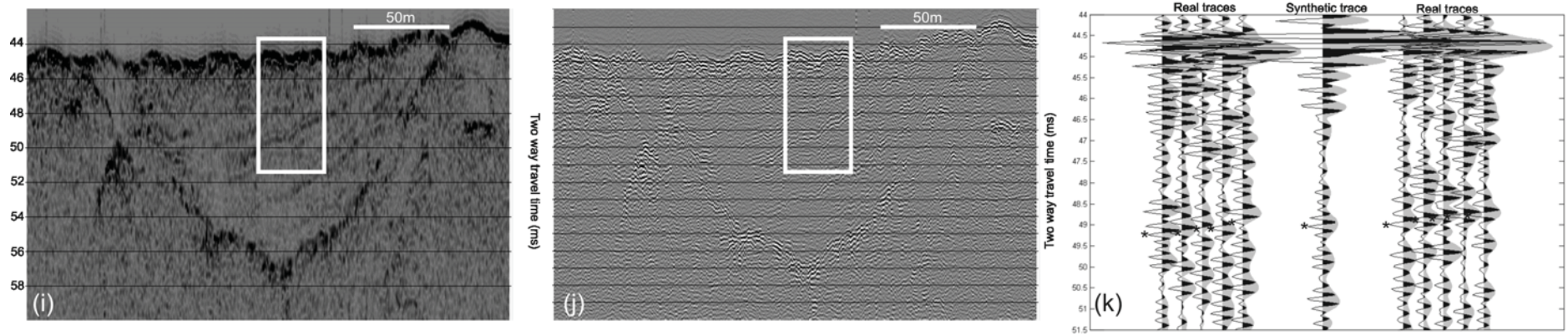


Figure 25: (a) The palaeo-channel section acquired with Chirp Sweep 3 with reflection strength applied and (b) without reflection strength. (c) Shows a comparison between real Chirp Sweep 3 traces and the synthetic trace. * indicates a distinctive negative reflector which corresponds to a silty clay layer in the core.

#### **5.2.3.2.** *Ryde Middle Bank and West Solent Data*

No core or grab were obtained from Ryde Middle Bank, however, the sand is generally accepted to be of medium to coarse sand (Section 4.2.4.1.). From Figure 26, the difference in detail between the Boomer (a) and Chirp (b) profile (with reflection strength applied) is remarkable. Although Boomer sources supposedly have a much better penetration, and Chirp sources often fail to penetrate coarse sediments, the Chirp profile, acquired with Sweep 2, still depicts a palaeo-channel under the sand bank very clearly (at a depth of 18 m beneath the seabed). This channel is hard to distinguish on the Boomer data. Higher up in the profile, both datasets show a second buried channel to the left of the sand bank, but again the Chirp data visualises it better. Finally, on the Chirp section, a horizontal stratification is visible in the sand bank itself, while the Boomer profile does not resolve any horizontal reflectors.

Similarly, Chirp II data acquired over the west Solent block (Section 4.2.4.2.) consistently penetrates through a thin < 3 m layer of gravel and sand and then some further 20 m in to Eocence – Oligocene bedrock (Figure 10). Although qualitative in comparison it does show that under certain conditions Chirp II is capable of pentrating coarser stratigraphies.

#### **5.2.3.3.** *Gravel bar deposits*

For the final coarse grained environment, a gravel bar deposit has been surveyed. This gravel bar is part of the same palaeo-channel system off Littlehampton and data has been acquired with Boomer and the three Chirp sweeps. As for the sand bank, the comparison is limited to a visual evaluation of the seismic profiles.

Within the gravel bar the Boomer data shows inclined reflectors, downlapping onto the base of the palaeo-channel (Figure 27a). None of the Chirp profiles, with or without reflection strength applied, depict any structures within the gravel deposit. Even the low frequency Sweep 3, the hypothetical challenger for the Boomer sources, was unable to penetrate through the gravel on the seabed (Figure 27b).

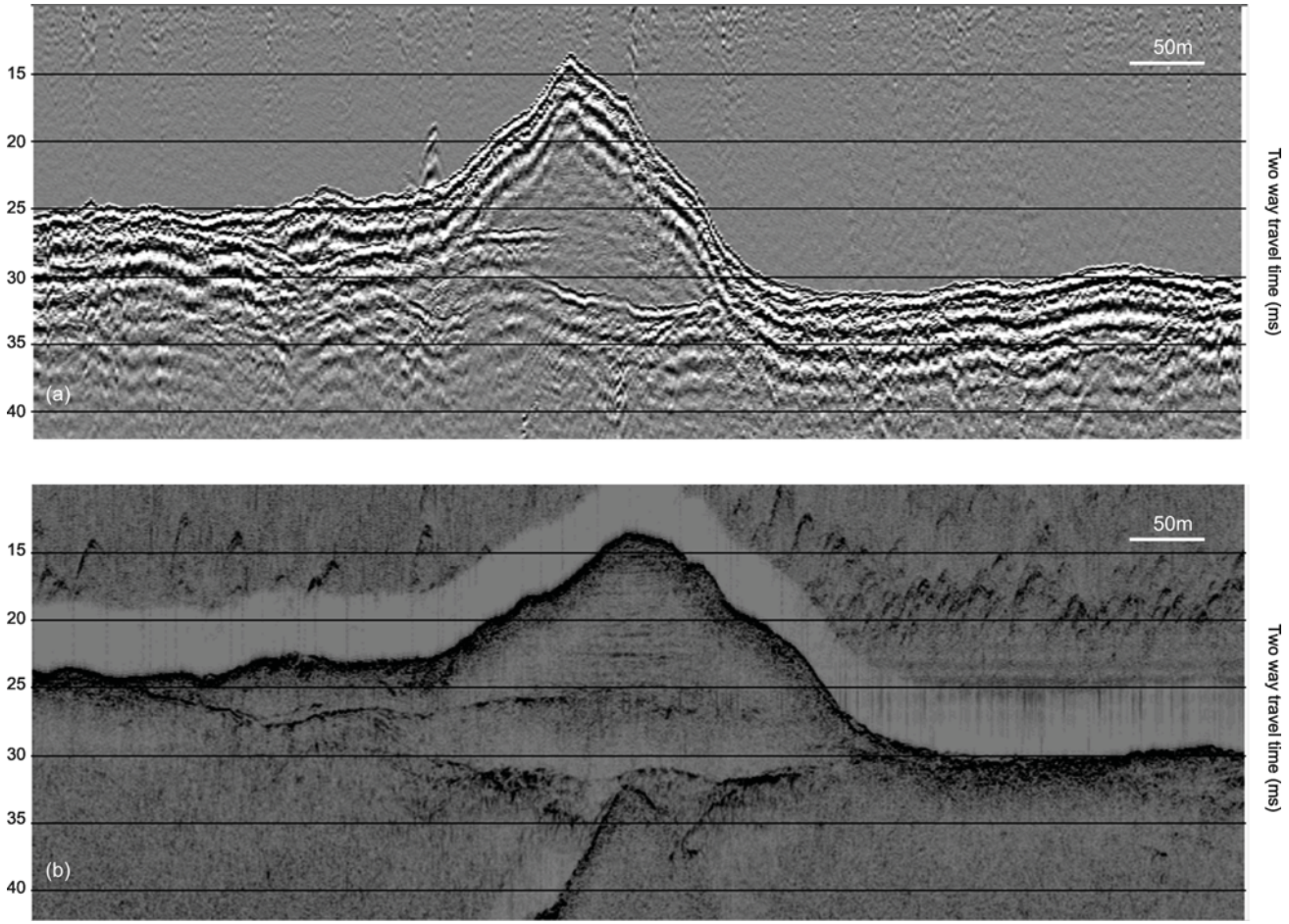


Figure 26: Seismic profile over Ryde Middle Sand Bank acquired (a) with a Boomer source and (b) with a Chirp system using Sweep 2.

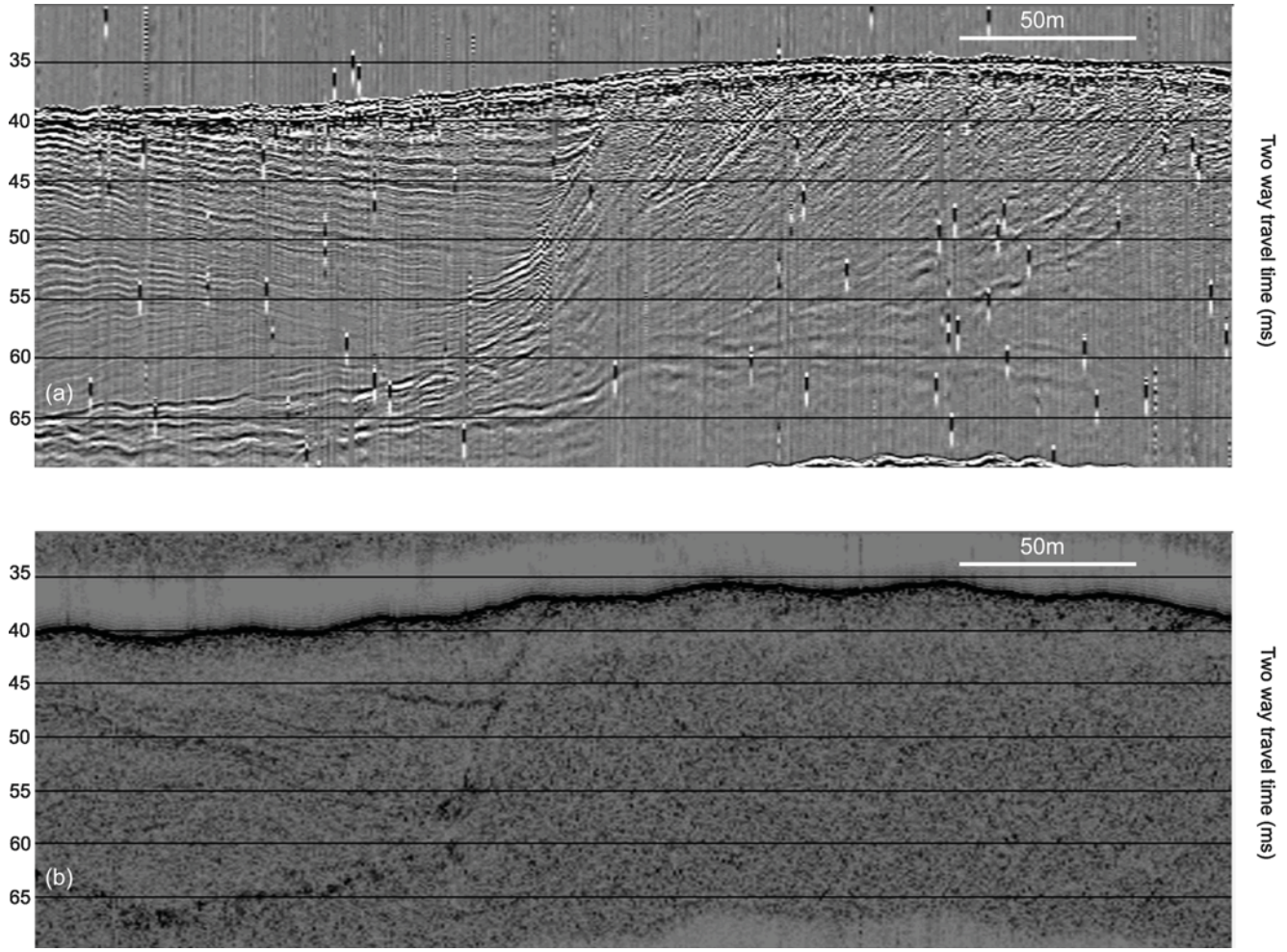


Figure 27: Seismic profile over a gravel bar deposit acquired (a) with a Boomer source and (b) with a Chirp system using Sweep 3. Note the dipping reflectors in the Boomer section (a) versus acoustic blanking in the Chirp profile (b).

### 5.2.4. *Discussion*

One of the main goals of the development of Chirp systems and their frequency modulated sweeps was to build a sub-bottom profiler with a wide bandwidth to ensure optimum penetration and decimetre resolution (Schock and LeBlanc, 1990). Since Boomer is known to be capable of penetrating coarse grained stratigraphies fairly easily, qualitatively comparing Boomer and Chirp data over identical sites can test the 'optimum penetration potential' of Chirp. Examination of the ability of the sources to image the channel base (Figure 22-25) shows that penetration of the Boomer source undoubtedly surpasses that of the Chirp source for this site. Only Sweep 3, with its relatively low fundamental frequency, images the base of the channel very clearly. Despite the inconsistent ability of the Chirp source to penetrate coarser grained sediments, the example of Ryde Middle Sand bank demonstrates that the newly developed transducers, in this case using Sweep 2, are able to penetrate the coarse sand to the same depth as the Boomer source, and, further, are capable of depicting a more detailed picture of the finer stratigraphy. However, in even coarser deposits, i.e. marine gravels (Section 5.2.3.3.), the Chirp source loses the ability to penetrate the seabed. Stevenson et al. (2002) demonstrated that the presence of material large enough (>3cm) to act as point scatterers, greatly increases attenuation, leading to a deficit in energy in the Chirp source sweep, which reduces its ability to penetrate through the gravel. The Boomer wavelet, with its higher power, lower frequency and, consequently, longer wavelength, is less affected by this possible scattering and therefore will experience less attenuation. This explains the total blanking seen in the Chirp profile of the gravel bar deposit under the seabed, while the Boomer source images dipping reflectors. In general, despite the best efforts of manufacturers to ensure optimum penetration with Chirp sources, these still cannot compete with the Boomer source in terms of penetration.

In practical terms, the resolving power of the two systems can be verified by analysing seismic traces of a complex stratigraphy such as found in the palaeo-channel described earlier. To the authors' knowledge, this is the first time that theoretical vertical resolution has been tested against real data and calculated synthetic seismograms. Plets et al. (in preparation) have already compared theoretical values (Widess, 1973; Clay and Medwin, 1977; Kallweit and Wood, 1982; Widess, 1982; Quinn, 1997) with resolution values obtained from a modelling exercise for a number of different Chirp sweeps. In the model, two spikes of equal amplitude are moved apart in small steps and convolved with the Klauder wavelet of the Chirp sweeps, after which an envelope function is applied. The availability of seismic profiles combined with core data can now allow further quantitative comparison with these theoretical and model values. Minimum vertical resolution of the real data was estimated by counting reflectors of equal polarity from the real traces over a certain depth range. The same procedure has been repeated for the modelled synthetic trace.

Since it has been demonstrated that applying reflection strength to Chirp Sweep 1 and Sweep 3 data enhanced stratigraphic interpretation, only their envelope function was considered for comparison of vertical resolution. Table 4 shows the results from this experiment, from which three observations can be made. Firstly, vertical resolution in the real data is never as high as the theoretical expressions or models predict. Secondly, vertical resolution estimated from the synthetic data is very similar to the real data for all Chirp sweeps; for the Boomer data there is less of an agreement due to a broader, more ringy output pulse than originally anticipated for the synthetic seismogram modelling. Finally, the real data, the synthetic seismograms and the

theoretical expressions/model values all exhibit the same pattern of increasing vertical resolution. i.e. Chirp Sweep 2 has greater vertical resolution than the Boomer source which in turn is better than Chirp Sweep 3, while Chirp Sweep 1 has the lowest resolution. The poorer resolution in the real Chirp data is simply caused by the fact that many thin layers, each with different reflection coefficient values, interfere with each other when convolved with the source sweep, while the theoretical expressions and model are simplifications of a reflection coefficient series with only two spikes of equal amplitude. These thin layers, which are also present in the real sedimentary column, are not necessarily due to changes in lithological boundaries, but can indicate changes, mainly in bulk density, within the same lithological unit. Nevertheless, these changes can be of geological importance e.g. for the interpretation of the internal architecture of larger structures such as channel in fill.

| | Theoretical expressions | | Model | Seismic data | | Synthetic data | |
|---|---|---|---|---|---|---|---|
| | Min | Max | | Reflection Strength | No Reflection Strength | Reflection Strength | No Reflection Strength |
| Boomer | 4cm | 25cm | - | - | 80cm | - | 35cm |
| Chirp Sweep 1 | 4cm | 85cm | 52cm | 200cm | - | 150cm | - |
| Chirp Sweep 2 | 2.5cm | 15cm | 12cm | 40cm | 22cm | 46cm | 31cm |
| Chirp Sweep 3 | 4cm | 51cm | 38cm | 150cm | - | 120cm | - |

Table 4. Quantitative comparison of the vertical resolution for theoretical expressions, modelled values and real and synthetic data.

### 5.2.5. *Conclusions*

This part of the project provided the opportunity to quantitatively compare the practical penetration and resolution of a Boomer pulse and a selection of Chirp II sweeps in coarse grained stratigraphies. The results of this study show that for gravel deposits none of the Chirp II sweeps had the capability to penetrate reliably. However, these quantitative results contrast with the qualitatively interpreted data from the East and West Solent which demonstrates consistent penetration through thin (< 3 m) sand and gravel horizons as well as excellent penetration (up to 18 m) through purely sandy deposits. Of the three Sweeps, Chirp Sweep 2 provides the best resolution of the four sources, with this being optimized when no reflection strength is applied. In conclusion Chirp Sweep 2 has been shown to provide the best resolution and penetration data in sand and finer stratigraphies whilst the boomer source is still the most reliable for thick gravel based stratigraphies.

## 5.3. Characterisation of buried inundated peat on seismic (Chirp) data, inferred from core information (Plets, Dix, Bastos and Best)

### 5.3.1. *Introduction*

The following text is based on a paper submitted to a Special Edition of Geoarchaeology:

Crux to many palaeo-landscape reconstructions is the identification and analysis of peat horizons. Peat is an organic sediment, consisting mainly of undecomposed or partially decomposed vegetation. It is formed in a water-saturated (anaerobic) environment where organic substances are not completely degradable and, therefore, accumulate as an organic soil (Bozkurt et al., 2001). Peat provides a wide range of essential data useful for archaeological site interpretation. Its successful identification and analysis can provide: chrono-stratigraphic index points; vegetational and proxy-climatic records; a reliable indicator of sea level rise; and a source of well preserved organic and non-organic archaeology.

The high organic content of peat and its good preservation of pollen and spores make it ideal for dating. Radiocarbon dates combined with the knowledge that peat represents intervals of stable or falling sea level and that silt records episodes of rapid rise, means that stratigraphers can construct or update local relative sea-level curves (e.g. Behre, 2004; Cooper et al., 2002; Fedje & Rosenhans, 2000; Waller & Long, 2003). Consequently, from an archaeological perspective, a buried peat layer may represent a fossil coastal land surface. Moreover, archaeological investigations on land indicate that peat marshes have been favourable occupation sites since early prehistory because of their proximity to fresh-water sources and the fact that they constitute terrain suitable for grazing, salt-making, hunting, wild-fowling, fishing and reed-cutting (Allen, 2000; Fedje & Josenhans, 2000). Peat also has a high preservation potential for both non-degradable and, more importantly, degradable artefacts, often in primary context and is easily radiocarbon dated. As Coles (1986) puts it “Peat is a sealed deposit of information”. On top of that, plant remains in peat provide the archaeologist with information to reconstruct palaeo-environments and palaeo-climates, and thus allows sites and artefacts to be placed within a broader context.

The majority of studied Late-Pleistocene and Holocene peat layers are acquired by coring or excavation on land (e.g. Behre, 2004; Coles, 1986). However, during the Last Glacial Maximum (22.000 – 18.000 $^{14}$C BP), the global eustatic sea-level was on average 120 m below present-day levels and climatic amelioration in the Late Pleistocene and Holocene resulted in a trend of gradual sea-level rise with episodes of still-stands and occasional sea-level falls. Hence, over the last 10000 years, the present day continental shelf has undergone different stages of swamp and marsh evolution with associated peat formation, lagoonal, brackish, tidal flat sedimentation and, finally, total inundation with the development of the present shallow marine conditions (Gerdes et al., 2003). Consequently, it is probable that Late-Pleistocene and Holocene peat layers and their associated palaeo-landscapes are now situated on the continental shelf, buried under marine sediments. Records have been obtained from offshore cores (e.g. Wessex Archaeology, 2004) but they tend to be scattered finds which are frequently difficult to place in their wider environmental context.

Section 5.3. will demonstrate that peat horizons buried in unconsolidated marine sediments have a characteristic acoustic signature enabling them to be detected and mapped using high-resolution sub-bottom profilers. The ability to not only identify such horizons at depth beneath seabed but produce three-dimensional reconstructions of these surfaces will significantly enhance our understanding of these deposits with the archaeological and geological record.

It is also worth noting that since peat is a very porous and permeable material, (auto)compaction under overburden load is an irreversible attribute that cannot be ignored (Allen, 2000). From an engineering perspective, such high compressibility causes construction difficulties and foundation problems (Nichol, 1998), making the acoustic characterization of such horizons of significant importance to the offshore engineering industry. Further, peat and any sediments with high organic concentration are potential contaminants to aggregate resources and therefore the ability to identify them prior to aggregate extraction can significantly increase yield.

### 5.3.2. *Methods*

The data used for the acoustic characterisation combined core data acquired by Wessex Archaeology from the outer section of the palaeo-Arun river (Section 5.1.) and Chirp II data acquired by SOES. The core and Chirp II data were processed following the methods described in Sections 5.2.2. and 5.2.1.2. respectively. Further, the construction of a synthetic seismogram followed the method also described in Section 5.2.2..

### 5.3.3. *Results*

The core used for this part of the project was taken from the edge of the Arun palaeo-valley and comprised of a fining upwards sedimentary sequence, overlain by a 15 cm surficial gravel unit (Figure 28). The sediment at the bottom of the sequence is a uniform unit of very fine sand, progressing into about 1.5 m of silty very fine sand and more silty clay layers. The top 3 m of the sequence consists mainly of silty clay within which three easily distinguishable peat layers were found (P1, P2 and P3). The two lower peat layers (P2 and P3) are separated only by a 6 cm thick silt layer. From the available core data, it was possible to create a reflectivity series (Figure 28), from which it was clear that each peat layer corresponds to a strong negative peak. A strong positive peak follows each of these negative peaks at the boundary of the peat and the underlying silty clay. Except for these large peaks, the reflectivity coefficients are generally low.

By convolving and correlating the estimated reflectivity series with the original Chirp sweep (Equation (5): Section 5.2.2.), a synthetic seismogram was constructed (Figure 29). In this theoretical synthetic seismogram, each peat layer is resolved and is represented by a strong negative reflector. However, application of reflection strength (envelope) to the synthetic results in decreased resolution. In the case of P1, the envelope's peak is situated beneath the peat layer; in the case of P2 and P3, a single envelope includes both layers and, again, the underlying silty clay layer is accentuated most.

Unfortunately, the seismic data acquired over the site, has few good traces directly over the core location area (Figure 30). Nevertheless, two very distinct, strong dark, reflectors are clearly seen on the reflection strength data (Figure 30a) immediately

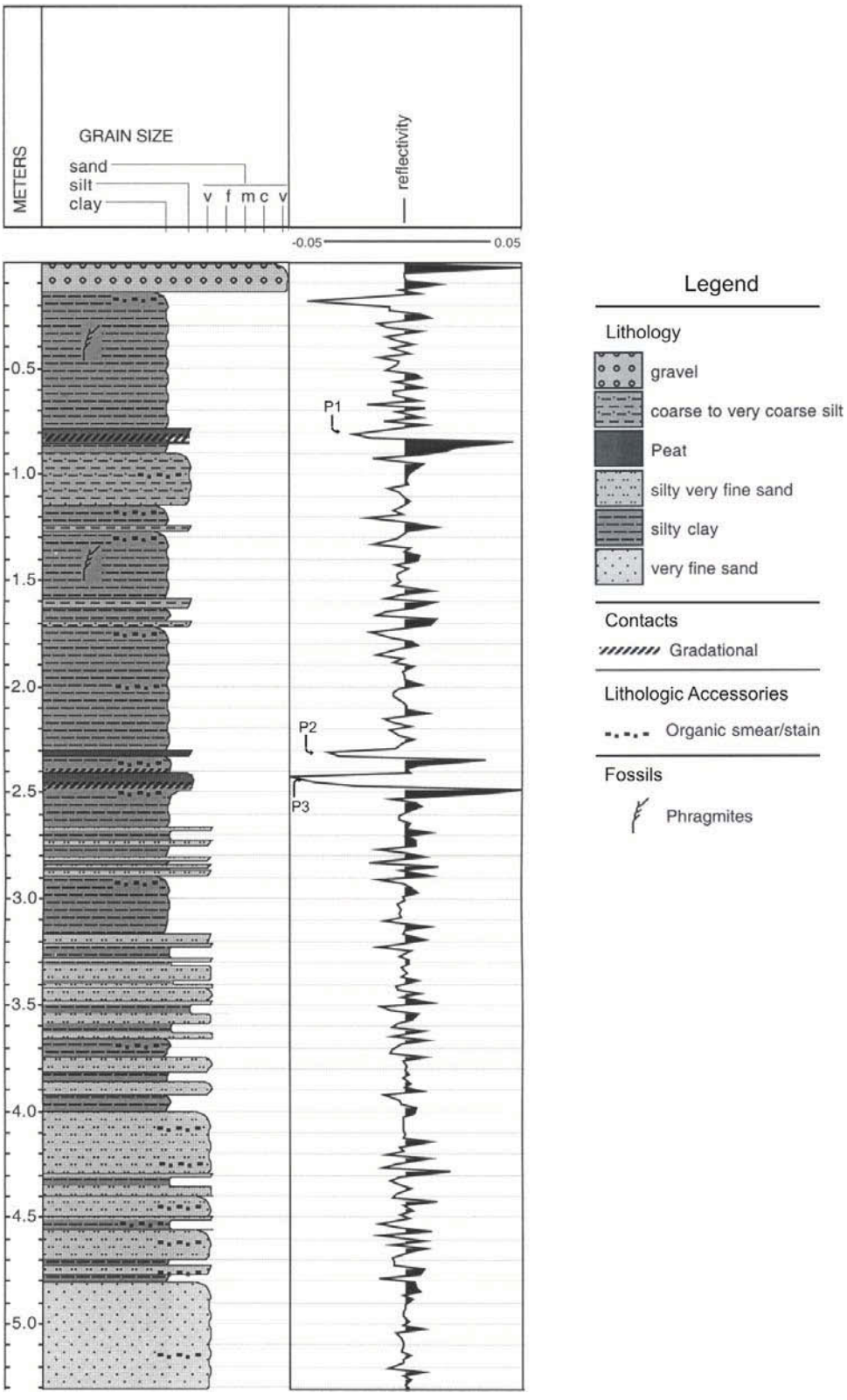


Figure 28: Log of the core recovered from the edge of the palaeo-valley. Sedimentary features and the reflectivity series are shown. P1, P2 and P3 indicate peat layers (see Figure 29 and Figure 30 for further analysis).

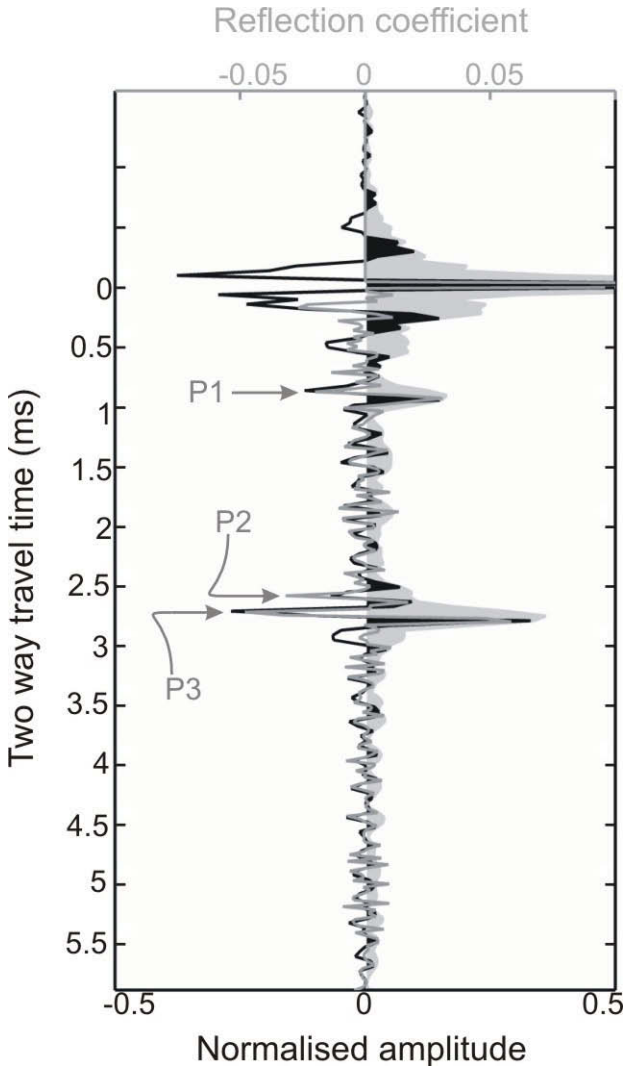


Figure 29: Synthetic seismograms constructed for the peat core, convolved with the Chirp Sweep 2. The grey line represents the reflectivity series as seen in Figure 1; the black line is the synthetic seismogram; and the dark grey envelope shows the application of reflection strength on Chirp data. P1, P2 and P3 indicate peat layers.

adjacent to the core location (white arrows). From comparison with the theoretical synthetic seismogram (Figure 29) these strong reflectors interpreted as being a combination of the peat and the underlying silt. Furthermore, it should be noted that the envelope seems to accentuate the peat-underlying silt boundary more than the peat layer itself. The image without the reflection strength (Figure 30b), on the other hand, clearly shows a bright reflector between two hard, dark reflectors. Even more promising is the presence of two closely spaced white reflectors in some parts of the lower peat layer (arrows Figure 30b), which are interpreted as being P2 and P3. To verify this, six individual traces were extracted from the seismic profile to be compared with the synthetic seismogram (broken white box in Figure 30b). Although the traces are not positioned exactly at the core site, an acoustical characterisation of the peat layers is still possible by comparing the reflector response of peat in the synthetic seismogram with the characteristic features, of the reflectors associated with P2 and P3, seen on the seismic data. This is done by simply shifting the synthetic trace down until the negative peaks depicting the peat layers correlate with the strong

negative reflectors of the seismic data. All negative spikes representing the three peat layers can easily be extrapolated to the real traces and match up perfectly with similar negative reflectors (Figure 30c). As predicted by the theoretical model (Figure 29), resolution decreases when the reflection coefficient is applied. Although the envelope function concurs rather well with P1 in the real traces, P2 and P3 are no longer resolved after using the reflection strength operation.

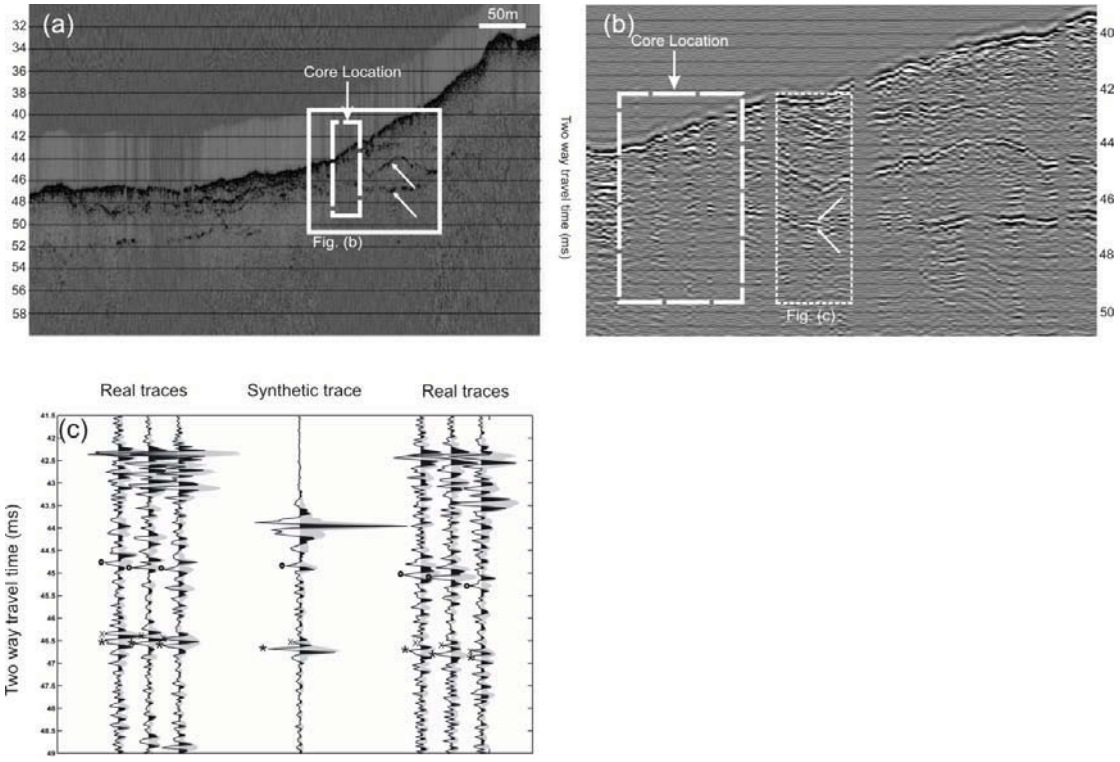


Figure 30: (a) Processed (reflection strength) seismic Chirp data of the palaeo-valley with location of the vibro-core position (with an error of 15 m on either side of a central coordinate). (b) Detail of the core location, without reflection strength applied. (c) Shows a comparison between Chirp traces extracted from the seismic data and the synthetic trace. O = Peat layer 1, X = Peat layer 2 and * = Peat layer 3.

### 5.3.4. *Discussion*

No information on the geotechnical properties of buried, inundated peat could be found in the literature. With the help of vibro-cores and synthetic modelling we have finally been able to identify the impedance response of peat and verify its typical acoustic signature in seismic profiles. The peat layers found in the Arun core, taken from the edge of the palaeo-valley, correspond to very large negative reflectors. In correlated Chirp data, acquired with a broad bandwidth sweep and with no reflection strength applied, a peat layer is depicted as a bright white reflector sandwiched between two black reflectors.

As described above the reflectivity series is dependent on the impedance response of sedimentary layers which in turn is determined by its acoustic velocity and bulk density. The density of a sediment is primarily controlled by its porosity, with density decreasing as porosity increases. It is known that an increase in percentage of carbon results in an increase in the specific pore volume (Emerson & McGarry, 2003) i.e. the

presence of organic matter gives the sediment a more open granular structure. Since peat is an organic rich sediment, its porosity is higher than the surrounding sediments, and, therefore, can easily be discriminated from the other sediments by its low density in a density profile. It is this density decrease that dominates the creation of the negative reflection coefficient in the reflectivity series. Typical values for the bulk density of peats are not common within the literature but Hobbs (1986) suggests values of between 950 to 1300 $kgm^{-3}$ for UK mire peats (although the effect of further burial and compaction beneath siliciclastic material is not discussed). Industrial geotechnical measurements of peat from two cores in the Southern North Sea provided density values of 1340$kgm^{-3}$ and 1080$kgm^{-3}$ and corresponding porosity values of 76% and 89% for two buried peat layers (METOC Ltd, pers. comm.). These values are comparable to the densities record within the Arun core (c. 1330 $kgm^{-3}$) and strengthen our interpretation that the low density / high porosity values of buried Holocene peat in a marine environment, relative to the sediments they are buried in (which have typical bulk densities of between 1600 $kgm^{-3}$ and 2000 $kgm^{-3}$: Bachman, 1985), results in an identifiable bright reflector in the acoustic data.

However, this large negative reflector seen in the reflectivity series in the peat core (Figure 28) is not a unique signature. Any significant drop in density or acoustic velocity, can create a spike similar to that seen in the peat core. Nonetheless, the environmental settings in which peat can be found should not be forgotten. Most buried peat layers of Holocene date, presently located in shallow marine environment, formed on marshes and mudflats which are dominated by a range of silts and silty clays (Allen, 2000). Generally, these fine-grained sediments already have a relatively low density, high porosity and low acoustic velocity. A significant drop in this density resulting in a strong negative reflector must be attributed to an increase in organic matter and, thus, is a good indicator for peat. Sand and gravel deposits in coastal sequences occur only as laterally restricted bodies such as channel in fills and beach barriers (Allen, 2000). If a peat layer were to be found in a more sandy sequence (e.g. Cooper et al., 2002), the reflection coefficient would be even more negative since sand has a higher bulk density and higher acoustic velocity than silts and clays. So, before interpreting a large negative reflector on a seismic profile as a peat layer, one must bear in mind the geomorphology and sedimentary palaeo-environment of the area. In the case of a palaeo-landscape with indications of relict fluvial systems, bright reflectors within the sandy channel fill could be attributed to sediments with a higher carbon content, but well developed peat layers are more likely to be found in the alluvial valley flanking the channel. This plain or valley is generally characterised by low energy sedimentation, i.e. muds and silts, and marshland vegetation, ideal for the formation of peat. Bright negative reflectors within these geomorphologic environments almost certainly suggest the presence of peat, since it is the only sediment in such settings that can have a lower bulk density than the mud/silt itself.

The implications of this work are already being utilised for the re-assessment of the Late Quaternary history of the Solent Estuary, Hampshire, UK. Re-analysis of a decade of seismic data from this region has identified this acoustic signature throughout the margins of the currently submerged sections of the Eastern Solent (Figure 31). Core data is not currently available from this area but interpretation of the acoustic facies and knowledge of the surficial sediments suggests that the region represents a similar sedimentary environment to that of the palaeo-Arun river. The interpreted “peat” reflectors in this area describe five lateral traceable horizons, located at the margins of the bedrock incised palaeo-Solent River, and at depths

between -5.5 and -29.2 m OD. Currently, the deepest recorded and dated peat horizon within the Solent system occurs at -9.4 m OD and is dated to 7320 cal BP (Waller and Long, 2003). We therefore hypothesise that the sediments of the East Solent contain a potentially detailed record of Late-Glacial to early Holocene pre-inundation land surfaces in an area that has a dearth of such information. This information is currently being worked in to the final draft of the Geological Society of London paper that is based on the data described in Section 4.2..

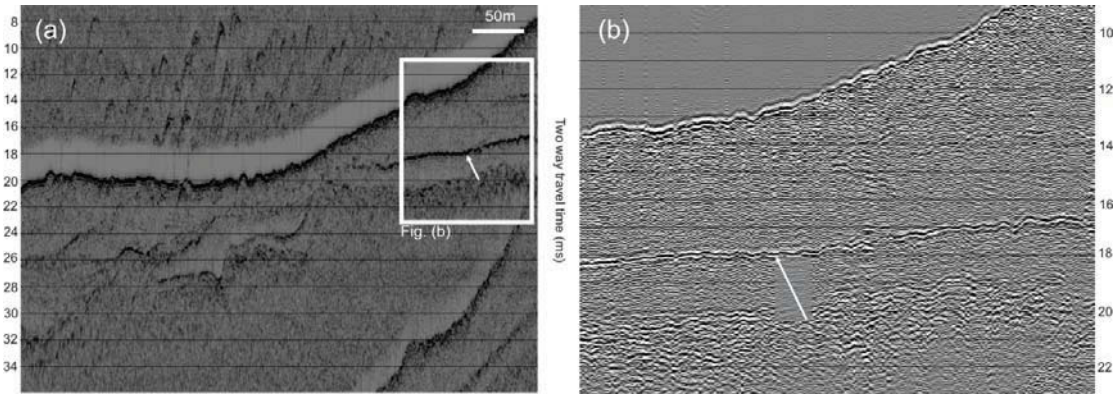


Figure 31: (a) High amplitude reflector (white arrow), believed to be a peat horizon, detected on Chirp data (with reflection coefficient) acquired in the East Solent. (b) A detail of the peat horizon, without reflection coefficient applied, shows a bright, negative reflector (white arrow).

One of the most important implications of this study relates to future work on the continental shelf, be it for archaeological or industrial purposes. At present, the modelling of peat surfaces in the coastal zone is still mostly done by coring. Due to correlation issues between sites, cores have to be obtained at regular intervals, which is a costly, time-consuming exercise (Bates and Bates, 2000) and relatively inaccurate. Now that the seismic characterisation of peat has been identified, large areas that potentially contain peat layers, can be surveyed in relatively short time periods with sub-bottom profilers. By surveying with relatively narrow line spacing (10 – 50m) and by digitising these horizons from the processed data, mapping each layer out and reconstructing a three dimensional grid of these fossil coastal land surfaces can be done relatively easily. This process could even help archaeologists to determine locations of high archaeological potential, prior to coring.

### 5.3.5. *Conclusion*

Peat is an important sedimentary facies, which can provide essential information for archaeological, geological and engineering research. Although terrestrial peat has been studied in depth, there is a general lack of geotechnical data for buried inundated peat horizons. Such horizons are believed to be detectable with marine high-resolution sub-bottom systems, but so far there has been no evidence that high amplitude reflectors, seen in palaeo-river environments, are indeed related to peat.

The availability of a core with peat horizons, and seismic Chirp data acquired within the same area made it possible to study the impedance response of such peat layers with in fine to medium grained silici-clastic sediments. Such an analysis suggests peat horizons buried within typical marine sediments produce a strong negative peak in the reflectivity series, mainly due to the very low densities of these

organic accumulations. Comparing an analytically created synthetic seismogram from such a reflectivity series and Chirp traces acquired in situ clearly demonstrates that high resolution seismic systems are able to resolve and characterize peat layers found buried beneath the seabed. Moreover, it gives us confidence to interpret similar reflectors seen on sub-bottom data in analogous environmental settings (e.g. Solent River) as indicators for peat horizons. The knowledge of occurrence of peat layers in specific contexts and the ability to detect these layers in shallow marine environments using sub-bottom profilers, equips the archaeologist, engineer or geologist with a cost-effective, quick method to reconstruct palaeo-land surfaces.

# 6. PHASE 3: 3D Chirp for the archaeological mapping in aggregate grade deposits

## 6.1. Introduction

Following discussions with Ian Oxley (Head of Maritime Archaeology, English Heritage) and the Project Officer, it was decided to undertake the first true high resolution 3D Chirp survey of an archaeological site, on the wreck of the first *Invincible*. Although not in an active dredging area it is partially buried within the sandy sediments of the East Solent, which are very similar to those that had been consistently penetrated with the new Chirp II sweeps, as described in Sections 4 and 5. The *Invincible* sank in unusual circumstances on Horse Sand Spit in the East Solent on February 19, 1758. She has been the subject of extensive historical work (Lavery, 1988: the historical descriptions given here are all from this text unless otherwise stated) and short periods of intense archaeological investigation (Bingemann, 1981; 1985; 1990; 1996). This combination of a wealth of historical data and a lack of extensive excavation made her an ideal test site for geophysical exploration. The site had also been subject to recent geophysical study by Wessex Archaeology who were able to provide recent swath bathymetry imagery, which was used to plan the survey.

It should be emphasised that this was not only the first successful 3D Chirp survey of an archaeological site but was also the first ever successful 3D Chirp survey. This dataset has therefore been the central focus of our research team at the National Oceanography Centre over the last three years, as each stage of the process (acquisition, processing, interpretation and visualization) has been in continual development throughout this period. However, through the analysis of this dataset and two others (one of which was acquired over the Grace Dieu wreck site: Section 6.3.) we have now developed a system that is capable of reliably collecting a true 3D dataset. The research has been so successful that we are now in the commercialization stage with our industrial partner GeoAcoustics Ltd.. We believe the system will not only radically change the abilities of marine archaeologists to non-destructively and non-intrusively investigate buried sites but which is also attracting significant commercial interest in the aggregate and a wide range of other marine industry sectors. This would not have been possible with out the contribution of the work undertaken as part of this ALSF grant.

## 6.2. Method

This section is based on the text from the published paper “Design of a 3D Chirp sub-bottom imaging system” (Bull et al., 2005; and which acknowledged the funding contribution of the ALSF programme).

Lower frequency (10-200 Hz) 3D seismic volumes have been collected for the oil industry for several decades. Although many of the principles and seismic processing algorithms are directly applicable to high frequency data, there needs to be careful consideration of the physical basis for the collection of true 3D data. The following need to be carefully considered: (1) Horizontal positioning and spatial aliasing; (2) Horizontal and vertical positioning accuracy requirements; and (3) Source signature considerations and frequency aliasing. The first two of these are discussed in detail in

the following sections, whereas the third is discussed in detail in Section 5.2. This work identified that an optimal chirp sweep, Chirp Sweep 2, for both penetration and resolution used a broad bandwidth and a sine-squared taper function. With regard to frequency aliasing, the sampling interval (40 μs) of the digital acquisition system used in this work was sufficient to ensure that the highest frequencies contained within the source sweeps (13 kHz) were over-sampled.

### 6.2.1. *Horizontal Resolution and spatial aliasing*

The horizontal resolution of seismic data indicates how closely spaced two point diffractors may be while still being distinguished. In raw data this is controlled by the Fresnel zone radius, the region over which energy scattered at depth interferes constructively at the surface. Theoretically the horizontal resolution may be improved by processing algorithms such as migration to be as low as $\lambda/2$, where $\lambda$ is the dominant wavelength, although in practice it will be limited by the range of horizontal wave numbers present in the data.

In order to apply wavefield-based methods such as migration, it is essential that the recorded energy is fully sampled in space as well as in time, i.e. that spatial aliasing of the data is avoided (e.g., Yilmaz, 1987). With a receiver spacing $\Delta x_{rec}$ in the array, and energy with wavelength $\lambda$ incident on the array at angle $\alpha$ from the vertical, this requires that:

$$\Delta x_{rec} < \frac{\lambda}{2 \sin \alpha}.$$

The receiver spacing required for this is smaller for shorter wavelengths or for incident energy that travels more horizontally. Clearly there is an additional factor that for a fixed number of channels, the smaller the receiver spacing used, the smaller will be the overall footprint of the array, and the more closely spaced must be individual sail-lines. Hence for efficiency $\Delta x_{rec}$ must be maximized while minimizing potential problems of spatial aliasing. The most likely origin for problematic aliased energy is by scattering at the seabed because, for a given recording time, the energy will travel most shallowly and have the highest amplitudes. Hence the effect of such scattered energy, including the directivities of each element in the hardware, has been modelled.

The model calculates the amplitude of the energy that would be returned from a given point on the seafloor for specular reflection at that point with a reflection coefficient of 1 and assuming no transmission losses in the water column; this will overestimate the amplitude of any possible return. In this analysis we are modeling the worst-case scenario for spatial aliasing. It is assumed that the source array and hydrophone group are centered at the same location; the actual offset between these is less than about 1m (which is small compared with typical likely water depths of 10-30m). The recorded amplitude of the frequency dependent energy returned from any given point on the seabed will be the product of the following factors: the directivities of the individual source transducer, the transducer array, the hydrophone group; and geometric spreading (Figure 32). All the directivities have been normalized by the amplitude of the specular reflection from the seabed immediately beneath the origin. The water depth and the recording time control the region over which the amplitudes are calculated; the example in Figure 33 assumes a frequency of 7.25 kHz and a water depth of 20 m.

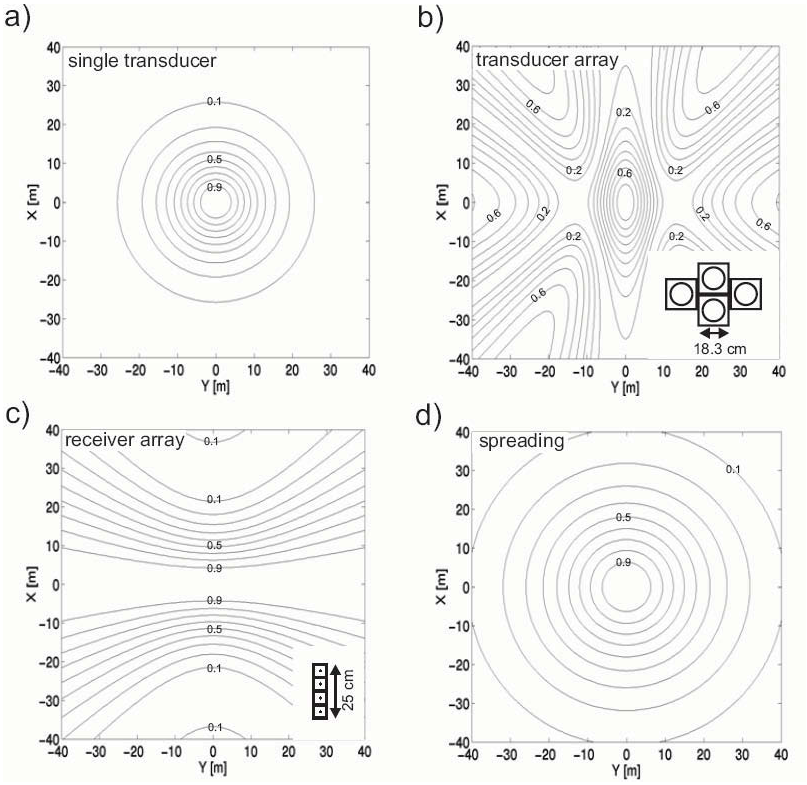


Figure 32: The modelled directivities of the component parts of the 3D Chirp system with contours of normalised amplitude. (a) The single transducer directivity (b) The directivity of the Maltese Cross arrangement for four point transducers; inset shows orientation of transducers (c) Hydrophone group directivity for a group comprising four elements at 7 cm spacing; inset shows orientation of hydrophone group. (d) The effect of geometrical spreading has spherical symmetry and is calculated as $1/r^2$.

The single transducer directivity due to the finite size of the transducers and any intrinsic effects, $D_t$, was provided by Neptune Sonar Ltd for the T135 transducers used in the system (Figure 32a). Although the discussion here focuses on a transducer configuration in which transducers were arranged as a Maltese Cross (Figure 32b), a number of other different transducer configurations were modelled including four arranged as a square, and two as a pair. The directivity of the Maltese Cross arrangement for four point transducers, $D_a$, was calculated based on the intended source array geometry (Figure 32b); the wide axis of the Maltese cross is in the y direction leading to a reduced footprint. The hydrophone group consists of four elements at 6.25 cm spacing, leading to a directivity $D_r$; the long axis of the element is oriented parallel to the x direction, so that there is no array effect in y (Figure 32c). Each individual hydrophone element is much smaller than the wavelengths used so that they may be considered omnidirectional. The effect of geometrical spreading is considered to have spherical symmetry and is simply $1/r^2$.

The final amplitude, $A$, as a function of seabed location can be calculated as

$$A = \frac{D_t \cdot D_a \cdot D_r}{r^2}$$

and is shown in Figure 33a. Note that the seabed returns with significant amplitude are limited to a zone close to the specular direction; although the transducer array

response has strong sidelobes, these are suppressed by the directivity of the individual transducers and the spreading factor. The perpendicular orientation of the long axes of the source array and hydrophone group also minimises the overall footprint.

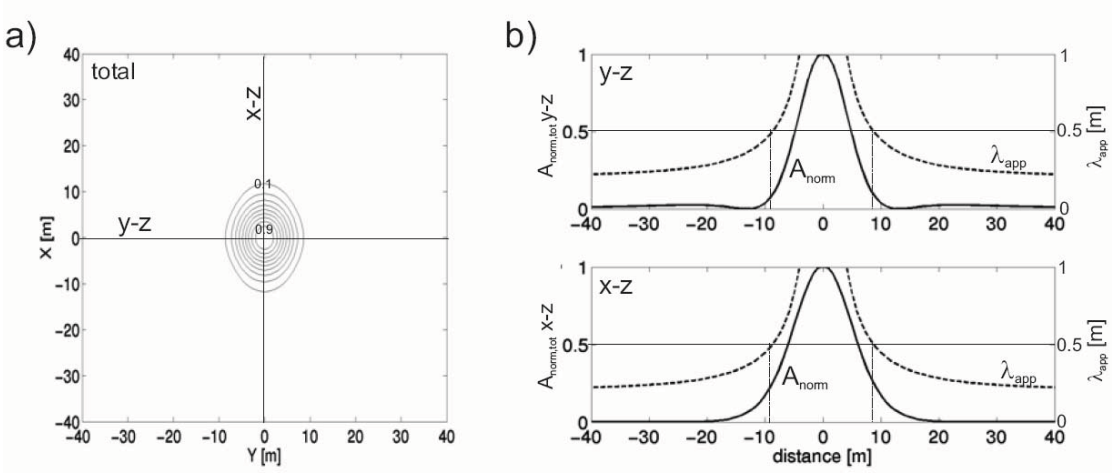


Figure 33: (a) The modelled final amplitude, $A$, as a function of seabed location with contours of normalised amplitude. (b) Cross-sections through the returned amplitude function along the x and y axes. For each point on the cross-section the apparent wavelength is also calculated. See main text for more discussion.

Figure 33b shows cross-sections through the returned amplitude function along the x and y axes. For each point on the cross-section the apparent wavelength, $\lambda_{app} = \lambda / \sin\alpha$ is also calculated. This modelling enabled the selection of an appropriate receiver spacing that would avoid spatial aliasing, but still provide a practicable solution that will enable the acquisition of a true 3D volume. Figure 33b shows that for aliased energy to have amplitudes less than 10% of that reflected immediately beneath the array if it is scattered in the crossline direction, and less than 25% in the inline direction, then apparent wavelengths of greater than 0.5 m must be fully sampled. This shows that a receiver group spacing of 0.25 m would be necessary, although this is an extreme case as we overestimate the amplitude of any recorded return. In summary, for the range of frequencies generated by the chirp source signature, it is concluded that a receiver separation of 25 cm in both x and y directions will result in negligible spatial aliasing.

### 6.2.2. *Horizontal and Vertical Positioning Accuracy Requirements*

The accuracy required for the positioning of the source and receiver elements of the 3D chirp system depends on the characteristics of the source signature used. In order to ensure that requirements are met for all sweeps, the source signature which produces the tightest auto-correlation function (Klauder wavelet) to be used with the system is considered. This signature Chirp Sweep 2 has a linear Instantaneous Frequency Function on a frequency band from 1.5 – 13 kHz and a sine-squared taper function with a mean frequency of 7.25 kHz.

The required accuracy in the vertical direction results from the necessity to stack seismic traces in a common mid-point bin defined in the geometry assignment during the 3D data processing. In order to avoid destructive interference by stacking the seismic traces, the error in its associated vertical positions need to be smaller then the distance between the main-lobe peak and the side-lobe trough of the signature's Klauder wavelet. This distance is 60 μs for the Klauder wavelet considered (Figure

19f), equivalent to ± 4.5 cm assuming a p-wave velocity of 1500 m/s in water. In order to reconstruct the wavefield adequately, the horizontal position needs to be known within a quarter of the wavelength, λ/4 of the highest frequency component. For the Klauder wavelet discussed, and the assumptions made, this is ± 1.45 cm. Furthermore, the positions need to be measured reliably with an update rate similar to the seismic shot rate. In summary navigational control is needed which will provide less than ± 4.5 cm vertical and less than ± 1.45 cm horizontal resolution.

#### **6.2.2.1.** *Positioning solution*

Positioning of the 3D chirp system is greatly simplified if the source and receiver elements are mounted on a plane and rigid array, so that the source-receiver offsets are known *a priori*. Given the absolute positioning accuracy required in both horizontal and vertical planes, the 3D chirp system uses a Real Time Kinematic GPS System (the Sagitta02 Long Range Kinematic, $LRK_{TM}$, GPS system) and a GPS attitude determination system (ADU5) both supplied by Thales Navigation. The knowledge of absolute position on the array together with its orientation: heading, pitch and roll allows the calculation of the absolute position of the source and receiver *element* positions. The RTK system uses a reference station with a GPS antenna at a known geographic location, sending GPS correction information via an UHF radio link to the roving station, providing the highly accurate absolute position of the roving station's GPS antenna in real-time. The GPS attitude determination is based on differential carrier phase measurements between the four antennas. One antenna is shared by the two systems.

In order to test the suitability of the system for marine work, two experiments were carried out. Firstly, to test system accuracy performance, the attitude and position were recorded in a static position over a period of time. Secondly, the system was mounted onto a catamaran and towed behind a survey vessel to simulate its application. Although the tests were completed using a catamaran rather than the final 3D chirp system, the worst-case errors in receiver element position could be simulated in a straightforward manner.

#### **6.2.2.2.** *Static test*

The GPS antennas were mounted onto a catamaran as shown in Figure 34. Antenna 1 is shared by the RTK GPS and the GPS attitude system; antennas 2, 3 and 4 are used only by the GPS attitude system. The radio-link with a local reference station was established and data recorded over a period of c. 20 minutes.

Figure 35a shows the absolute position data for Antenna 1 with the deviation of the x-, y-, and z-coordinate values from their mean value. Data from the attitude system are shown in Figure 35b showing the deviation of heading, pitch and roll for the catamaran from their mean value. Figure 35c shows the coordinates for a simulated *element* position, that is offset by 2 m in longitudinal and 2.5 m in transversal direction from antenna 1, which corresponds to the greatest offset between the GPS antenna and a receiver element on the final 3D chirp array (see later). Figure 35d shows an x-y-plot of this elements positional variation with time. The accuracy of the attitude system can be expressed as root-mean-square (rms) error, which, for the static test was 0.16˚ for heading, 0.32˚ for pitch and 0.22˚ for roll.

The *element* position error includes the error in the absolute position of Antenna 1 and the errors in heading, pitch and roll. The element position error represents the

worst-case expected error in position for a hydrophone element on the final 3D array. Hence positioning errors in the final 3D array are expected to be less than or equal to ± 0.7 cm in the horizontal direction, and ± 1.82 cm in the vertical direction. These errors are significantly less than the positioning requirement for the 3D array (± 1.45 cm in the horizontal and ± 4.5 cm vertically: Section 6.2.2.).

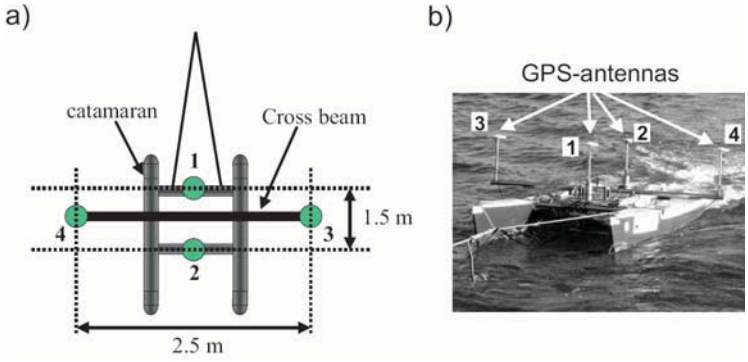


Figure 34: Experimental set-up. a) The GPS antenna positions on the catamaran as used for both the static and dynamic experiments. Antenna 1 determines the RTK GPS Position for the Sagitta02 system and is shared with the ADU5 system which additionally uses antennas 2, 3 and 4 to determine heading, pitch and roll. b) The catamaran being towed during the dynamic trials, which simulates the positioning requirements of the final 3D chirp system.

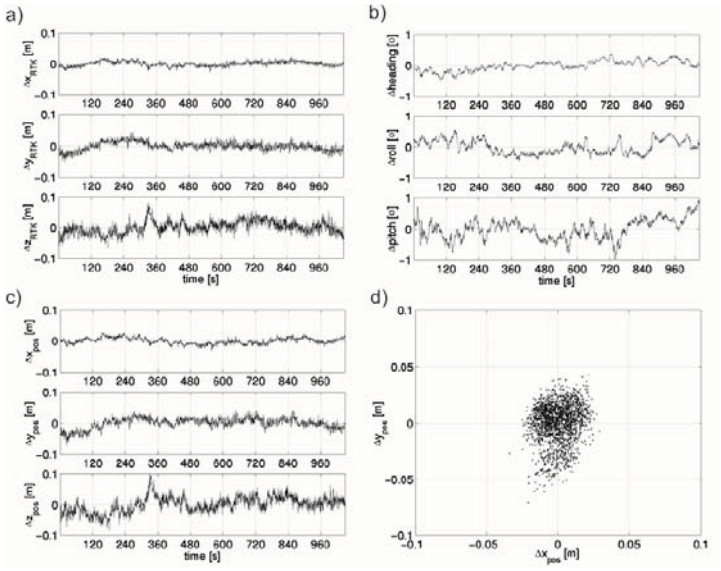


Figure 35: Static positioning experiment results using the Sagitta02 RTK ($LRK_{TM}$) GPS positioning and the ADU5 GPS attitude systems using configuration shown in Figure 4. a) The variation of the x, y and z-coordinates of Antenna 1 position from their mean value during a c 20 minutes period in which the catamaran remained static. b) The heading, pitch and roll variations for the catamaran from their mean value. c) The simulated variation of an *element* offset by 2 m in longitudinal and 2.5 m in transversal direction from the GPS antenna on a rigid plane determined from the RTK GPS position and attitude. This simulates the worst-case error in position of a receiver element on the 3D chirp system. d) The variation with time in the simulated elements position from its mean x and y position.

### 6.2.2. *3D Chirp Design and construction*

In the preceding section it has been demonstrated that: (1) for the highest resolution sweep a sampling interval of 40 μs will result in over-sampled data; (2) that a receiver spacing of 25cm in x and y directions will avoid significant spatial aliasing of the seismic data; (3) that a RTK GPS system together with an attitude system would give the required horizontal and vertical accuracy in positioning for the system. In this section the final design for the 3-D Chirp profiling system is described and illustrated.

As mentioned already one of the major problems in acquiring 3D data volumes at high frequencies is uncertainty in the position of sources with respect to receivers. The solution reported here is to use a rigid array with known source and receiver relative positions. Figure 36 and 37 show technical drawings of the 3D-Chirp system. The four transducers are shown arranged in the preferred Maltese Cross configuration, which gives enhanced directivity along-track, within the centre of the array together with the electronics bottles that drive the transducers. Careful consideration had to be given to achieving neutral buoyancy. This was solved by using a composite, low-density, reinforced foam central panel to support the transducers and electronics bottles. The design is modular so that the four transducers can be rearranged in a standard square configuration in the centre of the array, or as two pairs towards the edge of the mat to maximise ground coverage.

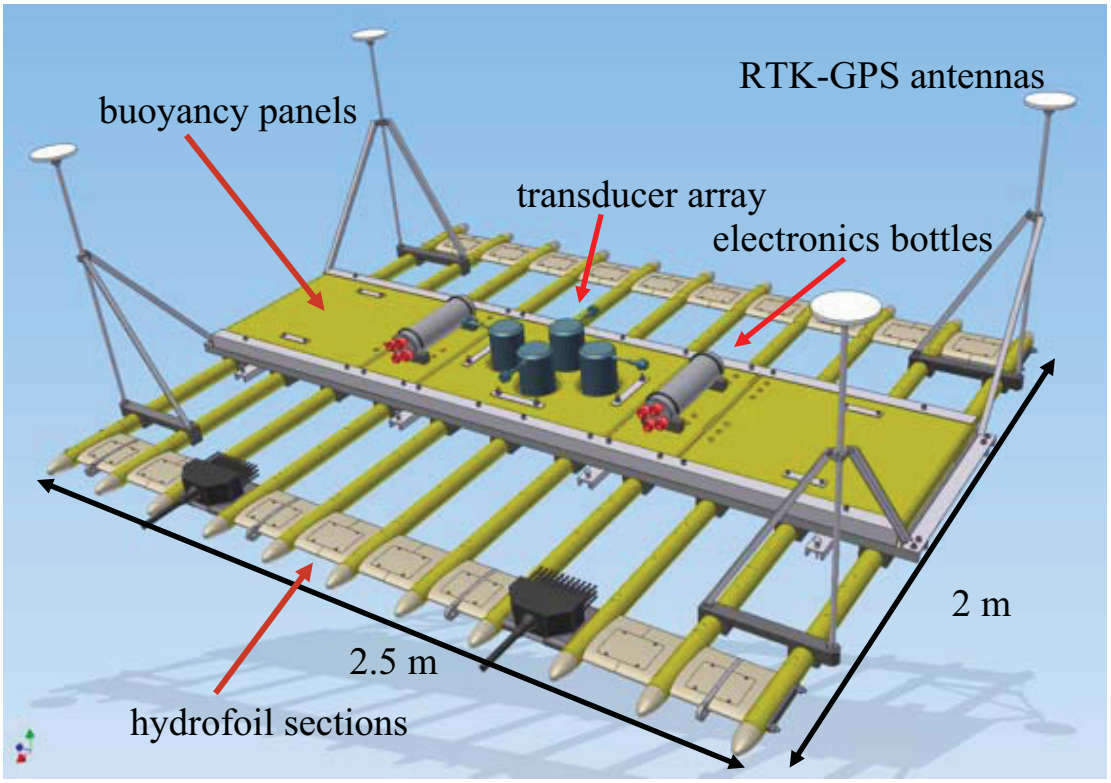


Figure 36: Top view of the 3D Chirp mat showing the key elements.

The four GPS antennas at the corners of the array provide positioning. Each of the antennas is 1 m above the top of the array, and as described previously one of these antennas provides absolute position, while all antennas are used in the attitude system to give heading, pitch and roll. Data from all four antennas is then used to produce the absolute position of each source point and hydrophone group within the array to

centimetric accuracy. This level of navigational accuracy enables not only correct within-line location of targets but also the effective merging of data from adjacent lines, including corrections for tidal variability.

Eleven longitudinal 2.25 m-long composite tubes containing the hydrophone groups are fitted on the underside (Figure 37). Each longitudinal sections contains between 4 and 6 hydrophone groups, such that there are 60 independent hydrophone groups within the array. Hydrophones positions can be changed within the array to accommodate different transducer positions. Each hydrophone group is 25 cm long and contains a pre-amplifier and four elements, each separated by 6.25 cm, which sum the arriving energy, and facilitate an increase in signal-to-noise. The design ensures that the hydrophone groups are protected from reverberation off the water-surface. The array has been designed so that hydrophone cabling is accommodated within the tubes, before being collected together within two splice blocks at the front of the array. The data is then sent up two cables to the recording system aboard the acquisition vessel.

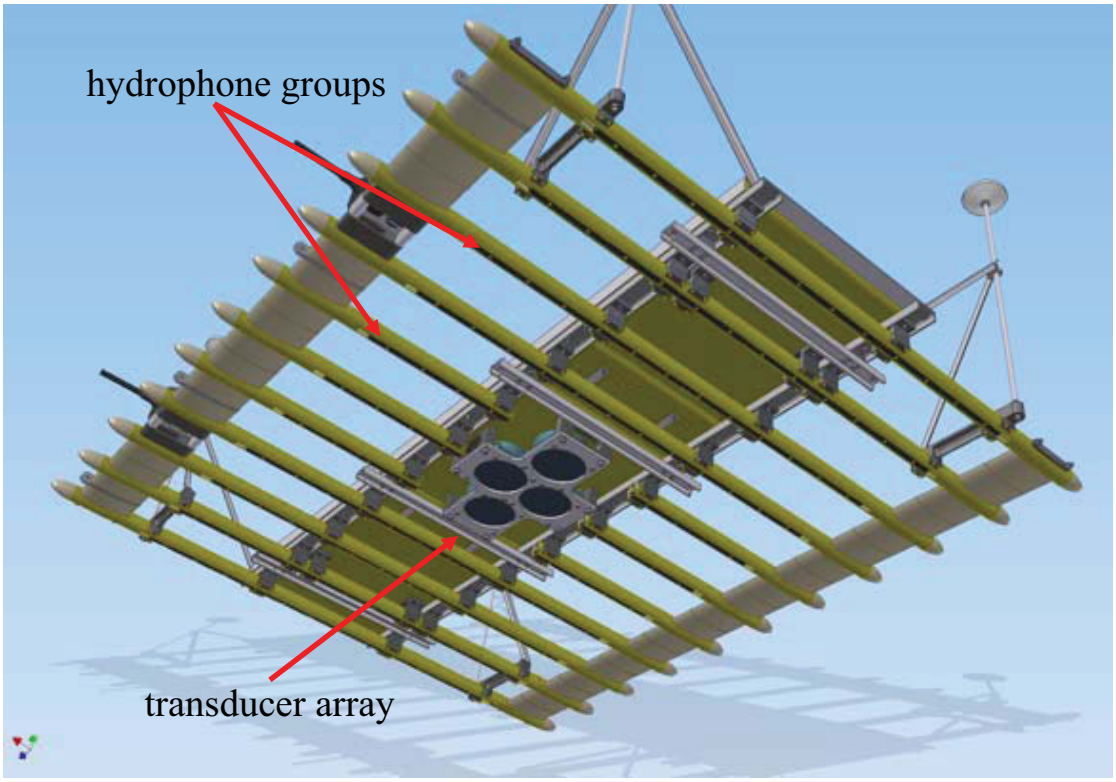


Figure 37: Underside view of the 3D Chirp mat showing the key elements.

The array has been hydrodynamically designed to tow smoothly and to ride swell and wave activity without tilting and to avoid acoustic noise generation. The total weight of the array including all elements is 176 kg and it has been designed to be deployable from small vessels (Figure 38). Trialling demonstrated that the system was neutrally buoyant and towed in a stable manner (Figure 38). The GPS antennas sit c. 0.7 m above the surface of the water with the base of the transducers and hydrophones sitting c. 0.4 m beneath the surface of the water. The system has been shown to operate in sea-states up to a Force 4 and an optimal towing speed through the water was found to be 2.0 $ms^{-1}$.

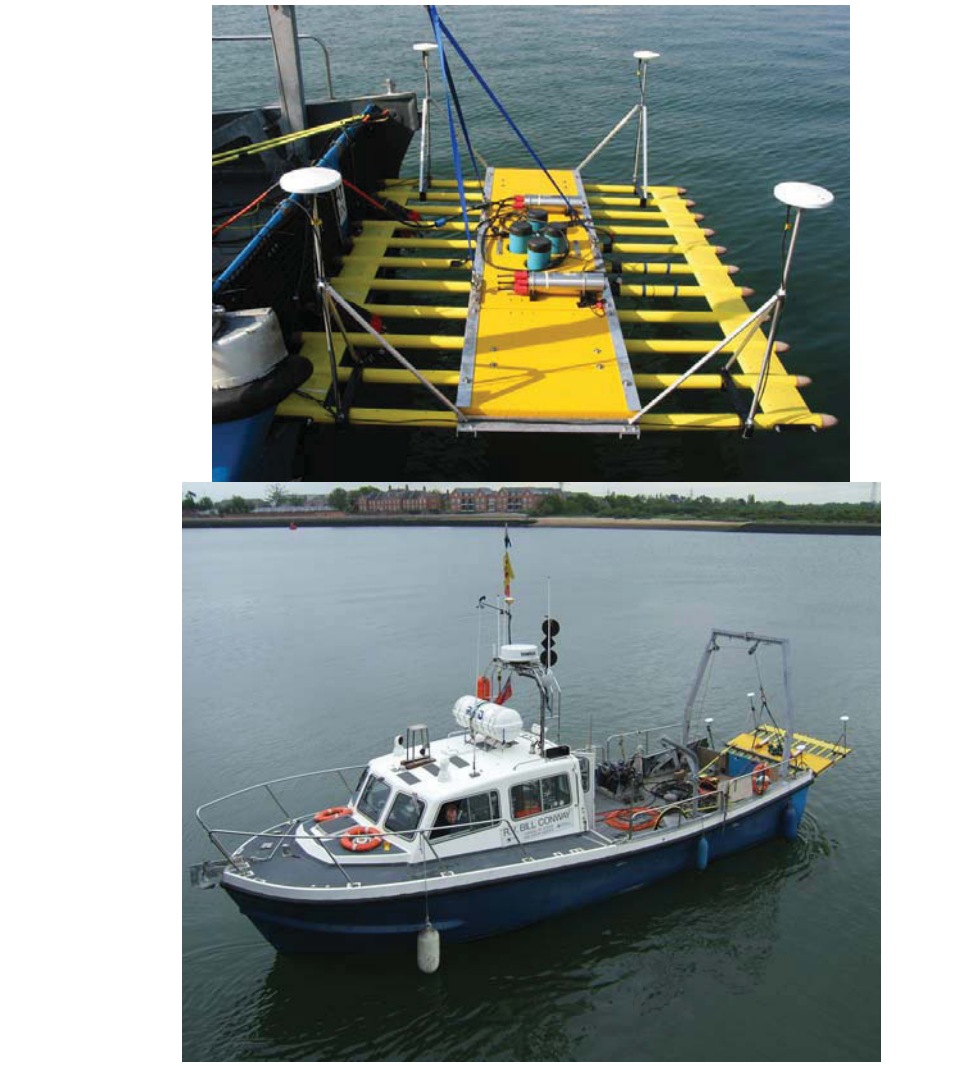

Figure 38: Top – constructed chirp mat; Middle – Chirp Mat deployed on back of small survey vessel; Bottom – Chirp Mat under tow.

The acoustic data from the system is recorded using a bespoke 60-channel logging system whilst the navigation (absolute position and heading, pitch and roll) is presently recorded separately. The seismic data is ultimately saved as standard SEGY files so the data can be processed and interpreted in standard oil industry packages. The crux of the system development and as such has caused the most development delays is ensuring the timing of the two datasets (navigation and seismic) are synchronised. This has finally been achieved through the combination of GPS clocks and two intenal clocks in the seismic logging system. These systems have to control both the shot interval of the system and the recording windows.

Once the data has been acquired the processing is split in to three stages: Geometry processing; Trace to trace processing; and either mid-point binning or 3D pre-stack Kirchoff migration. The Geometry processing has required the development of algorithms to take the single RTK-GPS absolute co-ordinate and the attitude data to calculate an absolute position for each hydrophone group for every shot in the survey. This data is then merge in to the header files of every seismic trace that has been acquired (in a single survey this can represent $10^7$ shots and so $10^8$ traces). It is though this large number of traces that make it a true 3D volume as it enables us to populate a post survey defined geometric grid (midpoint binning) to the survey data that can then be populated with a large number of traces ($10^1$ to $10^3$) to each bin. For the system we have designed, the smallest bin size we can grid to is 12.5 cm i.e. we have seismic data populating a regular grid with nodal points every 12.5 cm. In reality depending on the actual coverage (described as the fold coverage) the data can be binned at either 12.5 cm or 25 cm (or coarser if necessary). However, this should be compared to a typical 2D survey which although has similar along survey line coverage, at best you only have data every 1 – 10 m between lines and you are restricted in viewing data along the actual survey lines.

Having assigned the geometry the seismic data is then processed using 3D Promax using very similar flows as those described in Section 5.2.1.2.:

1. 'Bandpass Filtering' removes frequency components outside the frequency content of the original sweep (usually unnecessary)
2. *'Vibroseis Correlation'* correlates the raw uncorrelated data with the initial Chirp sweep
3. *'Automatic Gain Control'* varies the gain down the seismic section
4. *'Trace Math Transform'* applies an envelope function to the data (Reflection Strength) – this is optional because as has been described in Section 5.2. reflection strength may enhance strong reflectors aiding interpretation but do mask the true resolution of the data. Typically two data volumes are now produced: with and without reflection strength.

On completion of the seismic processing the data is then stacked at the binning interval determined earlier. Effectively, this represents the averaging of all traces within a single bin, a process which significantly enhances the Signal-to-Noise ratio of the data and thus it's clarity by suppressing transient acoustic anomalies. With good data coverage it is also possible to undertake 3D pre-stack Kirchoff migration. This is a process by which the reflection energy is mathematically placed back in its correct location. This is best illustrated when one considers the way a point reflector is

seen on a typical 2D trace. Figure 39 shows a Chirp section of a reflection from a pipeline (i.e. small diameter object).

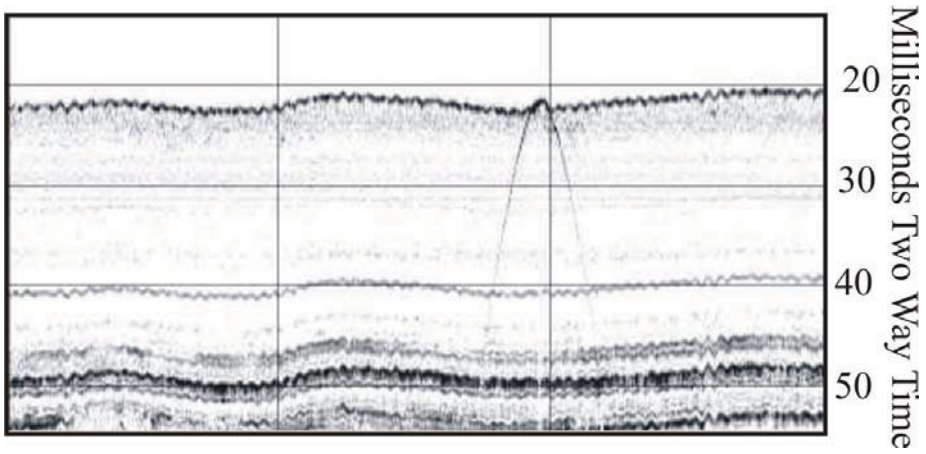


Figure 39: Typical point hyperbolae reflection from a small object in a 2D section.

This section shows the typical point hyperbolae produced by the reflections from a series of shots (i.e. those reflections proceeding and following the true normal incidence shot on the target create the reflection 'tails'). With migration these tails are all allocated to the shot location coinciding with the actual object position. With migration of this data this is obviously done in three-dimensions. However, we are currently still working on the appropriate application of 3D migration with this data and have subsequently taken on a new PhD student to cover this issue specifically. As such all of the data presented here will be show as a stacked volume. Finally, two industry packages have been used to interpret and visualize the data, Kingdom Suite (Seismic Micro-Technology Inc) and GeoFrame.

## 6.3. The *Invincible* Survey

The *Invincible* was the second ever 74-gun vessel to be built, this being the classic design which would dominate the major navies of the late eighteenth century. The Invincible was launched from the French port of Rochefort in the spring of 1745. The keel was made of elm but her principal timbers were of locally grown oak, with a total length of 171' 3" (52.2 m) and a maximum breadth of 49' 3" (15 m). Unfortunately, the vessel did not have an illustrious career being captured by the British on the 14 May 1747 at the First Battle of Finisterre. The vessel underwent a series of refits and then placed in active service with the British Navy. After a ten year career the *Invincible's* fate was met as it went to fight the French at Quebec the capital of French Canada.

The orders for the British fleet to set sail were given on the morning of Sunday 19 February, 1758. The *Invincible*, anchoured off St Helens on the northwest coast of the Isle of Wight, had problems in raising the anchour which had latched on to the bow of the vessel. As the crew attempted to free the anchour the vessel continued to move across the East Solent and towards the shallow sand banks of the northern shore. As she approached Horse Sand Spit the tiller fouled causing a tack to the deeper waters to the south east to fail. After further failed attempts to manoeuvre the *Invincible* into safer water the vessel went aground on Horse Sand Spit two hours before high water and facing to the north-north-east. A strengthening wind pushed the vessel further in

to the sand bank a situation exacerbated when on the next high water the Pilot and Master Attendant at Portsmouth dockyard attempted to run the vessel over the bank. Typically this failed, succeeding in only digging the vessel deeper into the sand bank, such that although actually afloat for the majority of the tide the *Invincible* was trapped in a whole. Over the next few days the majority of the ordnance and provisions were removed but a dramatic shift in the wind direction to the south south west and force to a violent storm resulted in the sea over running the decks and ultimately causing the *Invincible* to heel violently on to the port side. In March 1758 the vessel was officially abandoned. A survey in early May identified that the hull was lying on its portside at an angle of c. 30° to the vertical, in a hole, up to 22' (6.7 m) deep, and that it was "....greatly twisted, waving and cambered". By the autumn of that year all four of her masts had been recovered and records of the vessels condition or presence ceased.

The vessel was rediscovered on the bed of the Solent by Arthur Mack in 1979. The wreck site was licensed the following year and underwent extensive diver investigation between 1983 and 1987 (See Figure 40). This work indicated that the vessel was oriented north west/ south east, with the stern to the south east, and was lying on her port side at an angle of c. 45° at her bow, 15° at her stern and 30° amidships. As can be seen from the composite diver plan exposed coherent wreckage is represented by the linear exposure of the port side of the vessel (34 m long by 6.5 m wide) and a cluster of incoherent wreckage due north of the vessel, tentatively interpreted as the starboard side and superstructure of the vessel (Lavery, 1988). The area is covered by fine sands and with a predominant tidal flow direction in the area of 311° i.e. approximately parallel to the ships axis.

Simultaneous chirp and side scan sonar surveys were taken over the site in 1995, 1997 and 1998 utilising a survey grid oriented parallel to the wrecks axis (Quinn et al., 1998). The co-registration of the side scan sonar and the Chirp pulses (using standard Sweep 1) enabled the correlation of surface and sub-surface anomalies. Figure 41 shows the detail from a 100 kHz sonar image and a Chirp Section across the mid-section of the wreck. The image clearly shows that subsequent to the diver investigations movement of sand has exposed more inboard structures along the main axis of the wreck. Further, Quinn et al's interpretation of the 2D Chirp data suggested that the bulk of the wreck was to the NE of the area and in fact there were no identifiable wreck fragments to the south-west. This data also gave us confidence the newly defined Chirp II pulse (Sweep 2) would reliably image the buried timbers. Finally, Wessex Archaeology provided swath bathymetry data from a 2002 survey (Figure 42), this was used to plan the 3D Chirp survey. This dataset shows clearly the current location of the wreck site in a depression on the north-eastern margin of a linear sandbank that is broadly oriented south-east to north-west. Smaller scale parasitic bedforms with their long axes oriented north-east to south-west are migrating across the larger sandbank feature. Purely visual comparison shows the main structures identified in the eighties, during a number of dive seasons, are still present when the swath data was acquired in 2002. The GeoTiff provided by Wessex Archaeology also enabled the measurement of the basic dimensions of the site. A direct measurement off the swath gives a coherent port side wreckage length of 42 metres. However, this does not coincides with a measurement of 32 metres for the same part of the site from the published dive plan (although is still consistent with the

overall dimensions from the historic record). Also of interest is an isolated object, which sits in its own scour pit, 52 metres to the south-east of the wreck.

The 3D Chirp fieldwork acquired a total of 25 hours of survey data, at 4 shots per second culminating in the acquisition of approximately 150 Gb of data. This provided data coverage of c. 1 m line spacing in two directions (wreck parallel and at c. 20$^{o}$ to wreck) creating a survey box c. 160 m by 160 m. Based on previous knowledge of the site (Figure 41: Quinn et al., 1998) the survey was offset to encompass the exposed wreck sections and an area immediately to the north-east (Figure 43).

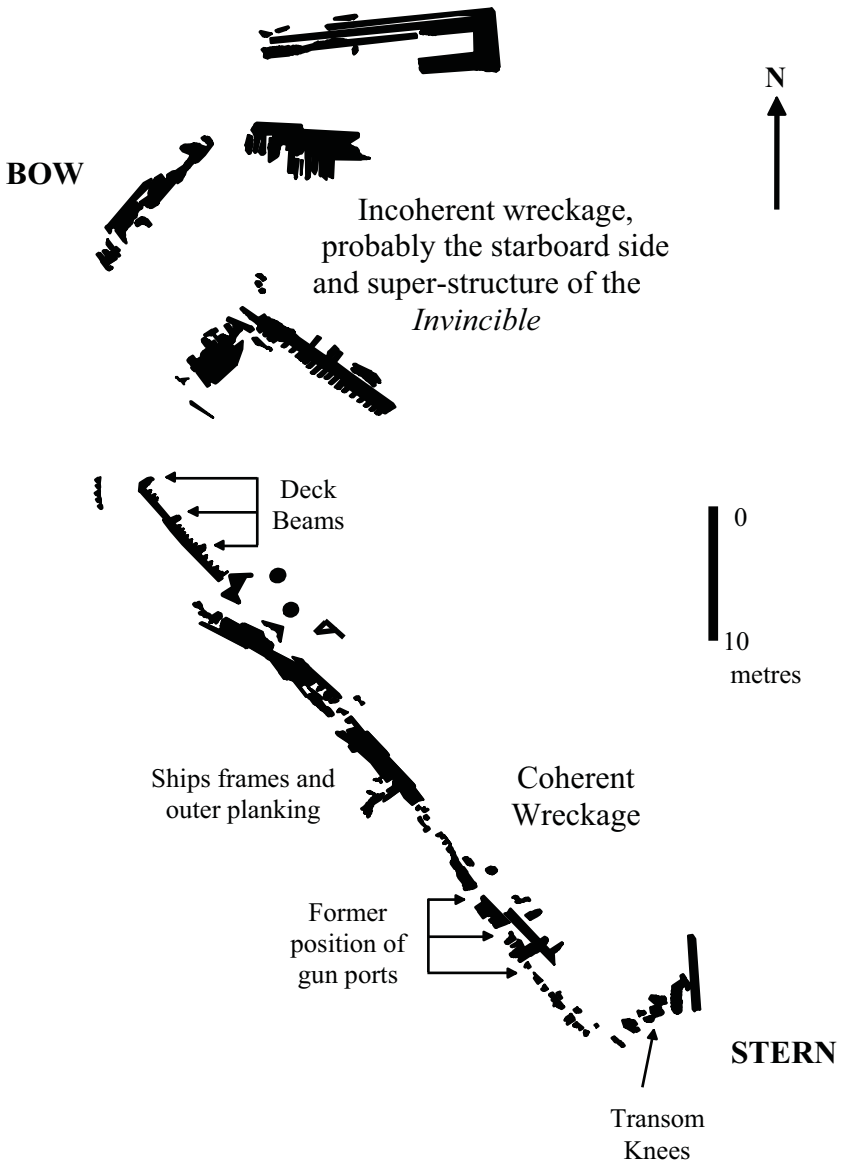


Figure 40: A detailed plan of the main *Invincible* site, based on diver survey, modified from Lavery (1988)

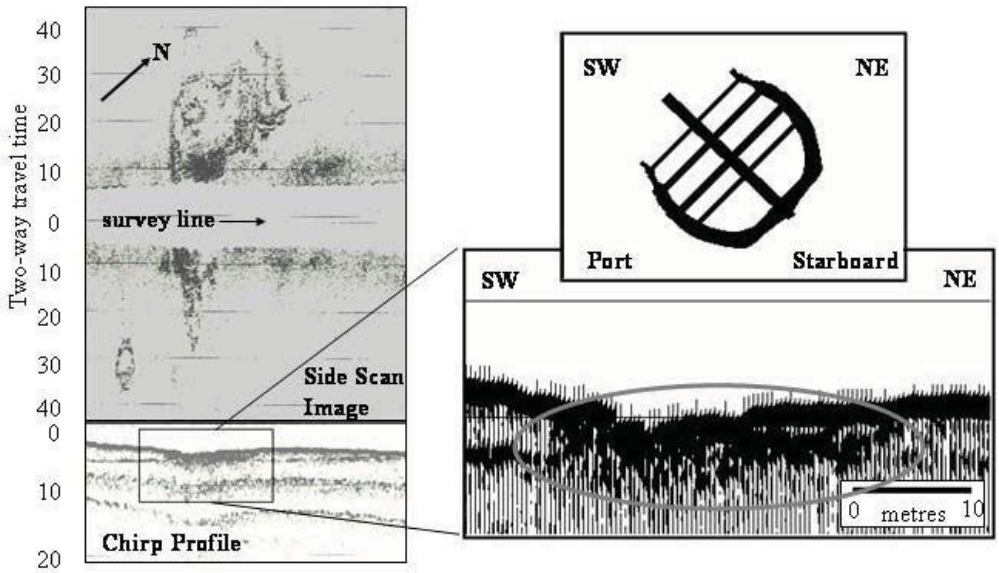


Figure 41: A side scan sonar and Chirp section taken from the *Invincible* wreck site in 1995. The high amplitude wreck reflectors are highlighted on the blow-up of the Chirp section (bottom right).

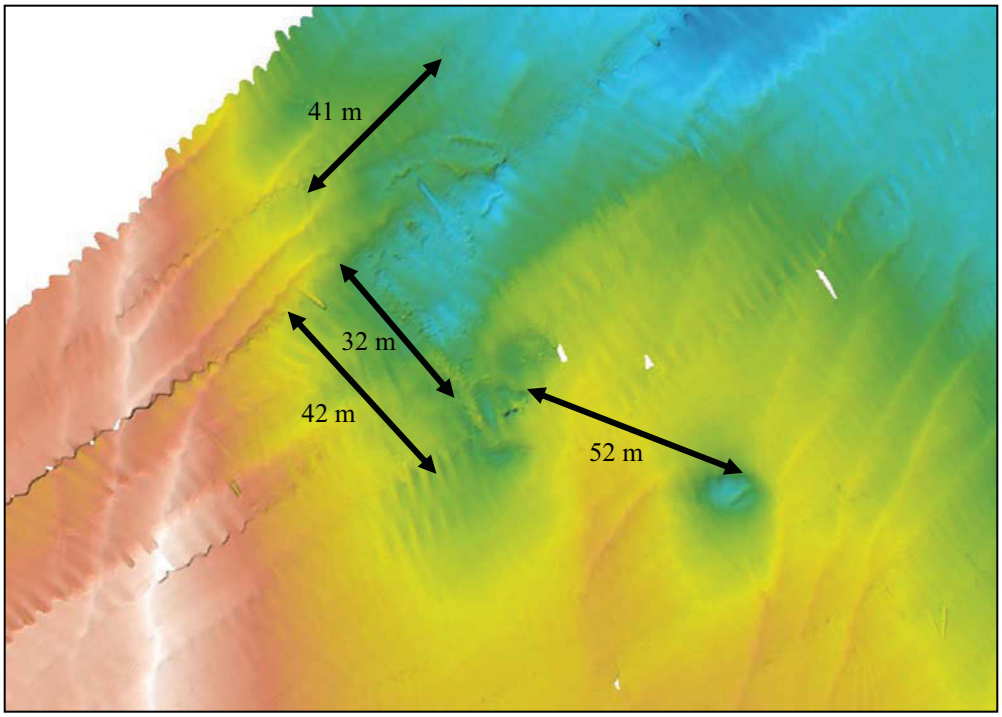


Figure 42: A swath bathymetry image of the wreck site taken in 2002 by Wessex Archaeology, showing key dimensions of the site. Depth is colour coded from White (shallow) to blue (deep).

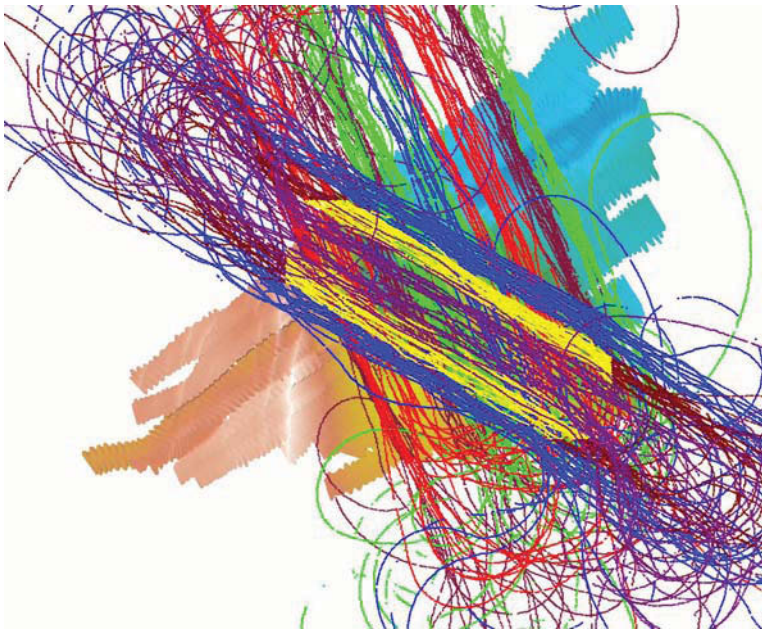

Figure 43: A shot-point map for the 3D Chirp survey overlying the swath bathymetry data provided by Wessex Archaeology, showing the excellent data coverage over the site.

Having binned the data at 25 cm bin size and processed the data using the flow described in Section 6.2.2. it is possible to produce a fold map to establish the number of traces per bin. As previously described, the higher the number of traces per bin the better the signal-to-noise ratio and thus the clarity of the image produced within the volume. It can be seen from Figure 44, that over the site the typical fold coverage is between 10 and 30 shots per 25 cm bin, this is exceptionally high. There are still a small number of data gaps, but over the site the largest of these is less than 2 metres.

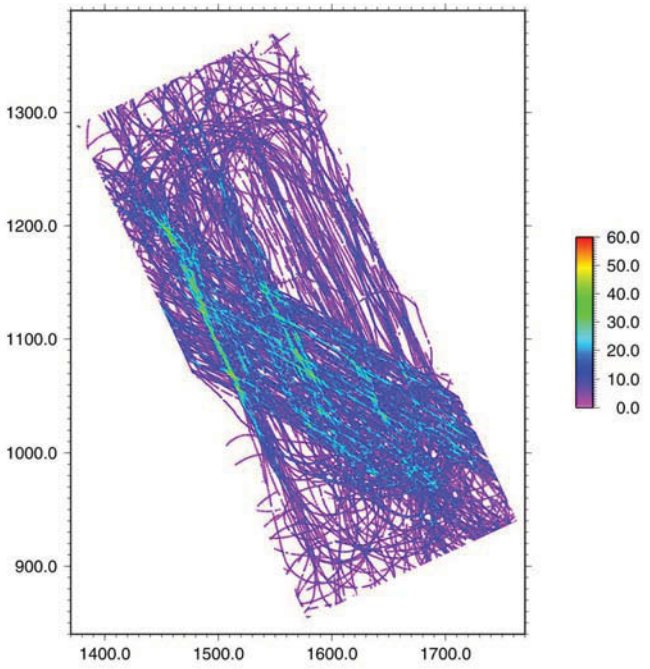


Figure 44: A fold coverage map produce from the 3D Chirp *Invincible* data.

Having produced the volume it is then possible to view the data as either in-line or x-line slices at intervals dictated by the 25 cm bin size. If required it is also possible to view lines drawn across the data volume in any chosen direction. However, the crux of this system is the ability to actually acquire time-slices i.e. horizontal planes taken at different depths through the volume. The minimum slicing interval is dictated by the sample interval which in this case is 50 kHz. This is equivalent to a slice every 0.02 ms two-way travel time which at 1600 $ms^{-1}$ (a typical velocity value for sound in fine sands) represents a slice every 1.6 cm. For the purposes of the visualization of the Invincible data the volume was sliced every 0.1 ms TWT, which is equivalent to every 8 centimetres (the middle of the theoretical resolution limits of Sweep 2: Section 5.2.4. Table 4).

Figure 45, is a single in-line vertical slice (in-line 539) taken through the 3D volume of the *Invincible* wreck. The section shows significant improvement on the data taken previously using a single channel system with Chirp Sweep 1, however, this will not only be the result of being able to stack the data, but also the improved nature of the sweep and the improved initial power input. The seabed can be clearly seen between 12 and 14 ms and the zone of high amplitude reflections highlighted represent the reflections associated with the known position of the wreck. There is also an easily identifiable horizontal reflector at c. 15 ms TWT, this can be clearly seen either side of the wreck but is not visible beneath the wreck reflectors. This is also a characteristic feature of wreck reflections, as they represent such high reflection co-efficients no energy is capable of penetrating beneath them creating a "shadow zone" (Arnott et al., 2005). However, it is fair to say that viewing the data in in-line slices enables the delimitation of the reflection zone related to the wreck but does not provide an easily interpretable section for the archaeologist.

The next stage of the interpretation was to pick the seabed horizon in order to create a high resolution picture of this surface. This should provide comparable data to the swath bathymetry image presented in Figure 42 and also act as a good control of the true z capability of the RTK system, as any mis-matches of the z value should be easily picked up during seabed map production. Figure 46, shows a colour coded contour map (white – shallow; blue – deep) from the 3D Chirp data. This provides an easily comparable (and arguably better) image of the seabed surface than the swath system (although it should be noted we are making no claim that this is an alternative to swath data). One or two artefacts (generally parallel to the ship-parallel lines) do occur but all of the major features of the sandbank and the wreck site are clearly resolved. The full detail of individual wreck related objects, at present, is not as well resolved within this stacked image as in the swath data. This is a product of not being able to properly migrate the data at present and hence point objects are presented as hyperbolae which are not easily picked within the interpretation software. We believe on a properly migrated volume we shall be able to resolve this point objects more clearly.

The true breakthrough of this development is shown in Figure 47a, this is a time-slice taken at 14.3 ms TWT which is equivalent to a depth of 25-50 cm (depending on overlying bed relief) beneath the seabed. This section clearly shows the full at depth distribution of the wreck material. By comparison to the swath data and diver information which is obviously restricted to a surface interpretation, the site consists of interconnected wreckage over an area, 77 metres in length and 42 metres in width. This suggests that the "incoherent wreckage" as described from the dive plan is in fact

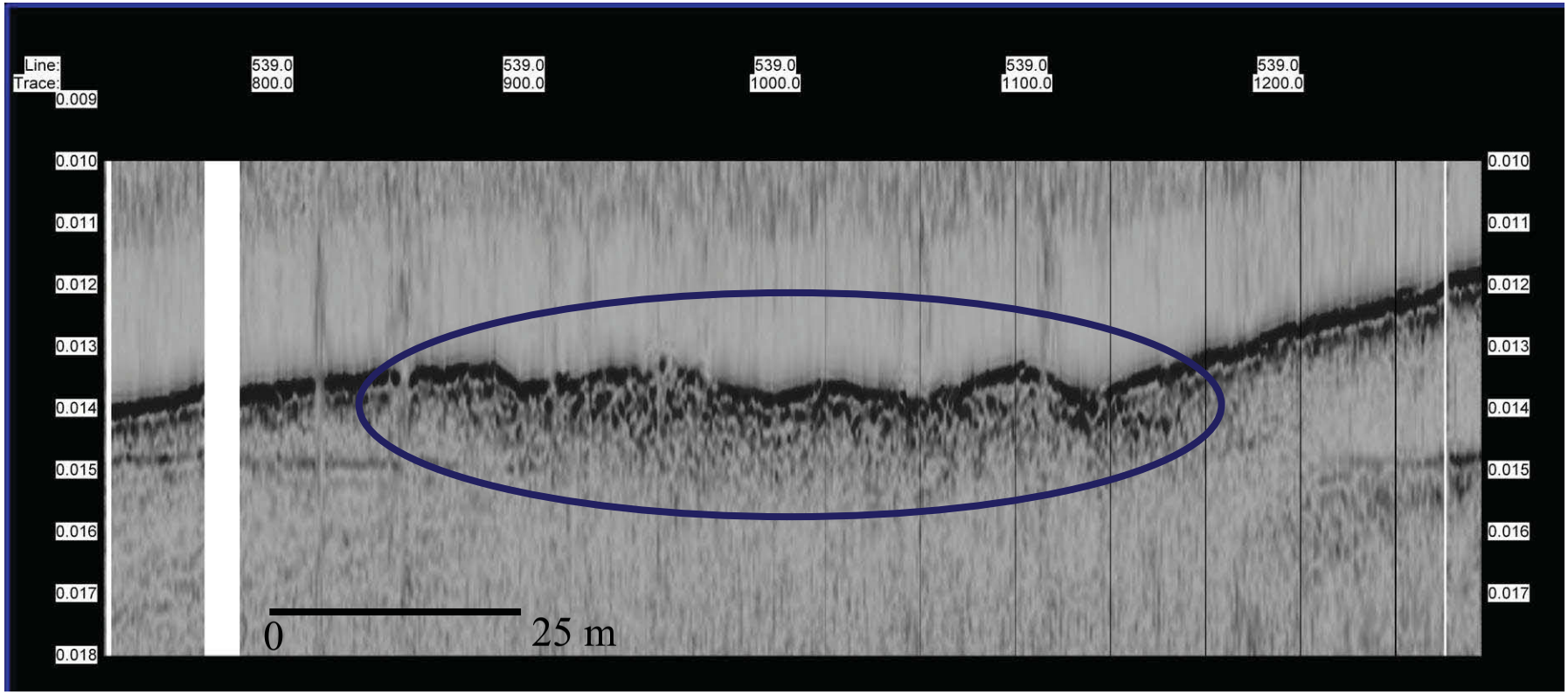


Figure 45. An in-line slice from the 3D Chirp volume of the Invincible wreck site, with the wreck area highlighted by the blue ovate. The vertical scale is in decimal seconds. The acoustic blanking caused by the wood of the wreck reflector can be clearly seen by the loss of the horizontal reflector at 0.015 seconds. This image should be compared with the single channel section seen in Figure 41.

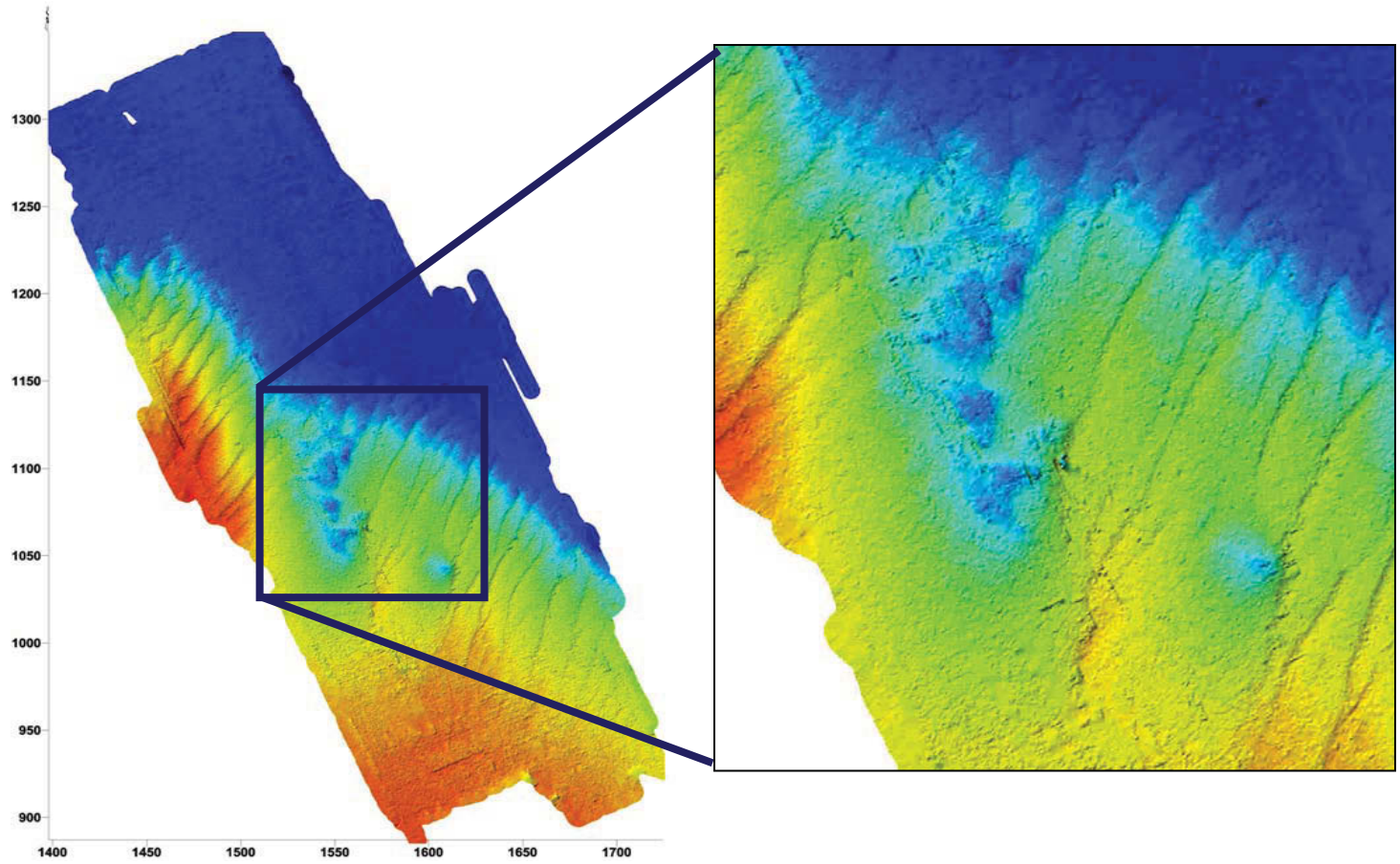


Figure 46. A bathymetric map of the Invincible wreck site produced from the seabed picks generated from the 3D Chirp volume. As with the swath data seen in Figure 42 all the key morphological features can be identified, including the bank, sediment bedforms and the scour associated with the main site and outliers. Depth code red shallow blue deep.

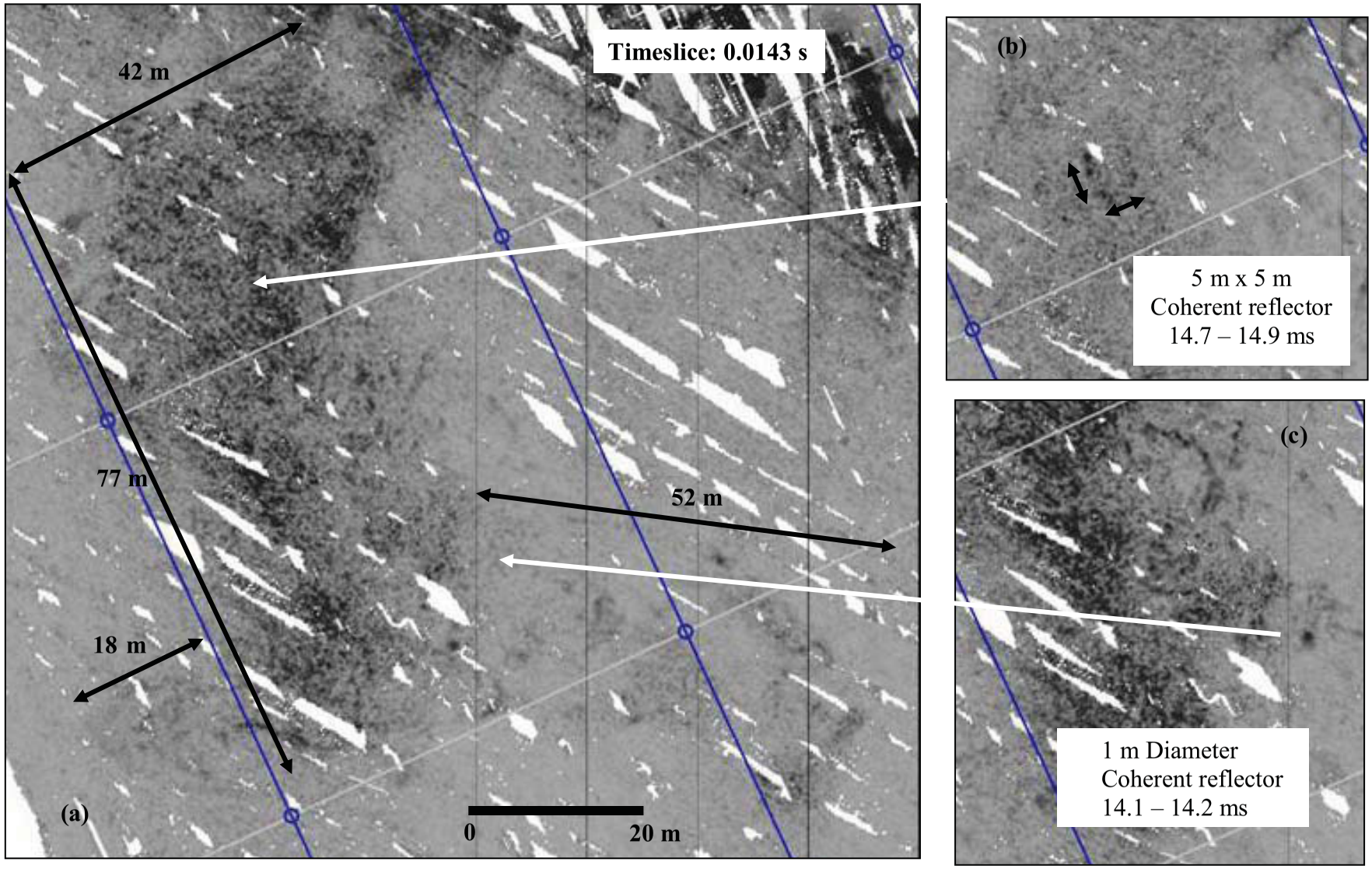


Figure 47: A series of timeslices through the *Invincible* wreck site, showing the full plan view at depth (a); coherent geometry on a metric scale (b) and individual metre scale objects (c) all buried beneath the sandbank.

connected at depth. Further, at this depth it seems apparent that the isolated object 52 metres to the south-east, identified in the swath, is also connected at this depth but with a more skeletal series of interconnecting "timbers". This image also suggests that although the majority of the wreck material is to the north-east of the port side margin as described by Quinn et al (1998) there is a significant (18 metre x 15 metre) section of wreckage to the south-west of the port margin at the stern end. In order to fully appreciate the changing stratigraphy of the site with depth a powerpoint presentation on CD is appended to this document. This presentation "EH timeslices.ppt", represents a series of timeslices taken at 0.1 ms (8 cm) intervals between 14 and 15.4 ms (which is equivalent to a 1.2 m thick volume).

Finally, Figure 47b and 47c show smaller objects within the actual wreck area. Firstly, Figure 47b shows a 5 m x 5 m square reflector which occurs between 14.7 ms and 14.9 ms TWT in the central bow section of the wreck, whereas Figure 47c actually shows a 1 metre diameter coherent reflector between 14.1 and 14.2 ms TWT. It is not possible at present to confirm the archaeological significance of these features, but they have been extracted to show the true resolution capabilities of object detection with this system.

Due to the broken and flattened nature of this particular wreck site any 3D rendering of the wreck does not provide significant additional information to that provided by the timeslices. However, to demonstrate the ultimate capability Figure 48a, b and c shows a 3D interpretation of the hull form of the Grace Dieu. This survey has been taken subsequent to Project 3364 and in very different conditions (only 4 metres of water and in muddy sediments), but the coherent nature of the wreckage makes for a more easily identifiable hull form. This work is currently being worked up by Plets as part of her PhD and it is fair to say that these data and the subsequent development of the 3D system would not have been possible without the work on the *Invincible*.

## 6.4. Conclusions

Chapter 6 covers the outcomes from Objectives 13 to 17 and shows the results from the World's first true 3D data volume acquired over an archaeological site. These data show the unprecedented capability to image buried and semi-buried shipwrecks to a resolution comparable with and arguably better than can be obtained from swath bathymetry systems (the state-of-the-art quantitative seabed imaging tools). Using the wreck of the Invincible which is buried in a sandy substrate it is possible to demonstrate the potential use of this tool for recording buried sites in some aggregate areas. This tool is rapid and through the lessons learnt during this project it is now possible to acquire a volume over a similar area in only two days of surveying and to have preliminary results within two weeks. The text of this section has formed the basis of a paper being submitted to the prestigious journal Science, with English Heritage being fully acknowledged for their support. The 3D system is now in the process of commercialization and we currently have had significant interest from many of the major nearshore surveying organizations including Fugro and Gardline. The implications from this work are therefore going to reach beyond just the aggregate industry and into the wider marine sector including wind farm work, harbour surveys, pipeline surveys and a number of military applications.

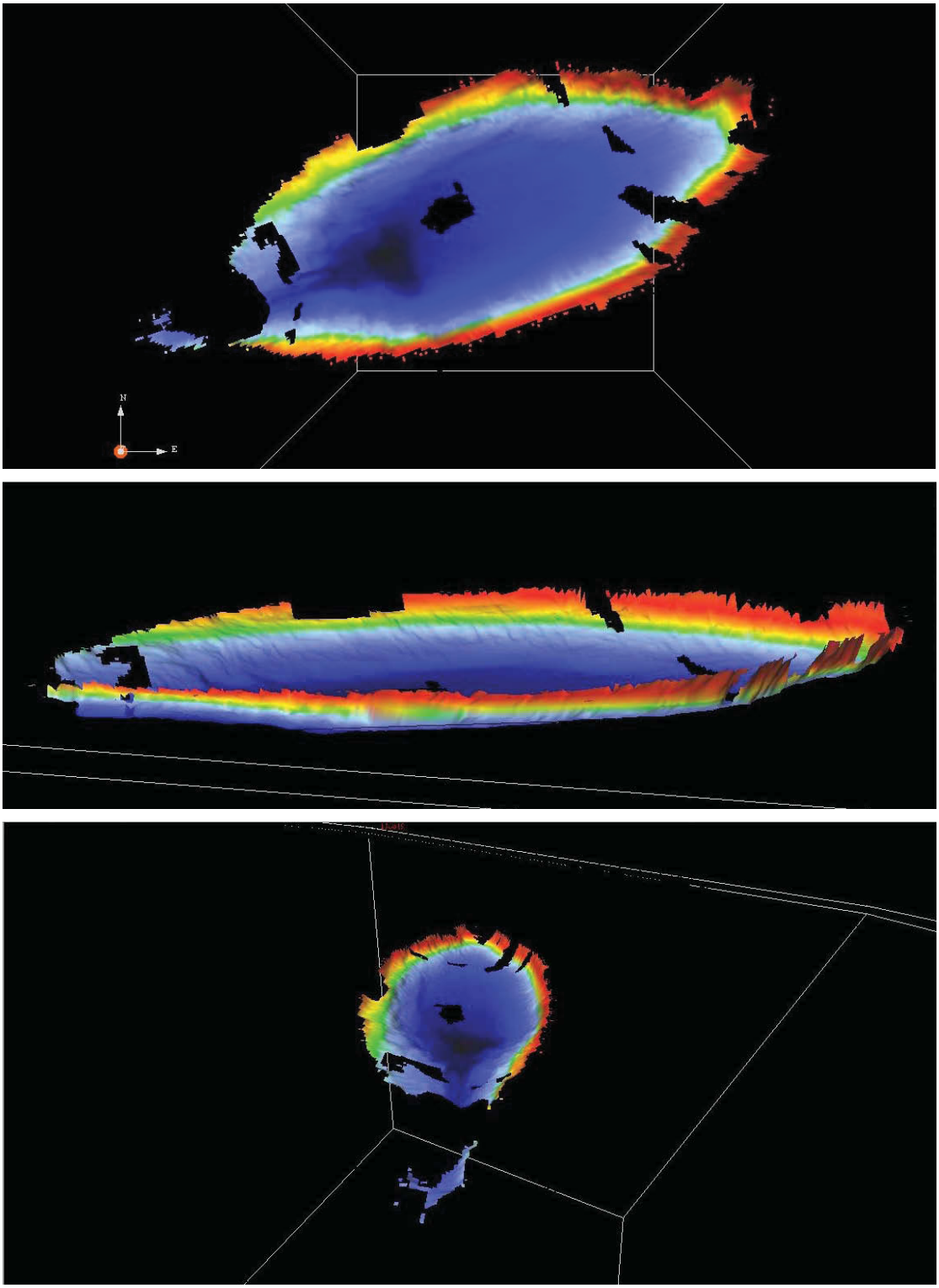


Figure 48. Reconstruction of the hull form of the Grace Dieu wreck site based on a 3D Chirp data volume: (a) Top View; (b) Side View); (c) Stern View. Courtesy Plets.

# 7. Conclusions and Dissemination

This project has successfully completed 16 of its 18 objectives as well as undertaking an additional study of significance to the marine archaeological interests of the aggregate industry. In terms of importance, the work has produced the following:

1. The world's first 3D survey of a buried wreck site, providing centimetric to decimetric resolution imagery of an eighteenth century wreck partially buried within a sandbank.
2. Through the combination of modelling, laboratory experiment and in situ data collection has established the acoustic characteristics of peat horizons buried in marine sediments.
3. A reconstruction of the palaeogeography of the offshore Solent region; showing both the course of the Palaeo-Solent River and the variable nature of the Holocene transgressive fill deposits.
4. Through modelling, laboratory experiment and in situ data collection the resolution capabilities of state-of-the-art Chirp II acoustic sweeps.

This work has been presented at six national and international conferences/workshops to both the academic and industry communities (see list below); and is currently the focus of five papers for academic journals (1 published; 1 submitted; three in the final draft stage). The work has also provided an essential component in our development of the 3D Chirp system particularly in terms of our knowledge of data acquisition, post processing and data visualization.

Conference Presentations:

Dix, J.K.. High resolution sonars for archaeological investigations. *English Heritage Underwater Survey and Recording Seminar*, *Centre for Archaeology, Fort Cumberland*, 2003.

Dix, J.K. & Henstock, T.. High resolution acoustics for the investigation of continental shelf archaeology: old and new approaches, a review. *English Heritage Workshop on North Sea Submarine Prehistory and Relations with Industry*, *London*, 2003.

Bull, J.M., Dix, J.K., Henstock, T., Gutowski, M., Leighton, T.G. and White, P.R.. The development of a 3D Chirp sub-bottom profiler system. *Seabed and Shallow Section Marine Geoscience: shared lessons and technologies from academia and industry*, *Geological Society of London, Burlington House, London.* 2004.

Dix, J.K., Bastos, A., Bull, J.M. and Henstock, T.. High resolution marine seismics: a method for detailed mapping of reservoir analogues. *Seabed and Shallow Section Marine Geoscience: shared lessons and technologies from academia and industry*, *Geological Society of London, Burlington House, London.* 2004.

Dix, J.K., Plets, R.K., Adams, J.R., Best, A.I. and Mindell, D.A., High resolution acoustic imagery from a shallowly buried shipwreck: A case study. *American Schools of Oriental Research Annual Meeting,* Philadelphia, 2005..

Dix, J.K, Bull, J.M., Gutowski, M., Henstock, T., Hogarth, P., Leighton, T.J. & White, P.R. True 3D High Resolution imagery of a Buried Shipwreck: the Invincible (1758), *American Geophysical Union, San Fransisco*, 2005.

## 8. REFERENCES


ADU, 2002. http://www.st-andrews.ac.uk/institutes/sims/Adu/

Allen, J.R.L. (2000). Morphodynamics of Holocene salt marshes: a review sketch from the Atlantic and Southern North Sea coasts of Europe. Quaternary Science Reviews, 19, 1155-1231

Applied Acoustic Engineering. http://www.appliedacoustics.com

Arnott S, Dix JK, Best AI, Gregory D. 2002. Acoustic propagation in waterlogged wood. *Acta Acustica United with Acustica* 88 (5): 699-702

Arnott, S., Dix, J.K., Best, A.I. and Gregory, D.. Imaging of buried archaeological materials: the reflection properties of archaeological wood. *Marine Geophysical Researches*, **26**, 2005,

Bachman, R.T. (1985). Acoustic and physical property relationships in marine sediment. Journal Acoustical Society of America, 78(2), 616-621.

Ballard RD, Coleman DF & Rosenberg GD. 2000. Further evidence of abrupt Holocene drowning of the Black Sea shelf. *Marine Geology* 170 (3-4): 253-261

Bates, M.R., & Bates, C.R. (2000). Multidisciplinary Approaches to the Geoarchaeological Evaluation of Deeply Stratified Sedimentary Sequences: Examples from Pleistoce and Holocene Deposits in Southern England, United Kingdom. Journal of Archaeological Science, 27, 845-858.

Behre, K.-E. (2004). Coastal development, sea-level change and settlement history during the later Holocene in the Clay District of Lower Saxony (Niedersachsen), northern Germany. Quaternary International, 112, 37-53.

Bellamy AG. 1995. Extension of the British landmass: evidence for shelf sediment bodies in the English Channel. In Preece RC (ed). *Island Britain: a Quaternary Perspective*. pp. 47-62. Geological Society Special Publication 96.

Best, A.I., & Gunn, D.E. 1999. Calibration of marine sediment core loggers for quantitative acoustic impedance studies. Marine Geology, 160, 137-146.

Best, A.I., Huggett, Q.J., & Harris, A.J.K. 2001. Comparison of in situ and laboratory acoustic measurements on Lough Hyne marine sediments. Journal of the Acoustic Society of America, 110(2), 695-709.

Bozkurt, S., Lucisano, M., Moreno, L., & Neretnieks, I. (2001). Peat as a potential analogue for the long-term evolutionin landfills. Earth-Science Reviews, 53, 95-147.

Buckingham, M.J., & Richardson, M.D. 2002. On tone-burst measurements of sound speed and attenuation in sandy marine sediments. IEEE Journal of Oceanic Engineering, 27(3), 429-453.

Bull. J.M., Gutowski, M., Dix, J.K., Henstock, T., Hogarth, P., Leighton, T.J. & White, P.R.. Design of a 3D Chirp sub-bottom imaging system. *Marine Geophysical Researches*, **26,** 2005, 157-169

Bridgland DR. 2000. River terrace systems in north-west Europe: an archive of environmental change, uplift and early human occupation. *Quaternary Science Reviews* 19 (13): 1293-1303

Bridgland DR. 2001. The Pleistocene Evolution and Palaeolithic Occupation of the Solent River. In Wenban-Smith F. & Hosfield R. (eds). *Palaeolithic Archaeology of the Solent River*. Lithic Studies Society Occasional Paper No.7. pp.15-21.

Bull JM, Quinn R & Dix JK. 1998. Reflection coefficient calculation from marine high resolution seismic reflection (Chirp) data and application to an archaeological case study. *Marine Geophysical Researches* 20 (1): 1-11

Chauhan OS & Almeida F. 1988. Geophysical methods as a tool to explore submerged marine archaeological sites. In Rao S (ed). *Marine Archaeology of Indian Ocean Countries*. pp. 3-4 Goa: National Institute of Oceanography.

Clay, C.S., & Medwin, H. 1977. Acoustical oceanography: principles and applications. New York: John Wiley & Sons.

Coles, J.M. (1986). Precision, Purpose and Priorities in Wetland Archaeology. The Antiquaries Journal*,* 67(3), 227-245.

Cooper, A., McErlean, T, Lenham, J. and Forsythe, F., 2002a. The Evolution of the Lough. In: Strangford Lough: *An Archaeological Survey of the Maritime Cultural Landscape.* McErlean, T., McConkey, R. and Forsythe, W. (Eds): Blackstaff Press, Belfast, ISBN 0-85640-723-2, 21-31.

Cooper JAG, Kelley JT, Belknap DF, Quinn R, McKenna J. 2002b. Inner shelf seismic stratigraphy off the north coast of Northern Ireland: new data on the depth of the Holocene lowstand. *Marine Geology* 186 (3-4): 369-387.

Dix JK. 2000. Principal Contributor in: Allen, M.J. and Gardiner, J. *Our Changing Coast: A survey of the intertidal archaeology Langstone Harbour, Hampshire*. CBA Research Report 124.

Dix JK. 2001. The Geology of the Solent River System. In Wenban-Smith F. & Hosfield R. (eds). *Palaeolithic Archaeology of the Solent River*. Lithic Studies Society Occasional Paper No.7. pp. 6-14.

Dix JK, Arnott S, Best AI & Gregory D. 2001. The geoacoustic characteristics of archaeological wood. *Institute of Acoustics, Underwater Acoustics Group Conference on Acoustical Oceanography*. pp. 299-305

Dix, J.K., Long, A.J. and Cooke, R., 1998. The Evolution of Rye Bay and Dungeness Foreland: New Evidence From the Offshore Seismic Record. In: Romney Marsh: Environmental Change and Human Occupation in a Coastal Lowland (Ed. Eddison, J., Gardiner, M. and Long, A.); *Oxford University Committee for Archaeology Monograph,* **46**: 1-12.

Dollar ESJ. 2002. Fluvial geomorphology. *Progress in Physical Geography* 26 (1): 123-143

Draper-Ali, S., 1996. Marine Archaeology and Geophysical Survey: A Review of Commercial Survey Practice and its contribution to Archaeological Prospection. Hampshire & Wight Trust for Maritime Archaeology, Southampton

Emerson, W.W., & McGarry, D. (2003). Organic carbon and soil porosity. Australian Journal of Soil Research*,* 41, 107-118.

Fedje, D.W., & Josenhans, H. (2000). Drowned forests and archaeology on the continental shelf of British Columbia, Canada. Geology*,* 28(2), 99-102.

Flemming NC. 1998. Archaeological evidence for vertical movement on the continental shelf during the Palaeolithic, Neolithic and Bronze Age periods. In Stewart I & Vita-Finzi C (eds). *Coastal Tectonics*. pp. 129-146. Geological Society of London, Special Publications 146.

Frey, D. 1971. Sub-bottom survey of Porto Longo Harbour, Peleponnesus, Greece. *International Journal of Nautical Archaeology*, **1**, 170-175.

Garrison EG. 1992. Recent archaeogeophysical studies of palaeoshorelines of the Gulf of Mexico. In Johnson LL & Stright MJ (eds). *Palaeoshorelines and Prehistory: an investigation of method*. pp.103-116. Boca Raton: CRC Press

GeoAcoustics. Retrieved 6th December, 2004, from http://www.geoacoustics.com

Gerdes, G., Petzelberger, B.E.M., & Scholz-Bottcher, B.M. (2003). The record of climatic change in the geological archives of shallow marine, coastal, and adjacent lowland areas of Northern Germany. Quaternary Science Reviews, 22, 101-124.

Gorgas, T.J., Wilkens, R.H., Fu, S.S., Frazer, L.N., Richardson, M.D., Briggs, K.B., & Lee, H. 2002. In situ acoustic and laboratory ultrasonic sound speed and attenuation measured in heterogeneous soft seabed sediments: Eel River shelf, California. Marine Geology, 182, 103-119.

Gregory, 2000. Underwater reconnaissance. Maritime Archaeology Newsletter, Roskilde Denmark, **14**: 20-22.

Gutowski, M., Bull, J., Henstock, T., Dix, J., Hogarth, P., Leigthon, T., & White, P. (2002). Chirp sub-bottom profiler source signature design and field testing. Marine Geophysical Researches, 23, 481-492.

Hamblin RJO, Crosby A, Balson PS, Jones SM, Chadwick RA, Penn IE & Arthur MJ. 1992. *The Geology of the English Channel*. British Geological Survey, United Kingdom Offshore Regional Report 10

Hamilton, E.L. (1970). Sound Velocity and Related Properties of Marine Sediments, North Pacific. Journal of Geophysical Research, 75(23), 4423-4446.

Hobbs, N.B. (1986). Mire morphology and the properties and behaviour of some British and foreign peats. Quareterly Journal of Engineering Geology, 19, 7-80.

Hosfield RT. 1999. *The Palaeolithic of the Hampshire Basin: a regional model of hominid behaviour during the Middle Pleistocene*. BAR British Series 286. Archaeopress, Oxford.

Hosfield RT. 2001. The Lower Palaeolithic of the Solent: 'Site' formation and interpretive frameworks. In Wenban-Smith F & Hosfield R (eds). *Palaeolithic Archaeology of the Solent River*. Lithic Studies Society Occasional Paper No.7. pp. 85-97.

ICOMOS, 1990 International Conference of Monuments and Sites, *Charter for the protection and management of the archaeological heritage*, http://www.international.icomos.org/e_archae.htm

Kallweit, R.S., & Wood, L.C. 1982. The limits of resolution of zero-phase wavelets. Geophysics, 47(7), 1035-1046.

Kearey, P., & Brooks, M. 1991. An introduction to geophysical exploration (2nd ed.). Oxford: Blackwell Science.

Koefoed, O. 1981. Aspects of vertical seismic resolution. Geophysical Prospecting, 29, 21-30.

Lawrence, M. L. and Bates, C. R. 2002. Acoustic Ground Discrimination Techniques for Submerged Archaeological Site Investigations. Marine Technology Society Journal, v. 35, No. 4, pp. 65-73.

Lewis SG, Maddy D & Scaife RG. 2001. The fluvial system response to abrupt climate change during the last cold stage: the Upper Pleistocene River Thames fluvial succession at Ashton Keynes, UK. *Global and Planetary Change* 28 (1-4): 341-359

Maddy D, Lewis SG, Scaife RG, Bowen DQ, Coope GR, Green CP, Hardaker T, Keen DH, Rees-Jones J, Parfitt S & Scott K. 1998. The Upper Pleistocene deposits at Cassington, near Oxford, England. *Journal of Quaternary Science* 13 (3): 205

Maddy D, Bridgland D & Westaway R. 2001. Uplift-driven valley incision and climate-controlled river terrace development in the Thames Valley, UK. *Quaternary International* 79:23-36

Mayer, L.A. 1980. Deep-sea carbonates: Physical property relationships and the origin of high-frequency acoustic reflectors. Marine Geology, 38, 165-183.

Mindell, D.A. & Bingham, B. 2001 D.A. Mindell and B. Bingham, 2001. A High-frequency, Narrow-beam Sub-bottom Profiler for Archaeological Applications. IEEE "Oceans" Engineering Conference, Hawaii, November 2001.

Momber G & Geen M. 2000. The application of the Submetrix ISIS-100 Swath Bathymetry system to the management of underwater sites. *International Journal of Nautical Archaeology* 29 (1): 154-162

Mosher, D.C., & Simpkin, P.G. (1999). Status and Trends of Marine High-Resolution Seismic Reflection Profiling: Data Acquisition. Geoscience Canada, 26, 174-188.

Muckleroy K. 1978. *Maritime Archaeology*. Cambridge: Cambridge University Press

Patterson, L., 1981. Outer continental shelf: preservation and rescue. *Journal of Field Archaeology,* **8**, 231-232.

Nichol, D. (1998). Construction over peat in Greater Vancouver, British Columbia. Proceedings- Institution of Civil Engineers Water and Maritime Engineering, 127, 109-119.

Parent, M.D., & O'Brien, T.F. 1993. Linear-Swept FM (Chirp) Sonar Seafloor Imaging System. Sea Technology, 49-55.

Plets, R.M.K., Dix, J. K., & Best, A. I., (in preparation). The concept of resolution for sub-bottom profiling systems (Chirp) revisited.

Quinn, R., 1997. Marine high-resolution reflection seismology: acquisition, processing and applications. Unpublished PhD thesis, *University of Southampton*.

Quinn R, Bull JM & Dix JK. 1997. Buried scour marks as indicators of palaeo-current direction at the Mary Rose wreck site. *Marine Geology* 140 (3-4): 405-413

Quinn R, Adams JR, Dix JK & Bull JM. 1998a. The Invincible (1758) site - an integrated geophysical assessment. *International Journal of Nautical Archaeology* 27 (2): 126-138

Quinn R, Dix JK & Bull JM. 1998. Optimal processing of marine high-resolution seismic reflection (Chirp) data. *Marine Geophysical Researches* 20(1):13-20

Quinn R, Cooper JAG & Williams B. 1999. Marine Geophysical Investigation of Belfast Lough, Northern Ireland. *Archaeology Ireland* 13 (1). Issue No. 47

Quinn R, Cooper AJA & Williams B. 2000. Marine geophysical investigation of the inshore coastal waters of Northern Ireland. *International Journal of Nautical Archaeology* 29 (2): 294-298

Quinn R, Rooney S, Barton K, O' Hara D & Sheehan K. 2001 An integrated marine geophysical investigation of the La Surveillante wreck-site. In Breen C. (ed.) *Integrated Marine Investigations on the Historic Shipwreck La Surveillante.* University of Ulster.

Quinn R, Forsythe W, Breen C, Dean M, Lawrence M & Liscoe S. 2002. Comparison of the Maritime Sites and Monuments Record with side-scan sonar and diver surveys: A case study from Rathlin Island, Ireland. *Geoarchaeology* 17 (5): 441-451

Rao S (ed). *Marine Archaeology of Indian Ocean Countries*. Goa: National Institute of Oceanography.

Redknap M. 1990. Surveying for underwater archaeological sites:- signs in the sand. *Hydrographic Journal* 58: 11-16

Robb, G.B.N. 2004. The *in situ* compressional wave properties of marine sediments. Unpublished PhD thesis, Institute of Sound and Vibration Research, Southampton.

Robb, G.B.N., White, P.R., Dix, J.K., Bull, J.M., Leighton, T.G. and Best, A.I., 2002. The estimation of geoacoustic properties from broadband acoustic data, focusing on instantaneous frequency techniques. *ISVR Technical Report No.298*.

Rule M. 1982. *The Mary Rose. The Excavation and Raising of Henry VIII's Flagship.* Greenwich: Conway Maritime Press

Rumsby B. 2002. Vertical accretion rates in fluvial systems: A comparison of volumetric and depth-based estimates. *Earth Surface Processes and Landforms* 25 (6): 617-631

Schock SG & Leblanc LR. 1990. Chirp sonar: new technology for subbottom profiling. *Sea Technology* 31(9):37-43

Selby I. 1992. An Introduction to Marine Aggregates and their Quaternary Origin. In *Quaternary Proceedings*. No.2: 25-31.

Sheriff, R.E. 1973. Encyclopedic dictionary of exploration geophysics. Tulsa, Oklahoma: Society of Exploration Geophysicists.

Sheriff, R.E., & Geldart, L.P. 1995. Exploration seismology (2nd ed.). Cambridge: Cambridge University Press.

Stevenson, I.R., McCann, C., & Runciman, P.B. 2002. An attenuation-based sediment classification technique using Chirp sub-bottom profiler data and laboratory acoustic analysis. Marine Geophysical Researches, 23, 277-298.

Stoll, R.D. 2001. Velocity dispersion in water-saturated granular sediment. Journal of the Acoustic Society of America, 111(2), 785-793.

Stright MJ. 1986. Evaluation of archaeological site potential on the Gulf of Mexico continental L-Shelf using high-resolution seismic data. *Geophysics* 51 (3): 605-622

Turgut, A., & Yamamoto, T. 1990. Measurements of acoustic wave velocities and attenuation in marine sediments. Journal of the Acoustic Society of America, 87(6), 2376-2383.

Van Andel TH & Llanos. 1983. Prehistoric and historic shorelines of the southern Argolid peninsula - a subbottom profiler study. *International Journal of Nautical Archaeology* 12 (4): 303-324

Vandenberghe J & Maddy D. 2001. The response of river systems to climate change. *Quaternary International* 79: 1-3

Velegrakis AF, Dix JK & Collins MB. 1999. Late Quaternary evolution of the upper reaches of the Solent River, Southern England, based upon marine geophysical evidence. *Journal of the Geological Society, London* 156: 73-87.

Verbeek, N.H., & McGee, T.M. (1995). Characteristics of high-resolution reflection profiling sources. Journal of Applied Geophysics, 33, 251-269.

Waller, M.P., & Long, A.J. (2003). Holocene coastal evolution and sea-level change on the southern coast of England: a review. Journal of Quaternary Science, 18(3-4), 351-359.

Wessex_Archaeology. (2004). Seabed Prehistory: Gauging the Effects of Marine Aggregate Dredging - Project Design (No. 53146.02). Salisbury: Wessex Archaeology.

Widess, M.B. (1973). How thin is a thin bed? Geophysics, 38, 1176-1180.

Widess, M.B. (1982). Quantifying resolving power of seismic systems. Geophysics, 47(8), 1160-1173.

Williams, K.L., Jackson, D.P., Thoros, E.I., Tang, D., & Schock, S. (2002). Comparison of sound speed and attenuation measured in a sandy sediment to predictions based on the Biot theory of porous material. IEEE Journal of Oceanic Engineering, 27(3), 413-428.

Yilmaz, O. (1987). Seismic data processing. Tulsa: Society of Exploration Geophysicists.